Aggregated Author Response Documents with Tracked Manuscript Changes

All *Referee comments are included below in italic black font* and the Author responses are in blue font.

Summary of Manuscript Revisions: In addition to specifically addressing each of the reviewer comments, we removed some of the less important technical description of the FT-ICR MS composition in sections 3.3 and 3.4. The manuscript has been edited for grammar corrections and clarity.

Author responses to comments from RC1 are given below in blue font. The original referee comments are provided in *black italicized font.*

This paper describes high resolution mass spectrometry (HRMS) and NMR analysis of water soluble organic compounds (WSOC) in four samples selected to represent fresh and aged aerosol particles as well as fresh and aged fog droplets. Results of this work generally support the importance of aqueous processing of organic aerosols. The data set is definitively interesting and worth publishing. The paper can be improved by addressing several issues described below. In addition, for the amount of new information presented in this paper it is too long. I would recommend shortening it and making it more focused on new findings.

My main criticism of this paper is its reliance on just one sample of each type (fresh aerosol, aged aerosol, fresh fog, and aged fog) to draw far reaching conclusions about chemical processes that are responsible for aging of WSOC. Furthermore, samples come from completely different dates making it quite difficult to faithfully compare them. This is much less satisfying and convincing than the approach taken by the authors in Gilardoni et al. (2016) that looked at the fog dissipation events. The authors rely on aerosol mass spectrometry (AMS) analysis, specifically on the f44-f60 correlation plots, to classify the samples. To prove to the readers that this classification works as expected the authors should compare at least two HRMS data sets from different filters that are supposed to be identical based on the f44-f60 AMS classification. Why not take a couple of samples (as opposed to a single sample) corresponding to closely spaced points in Figure 1 and compare their HRMS data? I am willing to bet that the authors would find very different molecular composition for these supposedly similar samples. If this is the case, the comparison of the HRMS data between different conditions becomes more difficult and potentially not even possible.

We thank the referee for their appreciation of the manuscript content and helpful comments. We understand the main criticism raised by the referee about the limited number of analyzed samples, in fact we are working on the analysis of a larger database collected during a more recent field experiment, specifically designed to investigate aqueous phase processing. Nevertheless, the complexity of ultrahigh resolution FT-ICR MS database generated from a single aerosol or fog water sample set some limitations on the number of samples that could be analyzed within a reasonable amount of time. One of the goals of this study is to analyze extremely different samples of aerosol and fog water in term of ageing of organic content and impact of wood burning emissions, to fully deploy the potential of ultrahigh resolution MS and identify the subset of information relevant for a larger database analysis. In addition, the low time resolution of ultrahigh resolution MS and ^{1}H-NMR analysis (hours or days) compared to HR-ToF-AMS analysis (minutes) requires a different approach in the data analysis compared to what was done in

Gilardoni et al. (2016), where we were able to follow the formation and dissipation of single fog events. For this reason, we rely on the high time resolution of HR-ToF-AMS analysis to identify aerosol samples for further analysis with ultrahigh resolution MS and ^{1}H-NMR techniques as described in the text.

The selection of aerosol samples was based on a detailed characterization of the field experiment data reported in a previous publication (Gilardoni et al., 2016), and is not the subject of the present manuscript. Instead, for the selection of fog water samples, we used the approach commonly employed by HR-ToF-AMS users for organic aerosol, investigating the f_{44} and f_{60} space, since it is recognized that f_{44} is a marker of ageing organic content and f_{60} is a proxy for wood burning organic molecules (Cubison et al., 2011). We are aware that this representation is an oversimplification of the complexity of organic fog water content, thus this approach is here employed exclusively to spot marked differences in term of different sources and atmospheric history of organic content. The following was added to section 3.1 on p. 7, line 5-8 to clarify this: "The f_{44} vs. f_{60} space was previously proposed to represent biomass burning vs. atmospheric aerosol aging (Cubison et al., 2011) and was extended here to fog samples. This representation is an oversimplification of the complexity of organic molecules in fog water, employed here exclusively to note the major differences in terms of emission sources and atmospheric history."

As mentioned above the goal of this work was to study very different samples. Even with these selections, we still observe many of the same molecular formulas across samples as indicated in the van Krevelen diagram Fig. 5. Thus, it is unlikely that similar samples as defined in Fig. 1 would yield "*very different molecular composition"*. However, the day to day composition of aerosol and fog and its evolution with respect to the local meteorology is the focus of a future publication.

Overall, this study provides evidence of the potential of combining high-field spectroscopic techniques (Hertkorn et al., 2007) to trace chemical changes in ambient aerosol in specific environmental conditions. We performed a screening of the possible organic compositions using HR-ToF-AMS and a simple functional group analysis by ^{1}H-NMR, and clearly chose extreme conditions in the chemical space (Fig. 1) for further in-depth chemical analyses. This is progressive with respect to previous explorative approaches employing combined ^{1}H-NMR and FT-ICR MS methods for aerosol analysis (Schmitt-Kopplin et al., 2010) which provided little information on the actual environmental conditions affecting the composition of the aerosol.

SPECIFIC COMMENTS

Abstract: To avoid confusing the readers I recommend removing the prefix "high resolution" in front of Tof-AMS in the abstract and in the text. I understand that this how this instrument was called when it was designed but it is a stretch to call it a high resolution instrument especially in a paper that relies on FT-ICR as the main method. Using simple "ToF-AMS" should be sufficient.

We agree that the terms high resolution and ultrahigh resolution are similar. However, the term "high resolution" refers specifically to the subclass of mass spectrometers that use the time of flight (ToF) to derive the measured mass. There are ToF instruments without high resolution. For this reason, we consistently refer to the instruments as HR-ToF-AMS and ultrahigh resolution FT-ICR MS (or simply FT-ICR MS).

P1L21: particles containing organosulfates might activate more easily accounting for the higher fraction of organosulfates in fog droplets compared to aerosol particles.

This sentence (now on p. 1 line 18-19) was changed to reflect the intended observational nature of the statement: "Higher numbers of organonitrates were observed in aerosol, and higher numbers of organosulfates were observed in fog water." While we agree that organosulfate compounds in aerosol may be more hygroscopic and aid in droplet activation, it is well documented that organosulfate compounds form in the aqueous phase of cloud/fog and wet aerosol particles (Darer et al., 2011; Ervens et al., 2011; Schindelka et al., 2013; Herrmann et al., 2015; McNeill, 2015); therefore, pre-existing organosulfates in aerosol may only indicate multiple cycles of fog formation and evaporation. We have added a statement about organosulfates in the fog from nucleation scavenging on p. 12 line 5-6: "…and nucleation scavenging from the preceding fog nuclei composition likely plays a significant role as well…"

P1L25: it would be useful to also add ranges for O:C and H:C for the "fresh" samples so that one can compare

This sentence (now p.1 line 21-23) was edited to compare the values of both the "fresh" and "aged" samples in O:C and H:C values, and the actual range of these values was added to compare more easily: "The average O:C and H:C values from FT-ICR MS were higher in the samples with an "aged" influence (O:C = 0.50-0.58 and H:C = 1.31-1.37) compared to those with "fresh" influence (O:C = 0.43-0.48 and H:C = 1.13-1.30)."

P5L26: it should also be pointed out that valence of 3 is used for N, so the extra double bond in the nitrooxy compounds is not counted

A sentence (p. 6 line 8-9) was added to clarify that the calculated DBE values do not include double bonds formed by pentavalent nitrogen, and tetravalent or hexavalent sulfur: "Note that S and O are divalent in equation (3); additional unsaturated bonds associated with pentavalent nitrogen, and tetravalent or hexavalent sulfur are not included in this DBE calculation."

P5L29: the authors should warn the readers that OS developed by Kroll et al. (2011) only works for CHO compounds, and that it also fails for peroxides. This formula cannot be used for CHOS and CHON compounds. The authors should check their text so that they do not over interpret results from this formula

We thank the referee for this reminder. We modified the OS_C calculation as described in Kroll et al. (2011) to more accurately calculate OS_C for formulas containing nitrogen and sulfur. However, this requires the assumption that when N is present it represents a nitrate functional group and when S is present it represents a sulfate functional group. This assumption is reasonable considering we analyzed the samples using negative ion electrospray, however, it is still an assumption. Furthermore, we assume that unstable peroxide species would not survive sample storage and sample preparation for analysis by FT ICR. This modified calculation is now included in the text (p. 6 line 9-12) along with the necessary assumption: "The average oxidation state of carbon (OS_C) in the molecular formulas was estimated using equation (4), based on the approximation described in Kroll et al. (2011); note that the inclusion of nitrogen and sulfur affects the oxidation state of carbon, and equation (4) assumes both are fully oxidized."

P12L20: the fact that these compounds show in a single daylight sample does not constitute proof that these compounds are related to photochemical properties. This is one example of several statements made by the authors for which they do not have sufficient data. To claim something like this, they would

need to demonstrate presence of these compounds in many daylight samples (not one!) and absence in many nighttime samples.

In our discussion of the results, we suggest that these molecular formulas may have been formed from photolysis reactions, because of the ~8.6 hours of daylight in sample collection. Furthermore, this was the major difference between the two aerosol samples. Thus, it would not have been appropriate to ignore such a major difference. We agree that photochemistry is not directly responsible for the N_2 and N_3 formulas, as there is a trend between the presence of these formulas and NO_X concentration during sample collection for all samples. We have modified this statement (now p. 13 line 27-28) describing them as such: "Compared to the other samples, BO0213D was collected during relatively high NO_X conditions, as well as high humidity and aerosol liquid water content compared to the other aerosol sample."

P13L15: another example where a conclusion is made (about sulfite radical involvement) without having needed data to prove it

Here we related our observation of organosulfates in these samples to literature sources as a suggestion for their origin. We agree that the involvement of sulfite radical is unlikely since most of the samples were collected at night. This statement (now p. 14 line 21-23) was revised to the following: "CHOS and CHNOS formulas were detected with high frequencies in samples with high water content during collection (all samples except BO0204N). This provided some evidence of the production of S-containing SOA species by reactions in the aqueous phase."

Figure 5: What message is conveyed by this figure that cannot be more easily conveyed with average O:C values? I do not see how it helps interpret the data. Two versions of this figure exist, one in the text and one in the SI section. I would just keep it in the SI section or remove altogether.

The van Krevelen space is useful for visualizing both oxidation (O:C) and saturation (H:C). In this work, we have identified thousands of individual molecular formulas. We observed both highly oxidized species and highly saturated species in the same samples, and this plot is able to show these differences. Furthermore, some of these formulas are observed in all of the samples, and some are unique to the individual samples. The van Krevelen plots in Fig. S2 includes all of these formulas, where the symbols in Fig. 5 are differentiated to indicate unique or common molecular formulas. The unique formulas in each sample help to further illustrate the differences between samples (outlined in multiple sections), hence we included two versions of the plot.

Figure 7: it would help explain how the spectra were normalized before the subtraction. The result of the subtraction obviously would depend on the choices made in the normalization.

The normalization procedure and its importance has been expanded upon in the supplemental text (p. S2): "The total ion abundance of the identified monoisotopic molecular formulas reported for each sample was determined by their summation. Then, these values were used to normalize the individual ion abundances within each sample using a ratio of the individual ion intensity to this total ion abundance. Then, the values were rescaled using a normalization constant (10,000). This normalization procedure was done to remove analytical biases introduced by trace contaminants with high electrospray efficiency."

Table 3 and Table S1: it would be useful to specify peak abundance (such as very high, high, medium, minor or something similar). Also, I would point out in the caption that the "identities" specified in one of the columns are for reference only – the fact that formulas match does not mean that this where these compounds came from.

We thank the reviewer for this helpful insight. Table 3 was moved into Table S1. We modified the extended Table S1 to indicate the normalized abundance of each formula. We revised the caption for Table S1 to include additional clarification regarding the nature of molecular formulas vs. chemical structures: "Table S1: Summary of the literature structural insights associated with the identified molecular formulas observed in this study. Because the identified molecular formulas may represent a variety of structural isomers, we note that matched molecular formulas do not necessarily correspond to the same molecular structure or atmospheric origin. The normalized abundances are indicated for each sample, where "ND" (not detected), "Low" (≤ 3%), "Med", (> 3% and ≤ 15%), "High" (> 15% and ≤ 50%) and "Very High" (> 50%). Molecular formulas from the literature are provided with their references." An additional paragraph was added to section 2.4 (p. 6 line 22-24) to further clarify the difference between molecular formulas and chemical structures: "Furthermore, it is important to note that the individual molecular formulas likely represent a mixture of structural isomers co-existing in atmospheric organic matter, as recently observed for deep-sea organic matter (Zark et al., 2017)." We also removed all references to specific IUPAC style chemical compound names, e.g. "2,4-dinitrophenol" was changed to "dinitrophenol" in the discussion of formulas matched to the previous literature.

S2: it states it there that the assignments were cut off above m/z 500 but assigned peaks in figure S3 go beyond 600

We describe the *de novo* cutoff in greater detail in the supplemental text (p. S2), as it does not perform a hard cut off for formulas of *m/z* > 500: "A de novo cut-off at *m/z* 500 was applied, indicating that no new formula assignments would occur above *m/z* 500, unless the formula was part of an existing CH_2 homologous series that began at a point lower than *m/z* 500. This is necessary because the number of possible molecular formulas increases at higher values."

S2: please explain the "rule of 13" – this must be some sort of a mass spectrometry jargon

Descriptions of the rule of 13 and the nitrogen rule, were added to the supplemental text (p. S2): "The rule of 13 checks for a reasonable number of heteroatoms in a formula. A base formula (C_nH_{n+r}) can be generated for any measured mass by solving: $\frac{M}{13} = n + \frac{r}{13}$ (Pavia, 2009). Then, the maximum number of "large atoms" (C, O, N, S) in a formula is defined as the mass divided by 13, because substituting for a heteroatom (O, N or S) involves a substitution for at least one carbon. This maximum number is then compared to the actual number of "large atoms" in a formula, and those formulas exceeding the maximum number are rejected. The nitrogen rule removes formulas with odd masses that do not contain an odd number of nitrogen atoms, and even masses that do not contain an even number (or no) nitrogen atoms; this is due to the odd numbered valence of nitrogen (Pavia, 2009)."

EDITORIAL COMMENTS

P1L34: remove "evolving"

This sentence (now p. 1 line 32-p. 2 line 1) now reads: "Atmospheric organic aerosol particles are comprised of a complex mixture of numerous individual organic compounds, produced by direct

emissions and secondary processes, of which a significant impact is from transformations in the aqueous phase."

P2L7: "and more" -> "and other compounds"

This sentence (now p. 2 line 9-11) now reads: "Biomass burning products include simple organic acids, sugars and anhydrosugars, substituted phenols, polycyclic aromatic hydrocarbons, and other compounds, depending on the type of fuel and burn conditions…"

P2L14: this sentence needs a revision (incompatible list items)

This sentence (now p. 2 line 17-19) now reads: "Atmospheric chemistry models are currently unable to replicate several key aspects of SOA, including SOA concentration levels, chemical oxidation states, degree of functionalization, and the occurrence of high molecular weight compounds, such as atmospheric humic-like substances."

P6L26: "rich of" -> "containing"

This sentence (now p. 7 line 18-20) was changed to use the same consistent descriptor with all portions describing the 3 categories of interest, and now reads: "These categories are: SOA (enriched in acyl groups, H-C-C=O), biomass burning aerosol (enriched in alkoxyls, H-C-O, and aromatics), and marine organic aerosol (enriched in aliphatic groups other than acyls and alkoxyls, mainly amines and sulfoxy groups)."

P10L30: two sets of references need to be joined in one

This paragraph was revised to be easier to understand. The respective set of references have been combined into the new revised paragraph. The paragraph is provided in response to the next comment below.

P10L31: "act" -> "acted"

This entire paragraph was revised for clarity. The revised paragraph (p. 12 line 3-13) now reads: "The unique molecular formulas found in the fresh fog (SPC0106F) were mostly of the $O_{5-13}S$ and $NO_{7-12}S$ subclasses. Organosulfates are known products of aqueous secondary processes, (Darer et al., 2011; Ervens et al., 2011; McNeill, 2015; Schindelka et al., 2013) and nucleation scavenging from the preceding fog nuclei composition likely plays a significant role as well (Darer et al., 2011; Gilardoni et al., 2014; Herckes et al., 2007; Hu et al., 2011). The aromatic organosulfates and nitooxy-organosulfates observed in fresh biomass burning aerosol (Staudt et al., 2014) were not observed here. In general, organosulfates are the products of aqueous-phase SOA reactions which are expected to be enhanced at acidic pH (Ervens et al., 2011; McNeill et al., 2012; Noziere et al., 2010). Because the pH of SPC0106F was only slightly acidic at 5.81, we propose that the formation of these organosulfates may have been promoted by low LWC, and thus relatively high solute concentrations, during the activation of the fog droplets or possibly in the fully formed fog droplets. Organosulfates may also efficiently nucleate droplets, leading to their eventual presence in the fog samples."

Figure 4: the choice of colors makes it hard to differentiate between them

This Figure was revised from a yellow scale, to a more discerning color palette including yellow, blue and red.

Table 2: “mass” -> “molecular weight (g/mol)”

The term “Mass” was changed in the Table to “Molecular weight (Da)” to include the unit. Though the Da unit is numerically equivalent to g mol^{-1}, Da is used more frequently as a unit in mass spectrometry literature.

References:

Cubison, M. J., Ortega, A. M., Hayes, P. L., Farmer, D. K., Day, D., Lechner, M. J., Brune, W. H., Apel, E., Diskin, G. S., Fisher, J. A., Fuelberg, H. E., Hecobian, A., Knapp, D. J., Mikoviny, T., Riemer, D., Sachse, G. W., Sessions, W., Weber, R. J., Weinheimer, A. J., Wisthaler, A., and Jimenez, J. L.: Effects of aging on organic aerosol from open biomass burning smoke in aircraft and laboratory studies, Atmos Chem Phys, 11, 12049-12064, 2011.

Darer, A. I., Cole-Filipiak, N. C., O'Connor, A. E., and Elrod, M. J.: Formation and Stability of Atmospherically Relevant Isoprene-Derived Organosulfates and Organonitrates, Environ Sci Technol, 45, 1895-1902, 2011.

Ervens, B., Turpin, B. J., and Weber, R. J.: Secondary organic aerosol formation in cloud droplets and aqueous particles (aqSOA): a review of laboratory, field and model studies, Atmos Chem Phys, 11, 11069-11102, 2011.

Gilardoni, S., Massoli, P., Giulianelli, L., Rinaldi, M., Paglione, M., Pollini, F., Lanconelli, C., Poluzzi, V., Carbone, S., Hillamo, R., Russell, L. M., Facchini, M. C., and Fuzzi, S.: Fog scavenging of organic and inorganic aerosol in the Po Valley, Atmos Chem Phys, 14, 6967-6981, 2014.

Gilardoni, S., Massoli, P., Paglione, M., Giulianelli, L., Carbone, C., Rinaldi, M., Decesari, S., Sandrini, S., Costabile, F., Gobbi, G. P., Pietrogrande, M. C., Visentin, M., Scotto, F., Fuzzi, S., and Facchini, M. C.: Direct observation of aqueous secondary organic aerosol from biomass-burning emissions, P Natl Acad Sci USA, 113, 10013-10018, 2016.

Herckes, P., Chang, H., Lee, T., and Collett, J. L.: Air pollution processing by radiation fogs, Water Air Soil Poll, 181, 65-75, 10.1007/s11270-006-9276-x, 2007.

Herrmann, H., Schaefer, T., Tilgner, A., Styler, S. A., Weller, C., Teich, M., and Otto, T.: Tropospheric Aqueous-Phase Chemistry: Kinetics, Mechanisms, and Its Coupling to a Changing Gas Phase, Chem Rev, 115, 4259-4334, 2015.

Hertkorn, N., Ruecker, C., Meringer, M., Gugisch, R., Frommberger, M., Perdue, E. M., Witt, M., and Schmitt-Kopplin, P.: High-precision frequency measurements: indispensable tools at the core of the molecular-level analysis of complex systems, Anal Bioanal Chem, 389, 1311-1327, 2007.

Hu, K. S., Darer, A. I., and Elrod, M. J.: Thermodynamics and kinetics of the hydrolysis of atmospherically relevant organonitrates and organosulfates, Atmos Chem Phys, 11, 8307-8320, 2011.

Kroll, J. H., Donahue, N. M., Jimenez, J. L., Kessler, S. H., Canagaratna, M. R., Wilson, K. R., Altieri, K. E., Mazzoleni, L. R., Wozniak, A. S., Bluhm, H., Mysak, E. R., Smith, J. D., Kolb, C. E., and Worsnop, D. R.: Carbon oxidation state as a metric for describing the chemistry of atmospheric organic aerosol, Nat Chem, 3, 133-139, 2011.

McNeill, V. F., Woo, J. L., Kim, D. D., Schwier, A. N., Wannell, N. J., Sumner, A. J., and Barakat, J. M.: Aqueous-Phase Secondary Organic Aerosol and Organosulfate Formation in Atmospheric Aerosols: A Modeling Study, Environ Sci Technol, 46, 8075-8081, 2012.

McNeill, V. F.: Aqueous Organic Chemistry in the Atmosphere: Sources and Chemical Processing of Organic Aerosols, Environ Sci Technol, 49, 1237-1244, 10.1021/es5043707, 2015.

Noziere, B., Ekstrom, S., Alsberg, T., and Holmstrom, S.: Radical-initiated formation of organosulfates and surfactants in atmospheric aerosols, Geophys Res Lett, 37, 2010.

Pavia, D., Lampman, G., Kriz, G., Vyvyan, J.: Introduction to Spectroscopy, 4th ed., Brooks/Cole, Cengage Learning, 656 pp., 2009.

Schindelka, J., Iinuma, Y., Hoffmann, D., and Herrmann, H.: Sulfate radical-initiated formation of isoprene-derived organosulfates in atmospheric aerosols, Faraday Discuss, 165, 237-259, 2013.

Schmitt-Kopplin, P., Gelencser, A., Dabek-Zlotorzynska, E., Kiss, G., Hertkorn, N., Harir, M., Hong, Y., and Gebefugi, I.: Analysis of the Unresolved Organic Fraction in Atmospheric Aerosols with

Ultrahigh-Resolution Mass Spectrometry and Nuclear Magnetic Resonance Spectroscopy: Organosulfates As Photochemical Smog Constituents, Anal Chem, 82, 8017-8026, 2010.

Staudt, S., Kundu, S., Lehmler, H. J., He, X. R., Cui, T. Q., Lin, Y. H., Kristensen, K., Glasius, M., Zhang, X. L., Weber, R. J., Surratt, J. D., and Stone, E. A.: Aromatic organosulfates in atmospheric aerosols: Synthesis, characterization, and abundance, Atmos Environ, 94, 366-373, 2014.

Zark, M., Christoffers, J., and Dittmar, T.: Molecular properties of deep-sea dissolved organic matter are predictable by the central limit theorem: Evidence from tandem FT-ICR-MS, Mar Chem, 191, 9-15, 10.1016/j.marchem.2017.02.005, 2017.

Author responses to comments from RC2 are given below in blue font. The original referee comments are provided in *black italicized font.*

This manuscript presents molecular-level analyses of fresh versus aged fog and samples influenced by biomass burning. The authors aim to explore the potential importance of aqueous phase processing on alteration of organic matter chemical compositions. The authors reported that aged aerosols and fresh fog samples show similarity in composition, indicating the possibility of aged aerosols that served as fog nuclei. One of my major concerns for this manuscript is that the authors attributed the CHON and CHOS compounds exclusively to organonitrates and organosulfates based on FT–ICR MS analyses, but this is not supported by NMR spectra! This seems to be a major finding but it was not discussed in great detail. It looks to me that other types of organic nitrogen and organosulfur compounds may contribute to formation of detected CHON and CHOS that need further investigations. In addition, nitro groups (R-NO2) and nitrooxy groups (R-ONO2) are different. They have distinct formation processes and physiochemical properties as well (e.g., lifetime against hydrolysis). The authors need to be clear when discussing their findings in context of literature.

For the results and discussion, the current form of manuscript is a bit lengthy and repetitive when reporting the FT-ICR MS data. A more concise presentation will greatly improve the readers' reading experience. Also, reactions in aerosol liquid water content and in fog should be discussed separately. Based on the results presented (with only 1 sample in each category), the aqueous processing does alter the chemical compositions of organic matter, but the pathways are rather inconclusive.

Overall, this is still a nice case study that provides useful information. Below I provide a few more specific comments for the authors' consideration and clarification.

We thank the referee for their helpful comments. As suggested, we made several edits to improve the readability and reduce redundancies in the manuscript. We also clarified the comparisons of fresh fog to aged fog compositions and fresh aerosol to aged aerosol compositions (Sections 3.3.3 and 3.3.4 respectively). Another comparison between the two types of samples was made because of the interesting observation of similar compositions between the aged aerosol and the fresh fog. It is plausible that some reactions in aerosol liquid water may also occur during fog activation as droplets begin to grow, helping to explain the similar compositions between these two samples of different types.

The results of the ^{1}H-NMR and FT-ICR MS measurements are only apparently in contradiction. While the ^{1}H-NMR analyses were performed on bulk aqueous samples, the electrospray ionization FT-ICR MS analysis requires the removal of inorganic ions present in the bulk aqueous extracts. Reversed phase SPE cartridges were used to isolate the water-soluble organic aerosol components. However, some losses of low molecular weight and ionic water-soluble organic compounds are expected. This may have included the low-molecular weight alkyl amines observed by ^{1}H-NMR analysis. Furthermore, the negative ion electrospray favors the detection of acidic compounds and thus is not ideal for the detection of reduced nitrogen or sulfur compounds. A statement was added to the end of section 2.4 (p. 6 line 19-22) to clarify this: "The resulting data set represents the SPE-recovered higher molecular weight water soluble organic aerosol and is expected to predominantly contain acidic compounds due to the negative ion ESI analytical bias. The observed molecular compositions represent the oxidized fraction of the atmospheric samples thus, useful insights can be made with these limitations in mind."

The concern as to whether the ^{1}H-NMR data actually support the hypothesis of the occurrence of organic nitrates and organic sulfates in these samples can be reassured by the clear signals in the spectral regions where aliphatic hydrogen atoms in alpha position to such functional groups are expected to occur (specifically between 4 and 5 ppm chemical shift, as described by Hsieh et al. (2014)). However, it is not as clear as to whether the ^{1}H-NMR analysis provides the same information on the relative abundance of organic nitrates and organic sulfates between samples as derived from the FT-ICR MS datasets, as the same spectral region can host many other possible functionalities (e.g., esters, peroxides, hydroxy-carboxylic acids). In summary, ^{1}H-NMR spectroscopy was not specific enough to trace the abundance of organic nitrates and sulfates in these samples in a useful manner for comparison with the FT-ICR MS data. The N and S containing molecular formulas observed with FT-ICR were attributed to organonitrates, organosulfates and nitrooxy-organosulfates, based on a previous study using negative mode electrospray ionization and MS/MS analysis for functional group determination of water-soluble atmospheric organic matter (LeClair et al., 2012), and the observed O:N and O:S ratios, which we clarified in the text.

Specific Comments:

1) Page 4, lines 7-9: The aerosol filter extracts were filtered with 0.45 um PTFE membrane, while the fog water was filtered through 47 mm quartz fiber filters. What is the pore size of 47 mm quartz fiber filters? Why did the authors use two different filtering methods here? Since the FT–ICR MS analysis is very sensitive, potential artifacts (even trace amounts) during sample preparation should be avoided.

These method differences result from the laboratory methods for the different analysis techniques. Aerosol filter extractions were performed at Michigan Tech (MTU) for FT-ICR analysis (Section 2.4) and at the Institute of Atmospheric Sciences and Climate (CNR-ISAC) for total carbon, ^{1}H-NMR analysis and HR-ToF-AMS analysis for fog samples (Section 2.1). Fog and aerosol samples prepared at MTU for FT-ICR analysis were prepared consistently with 25 mm quartz fiber filters, as described in section 2.4. We are not aware of a uniform pore size for quartz fiber filters, due to the nature of the material. Sample blanks were used to correct for artifacts that may have been introduced by the quartz fiber filter due to the sensitivity of FT-ICR MS. Additional statements were added to section 2.1 (p. 4 line 18-25): "The aerosol filters were extracted with deionized ultra-pure water (Milli-Q) in an ultrasonic bath for 1 h. The water extract was filtered with a 0.45 µm PTFE membrane in order to remove suspended particles. Fog water was filtered through 47 mm quartz fiber filters within a few hours of collection and conductivity and pH measurements were taken ... Aliquots of both aerosol water extracts and fog water prepared in this way were used to determine the total organic carbon content … and water soluble organic carbon (WSOC) concentration, (Rinaldi et al., 2007) as well as for ^{1}H-NMR analysis and HR-ToF-AMS analysis of fog samples described below (HR-ToF-AMS data for aerosol samples was collected in real time)." and 2.4 (p. 5 line 22-24): "Fog samples were later re-filtered using a 25 mm quartz filter before SPE. A portion of the aerosol filter samples were extracted with ultrapure water using sonication and the extracts were then filtered using a 25 mm quartz filter to remove insoluble materials…" to clarify these differences in methods.

2) Page 7, line 6: Does "SOA-like" mean oxygenated/or functionalized/or fragmented? It is not clear here.

We have revised the text to more accurately convey that the fog compositions were more oxidized, and thus more similar to SOA than the aerosols, according to the simplified source attribution scheme of Fig. 1. The text was changed to reflect this in the abstract (p.1 line 25-27): "Fog compositions were more

oxidized and "SOA-like" than aerosols as indicated by their NMR measured acyl vs alkoxyl ratios and the observed molecular formula similarity between the aged aerosol and fresh fog, implying that fog nuclei must be somewhat aged." In the ^{1}H-NMR discussion (p. 8 line 3-5): "So, according to the simple source-attribution scheme based on the major ^{1}H-NMR functionalities presented here, the fog compositions were more oxidized and "SOA-like" than aerosols." And in the conclusions (p. 14 line 18-20): "Overall, the fog composition was generally more oxidized and "SOA-like" than the aerosol, where the fresh fog composition was similar to the aged aerosol composition in both the ^{1}H-NMR analysis and the molecular formula trends."

3) Page 10, lines 25-35: Since aged aerosols could act as fog nuclei, scavenging of organosulfates resided in aged aerosols into fog might have contributed to the observed organosulfates in fresh fog water. Based on the data presented, I don't really see direct evidence here showing that aqueous processing leads to CHOS production. Similarly, on Page 13 lines 12-17: the authors concluded that the current data provide strong evidence of aqueous processing that dominates the production of S-containing organic matter. I would tone down this statement.

We have revised this paragraph to include statements on nucleation scavenging. The revised paragraph (p. 12 line 3-13) now reads: "The unique molecular formulas found in the fresh fog (SPC0106F) were mostly of the $O_{5-13}S$ and $NO_{7-12}S$ subclasses. Organosulfates are known products of aqueous secondary processes, (Darer et al., 2011; Ervens et al., 2011; McNeill, 2015; Schindelka et al., 2013) and nucleation scavenging from the preceding fog nuclei composition likely plays a significant role as well (Darer et al., 2011; Gilardoni et al., 2014; Herckes et al., 2007; Hu et al., 2011). The aromatic organosulfates and nitooxy-organosulfates observed in fresh biomass burning aerosol (Staudt et al., 2014) were not observed here. In general, organosulfates are the products of aqueous-phase SOA reactions which are expected to be enhanced at acidic pH (Ervens et al., 2011; McNeill et al., 2012; Noziere et al., 2010). Because the pH of SPC0106F was only slightly acidic at 5.81, we propose that the formation of these organosulfates may have been promoted by low LWC, and thus relatively high solute concentrations, during the activation of the fog droplets or possibly in the fully formed fog droplets. Organosulfates may also efficiently nucleate droplets, leading to their eventual presence in the fog samples."

The conclusion statement (now p. 14 line 21-23) was revised to the following: "CHOS and CHNOS formulas were detected with high frequencies in samples with high water content during collection (all samples except BO0204N). This supports an enhanced production of S-containing SOA species via reactions in the aqueous phase."

4) Page 12, line 32: "hygroscopic" is a better term to describe aged/oxygenated organics that contribute to droplet formation.

This sentence (now p. 14 line 4-5) now reads: "Hygroscopic species are expected to enhance droplet formation, indicating that organics acting as fog nuclei must be somewhat aged."

5) Page 13, lines 8-9: it is confusing when the authors stated "some evidence of dimerization" here. This was not presented in "results and discussion" but suddenly mentioned in summary.

We have revised the text to remove all references to dimerization.

References:

Darer, A. I., Cole-Filipiak, N. C., O'Connor, A. E., and Elrod, M. J.: Formation and Stability of Atmospherically Relevant Isoprene-Derived Organosulfates and Organonitrates, Environ Sci Technol, 45, 1895-1902, 2011.

Ervens, B., Turpin, B. J., and Weber, R. J.: Secondary organic aerosol formation in cloud droplets and aqueous particles (aqSOA): a review of laboratory, field and model studies, Atmos Chem Phys, 11, 11069-11102, 2011.

Gilardoni, S., Massoli, P., Giulianelli, L., Rinaldi, M., Paglione, M., Pollini, F., Lanconelli, C., Poluzzi, V., Carbone, S., Hillamo, R., Russell, L. M., Facchini, M. C., and Fuzzi, S.: Fog scavenging of organic and inorganic aerosol in the Po Valley, Atmos Chem Phys, 14, 6967-6981, 2014.

Herckes, P., Chang, H., Lee, T., and Collett, J. L.: Air pollution processing by radiation fogs, Water Air Soil Poll, 181, 65-75, 10.1007/s11270-006-9276-x, 2007.

Hsieh, P. H., Xu, Y. M., Keire, D. A., and Liu, J.: Chemoenzymatic synthesis and structural characterization of 2-O-sulfated glucuronic acid-containing heparan sulfate hexasaccharides, Glycobiology, 24, 681-692, 10.1093/glycob/cwu032, 2014.

Hu, K. S., Darer, A. I., and Elrod, M. J.: Thermodynamics and kinetics of the hydrolysis of atmospherically relevant organonitrates and organosulfates, Atmos Chem Phys, 11, 8307-8320, 2011.

LeClair, J. P., Collett, J. L., and Mazzoleni, L. R.: Fragmentation Analysis of Water-Soluble Atmospheric Organic Matter Using Ultrahigh-Resolution FT-ICR Mass Spectrometry, Environ Sci Technol, 46, 4312-4322, 2012.

McNeill, V. F., Woo, J. L., Kim, D. D., Schwier, A. N., Wannell, N. J., Sumner, A. J., and Barakat, J. M.: Aqueous-Phase Secondary Organic Aerosol and Organosulfate Formation in Atmospheric Aerosols: A Modeling Study, Environ Sci Technol, 46, 8075-8081, 2012.

McNeill, V. F.: Aqueous Organic Chemistry in the Atmosphere: Sources and Chemical Processing of Organic Aerosols, Environ Sci Technol, 49, 1237-1244, 10.1021/es5043707, 2015.

Noziere, B., Ekstrom, S., Alsberg, T., and Holmstrom, S.: Radical-initiated formation of organosulfates and surfactants in atmospheric aerosols, Geophys Res Lett, 37, 2010.

Rinaldi, M., Emblico, L., Decesari, S., Fuzzi, S., Facchini, M. C., and Librando, V.: Chemical characterization and source apportionment of size-segregated aerosol collected at an urban site in sicily, Water Air Soil Poll, 185, 311-321, 2007.

Schindelka, J., Iinuma, Y., Hoffmann, D., and Herrmann, H.: Sulfate radical-initiated formation of isoprene-derived organosulfates in atmospheric aerosols, Faraday Discuss, 165, 237-259, 2013.

Staudt, S., Kundu, S., Lehmler, H. J., He, X. R., Cui, T. Q., Lin, Y. H., Kristensen, K., Glasius, M., Zhang, X. L., Weber, R. J., Surratt, J. D., and Stone, E. A.: Aromatic organosulfates in atmospheric aerosols: Synthesis, characterization, and abundance, Atmos Environ, 94, 366-373, 2014.

Molecular insights on aging and aqueous phase processing from ambient biomass burning emissions-influenced Po Valley fog and aerosol

Matthew Brege[1], Marco Paglione[2], Stefania Gilardoni[2], Stefano Decesari[2], Maria Cristina Facchini[2], and Lynn R. Mazzoleni[1,3]

[1]Department of Chemistry, Michigan Technological University, Houghton, MI, USA.
[2]Institute of Atmospheric Sciences and Climate, Italian National Research Council, Bologna, Italy.
[3]Atmospheric Sciences Program, Michigan Technological University, Houghton, MI, USA.

Correspondence to: Lynn R. Mazzoleni (lrmazzol@mtu.edu)

Abstract. To study the influence of regional biomass burning emissions and secondary processes, ambient samples of fog and aerosol were collected in the Po Valley (Italy) during the 2013 Supersito field campaign. After the extent of "fresh" *vs.* "aged" biomass burning influence was estimated from proton nuclear magnetic resonance (^{1}H-NMR) and high resolution time of flight aerosol mass spectrometry (HR-ToF-AMS), two samples of fog water and two samples of PM_1 aerosol were selected for ultrahigh resolution Fourier transform ion cyclotron resonance mass spectrometry (FT-ICR MS) analysis. Molecular compositions indicated that the water-soluble organic matter was largely non-polymeric without clearly repeating units. The selected samples had an atypically large frequency of molecular formulas containing nitrogen and sulfur (not evident in the NMR composition) attributed to multifunctional organonitrates and organosulfates. Higher numbers of organonitrates were observed in aerosol, and higher numbers of organosulfates were observed in fog water. Consistent with the observation of an enhanced aromatic proton signature in the ^{1}H-NMR analysis, the average molecular formula double bond equivalents and carbon numbers were higher in the "fresh" biomass burning influenced samples. The average O:C and H:C values from FT-ICR MS were higher in the samples with an "aged" influence (O:C = 0.50-0.58 and H:C = 1.31-1.37) compared to those with "fresh" influence (O:C = 0.43-0.48 and H:C = 1.13-1.30). The "aged" fog had a large set of unique highly oxygenated CHO fragments in the HR-ToF-AMS, which reflects an enrichment of carboxylic acids and other compounds carrying acyl groups, highlighted by the NMR analysis. Fog compositions were more oxidized and "SOA-like" than aerosols as indicated by their NMR measured acyl vs alkoxyl ratios and the observed molecular formula similarity between the aged aerosol and fresh fog, implying that fog nuclei must be somewhat aged. Overall, functionalization with nitrate and sulfate moieties, in addition to aqueous oxidation, trigger an increase in the molecular complexity in this environment, which is apparent in the FT-ICR MS results. This study demonstrates the significance of the aqueous phase to transform the molecular chemistry of atmospheric organic matter and contribute to secondary organic aerosol.

1. Introduction

Atmospheric organic aerosol particles are comprised of a complex mixture of numerous individual organic compounds, produced by direct emissions and secondary processes, of which a significant impact is from

Formatted: Left: 1", Right: 1", Top: 1", Bottom: 1"
Formatted: English (US)
Deleted: Atmospheric organic matter is a complex mixture of thousands of individual organic compounds originating from a combination of primary emissions and secondary processes.
Formatted: English (US)
Deleted:) observations,
Formatted: English (US)
Deleted: Over 4300 distinct molecular formulas were assigned to electrospray ionization FT-ICR MS anions and were sorted into four elemental groups (CHO, CHNO, CHOS and CHNOS) and 64 subclasses. Molecular weight distributions
Formatted: English (US)
Deleted: , although some evidence of dimerization was observed for C_{10} compounds and especially for $C_{8\text{-}9}$ CHNO species in the "aged" aerosol.
Formatted: English (US)
Deleted: While higher
Formatted: English (US)
Deleted: (dry or deliquesced particles),
Formatted: English (US)
Deleted: mostly found
Formatted: English (US)
Deleted: , and so chemical reactions promoted by liquid water must be postulated for their formation
Formatted: English (US)
Deleted: , whereas the
Formatted: English (US)
Deleted: >
Formatted: English (US)
Deleted: 6
Formatted: English (US)
Deleted: >
Formatted: English (US)
Deleted: 2).
Formatted: English (US)
Formatted: English (US)
Deleted: mass spectra
Formatted: English (US)
Deleted: as
Formatted: English (US)
Formatted: English (US)
Formatted: English (US)
Formatted: English (US)
Deleted: evolving
Formatted: English (US)

transformations in the aqueous phase. Surface emitted primary organic aerosol and volatile organic compounds are transformed in the atmosphere by gas to particle phase conversion, heterogeneous reactions, and aqueous phase reactions in aerosol water, fog, and cloud droplets (Ervens et al., 2011; Herrmann et al., 2015). The products of these processes are collectively referred to as secondary organic aerosol (SOA). These aging reactions happen quickly in the atmosphere, and the observed mass fraction of SOA is larger than that of primary organic aerosol (Zhang et al., 2007; Ervens et al., 2011; Zhang et al., 2011; Paglione et al., 2014; Gilardoni et al., 2016). Biomass burning emissions, such as those from forest fires, agricultural land clearing, residential heating, and cooking with biofuels, are important sources of organic carbon to the atmosphere globally (Andreae and Merlet, 2001; Bond et al., 2004; Glasius et al., 2006; Laskin et al., 2015). Biomass burning products include simple organic acids, sugars and anhydrosugars, substituted phenols, polycyclic aromatic hydrocarbons, and other compounds, depending on the type of fuel and burn conditions (Mazzoleni et al., 2007; Pietrogrande et al., 2014a; Pietrogrande et al., 2014b; Gilardoni et al., 2016). These water-soluble emissions can serve as precursors for SOA once dissolved in the aqueous phase (Chang and Thompson, 2010; Yu et al., 2014; Yu et al., 2016), and upwards of 50% of organic matter in fog and cloud droplets remains unidentified (Herckes et al., 2013). Biomass burning emissions can even facilitate droplet nucleation. In fact, laboratory studies indicate that in addition to hydrophilic species, even refractory "tar balls," emitted from smoldering biomass burning begin to absorb water at high relative humidity (Hand et al., 2005; Laskin et al., 2015).

Atmospheric chemistry models are currently unable to replicate several key aspects of SOA, including SOA concentration levels, chemical oxidation states, degree of functionalization, and the occurrence of high molecular weight compounds, such as atmospheric humic-like substances (Ervens et al., 2011; Lee et al., 2013; Nguyen et al., 2013). Aqueous phase reactions in wet aerosol, cloud, and fog droplets have been proposed to improve these SOA observation gaps (Ervens et al., 2011; Gilardoni et al., 2016; Herckes et al., 2013; Laskin et al., 2015), but the current level of understanding regarding aqueous phase processes is insufficient to include them in models. Laboratory studies focusing on simplified systems of only one or two precursor components have successfully recreated some of the complexity of ambient atmospheric samples (De Haan et al., 2011; Lee et al., 2013; Nguyen et al., 2013; Hawkins et al., 2016; Yu et al., 2016). A number of recent studies focusing on the molecular composition of cloud (Lee et al., 2012; Desyaterik et al., 2013; Pratt et al., 2013; Zhao et al., 2013; Boone et al., 2015; Cook et al., 2017) and fog (Mazzoleni et al., 2010; LeClair et al., 2012; Xu et al., 2017) chemistry have been recently reported. Together these studies indicate a clear importance of aqueous phase reactions for the production of aqueous SOA, including the formation of organonitrates, organosulfates, and nitrooxy-organosulfates. Of these, organosulfate formation is thought to happen nearly exclusively in the aqueous phase (Ervens et al., 2011; Herrmann et al., 2015). Along with organonitrates, organosulfates are susceptible to hydrolysis in the aqueous phase, though high kinetic barriers under atmospheric conditions often slow these reactions and allow for the observation of these species in ambient samples (Darer et al., 2011; Hu et al., 2011). Organosulfates are often described in the literature as the products of acid catalyzed oxidation of biogenic terpenoids (Surratt et al., 2008; Pratt et al., 2013; Schindelka et al., 2013), but have also been observed in biomass combustion influenced cloud water (Zhao et al., 2013; Cook et al., 2017). The formation of aqueous phase products in aerosol, fog and cloud waters, greatly increase the complexity of organic aerosol. Although several analytical techniques have been used to address the challenge of resolving the complex mixture of

Formatted ... [1]
Deleted: , forest fires
Formatted ... [2]
Deleted: and dicarboxylic acids
Formatted: English (US)
Deleted: more
Formatted ... [3]
Deleted: ,
Formatted ... [4]
Deleted: Due
Formatted: English (US)
Deleted: their complexity,
Formatted: English (US)
Deleted: concentrations
Formatted ... [5]
Deleted: , are poorly represented in atmospheric chemistry models.
Formatted: English (US)
Deleted: the
Formatted ... [6]
Deleted: ; Gilardoni et al., 2016
Formatted ... [7]

atmospheric organic matter (Decesari et al., 2007; Hertkorn et al., 2007; Nizkorodov et al., 2011; Desyaterik et al., 2013; Dall'Osto et al., 2015; Noziere et al., 2015; Laskin et al., 2016; Willoughby et al., 2016), no universal analytical method exists.

The Po Valley (Italy) has ideal ambient conditions to study aqueous phase influences on atmospheric organic matter. The valley contains a mixture of densely populated areas and intensively cultivated agricultural regions. Surrounded by mountains to the north, west and south, the valley frequently has stable meteorological conditions with low ventilation and a low boundary layer, allowing for the accumulation of high concentrations of regional pollutants. Consequently, frequent fog events and high concentrations of anthropogenic biomass burning emissions are observed in months with cold temperatures (Larsen et al., 2012; Saarikoski et al., 2012; Giulianelli et al., 2014; Paglione et al., 2014; Gilardoni et al., 2016). The Po Valley has some of the highest reported carbon concentrations for fog water in the world (Herckes et al., 2013). In recent years, the analysis of fog water and aerosol from San Pietro Capofiume (SPC) (located 30 km northeast of the city of Bologna) has included Aerodyne high resolution time-of-flight aerosol mass spectrometry (HR-ToF-AMS) and proton nuclear magnetic resonance spectroscopy (^{1}H-NMR) to determine the fog scavenging efficiency of aerosol (Gilardoni et al., 2014) and source apportionment of aerosol (Decesari et al., 2007). In Saarikoski et al. (2012), HR-ToF-AMS data from SPC aerosol showed an extremely high concentration of aerosol nitrate (39%) and a somewhat typical concentration of organic carbon (33%) in agreement with Gilardoni et al. (2014). Positive matrix factorization (PMF) of HR-ToF-AMS organic mass fragments was used to identify several factors describing Po Valley organic aerosol, including factors for fresh biomass burning organic aerosol, and three types of oxygenated organic aerosol (Saarikoski et al., 2012). A similar study by Paglione et al. (2014) used PMF on ^{1}H-NMR data of SPC aerosol to identify factors for fresh biomass burning emissions, as well as SOA factors, including products formed from aged biomass burning emissions.

Further investigation with a focus on molecular markers and source apportionment was done as part of the Supersito 2013 field campaign in the Emilia-Romagna region, including samples from SPC and the urban site of Bologna (Pietrogrande et al., 2014a; Pietrogrande et al., 2014b; Poluzzi et al., 2015). The campaign has shown the significance of biomass burning emissions in the region. Approximately 35% of the organic carbon was from wood burning in winter months (Pietrogrande et al., 2015), biomass burning emissions were shown to increase with decreasing ambient temperature (Gilardoni et al., 2014), and aqueous phase SOA formation from biomass burning emissions and associated brown carbon formation was directly observed (Gilardoni et al., 2016). HR-ToF-AMS observations have shown similarity between atmospheric organic matter in fog water and aerosol formed following fog dissipation, indicating low volatility organics that were originally present in the fog are left behind upon evaporation; these particles are enriched in oxidized organic matter, and absorb solar radiation more efficiently than fresh emissions, contributing to atmospheric brown carbon (Gilardoni et al., 2016).

In this study, we analyzed fog from SPC and aerosol from Bologna, collected during the 2013 Supersito field campaign. Due to the intense time investment required for FT-ICR MS data analysis, we chose to focus our detailed analysis on a subset of samples, including two aerosol and two fog samples. The subset was selected to represent the influence of fresh and aged biomass burning emissions on fog and aerosol based on the HR-ToF-AMS and ^{1}H-NMR observations (Section 3.1). We used a combination of ^{1}H-NMR, HR-ToF-AMS and FT-ICR MS techniques to explore

Formatted ... [8]
Formatted ... [9]
Deleted: Ambient
Formatted ... [10]
Deleted: ideal for observations of the
Formatted ... [11]
Deleted: contributions to
Formatted ... [12]
Deleted: exist in the Po Valley (Italy).
Formatted ... [13]
Deleted: The valley contains a mixture of dense population areas
Formatted ... [14]
Formatted ... [15]
Formatted ... [16]
Formatted ... [17]
Formatted ... [18]
Formatted ... [19]
Deleted: ;
Formatted ... [20]
Formatted ... [21]
Formatted ... [22]
Formatted ... [23]
Formatted ... [24]
Formatted ... [25]
Formatted ... [26]
Formatted ... [27]
Formatted ... [28]
Formatted ... [29]
Deleted: .
Formatted ... [30]
Formatted ... [31]
Formatted ... [32]
Formatted ... [33]
Formatted ... [34]
Formatted ... [35]
Formatted ... [36]
Formatted ... [37]
Formatted ... [38]
Formatted ... [39]
Formatted ... [40]
Formatted ... [41]
Formatted ... [42]
Deleted: the
Formatted ... [43]
Deleted: which revealed detailed chemical information about

the molecular level details of the complex mixtures of atmospheric organic matter in the Po Valley. Similar studies focusing on analysis of atmospheric samples with ^{1}H-NMR and FT-ICR MS have been conducted in the past (Schmitt-Kopplin et al., 2010; Willoughby et al., 2016), but so far, this type of study with a focus on biomass burning and aqueous phase processing has not been previously reported.

2. Methods

2.1 Sample collection and chemical analysis

Sub-micrometer (PM_1) aerosol particles were collected in Bologna on pre-washed and pre-baked quartz fiber filters (PALL, 18 cm diameter) by a High-Volume Sampler (TECORA Echo Hi Vol) equipped with a digital PM_1 sampling inlet, at a nominal flow rate of 500 L min^{-1}. PM_1 samples were collected during winter 2013 (from 4 February 2013 to 15 February 2013), during the Supersito project. Fog water was collected at the SPC field station, where monitoring of fog occurrence and fog water collection has been performed every year systematically since 1989 (Giulianelli et al., 2014); during the 2013 winter fog samples were collected from 29 November 2012 to 12 March 2013. In the fog collector (Fuzzi et al., 1997), a short wind tunnel is created by a rear fan, where an air stream containing fog droplets are collected by impaction using a series of stainless steel strings. The collected droplets drain off the strings into a sampling bottle. The air flow through the tunnel was 17 m^3 min^{-1} with a 50% collection efficiency for individual strings (3 µm radius each). All parts of the fog collector coming into contact with the fog droplets, were made of stainless steel to avoid sampling artifacts from adsorption of organic compounds to the surfaces.

The aerosol filters were extracted with deionized ultra-pure water (Milli-Q) in an ultrasonic bath for 1 h. The water extract was filtered with a 0.45 µm PTFE membrane in order to remove suspended particles. Fog water was filtered through 47 mm quartz fiber filters within a few hours of collection and conductivity and pH measurements were taken (Crison microCM 2201 conductimeter and Crison micropH 2002 pH meter). Aliquots of both aerosol water extracts and fog water prepared in this way were used to determine the total organic carbon content (Multi N/C 2100 analyzer; Analytik Jena, Germany) and water soluble organic carbon (WSOC) concentration (Rinaldi et al., 2007), as well as for ^{1}H-NMR analysis and HR-ToF-AMS analysis of fog samples described below (HR-ToF-AMS data for aerosol samples was collected in real time).

2.2 ^{1}H-NMR analysis

Aliquots of the aerosol extract and fog water were dried under vacuum and re-dissolved in deuterium oxide (D_2O) for organic functional groups characterization by ^{1}H-NMR spectroscopy, as described in Decesari et al. (2000). The ^{1}H-NMR spectra were acquired at 600 MHz (Varian Unity INOVA spectrometer) with a 5 mm probe. Sodium 3-trimethylsilyl-(2,2,3,3-d4) propionate (TSP-d4) was used as an internal standard by adding 50 µl of a 0.05% TSP-d4 (by weight) in D_2O to the standard in the probe. The speciation of hydrogen atoms bound to carbon atoms can be provided by ^{1}H-NMR spectroscopy in protic solvents, on the basis of the range of frequency shifts, the signal can be attributed to H-C containing specific functionalities (Decesari et al., 2000; Decesari et al., 2007). Detection limits for an average sampling volume of 500 m^3 were of the order of 3 nmol m^{-3} for each functional group. ^{1}H-NMR spectra

Deleted: Molecular insights on aging and aqueous phase processing were gathered from the variations in the detailed molecular composition from ultrahigh resolution FT-ICR MS measurements within the chemical context provided by the ^{1}H-NMR, HR-ToF-AMS, and other measurements.
Formatted: English (US)
Formatted: English (US)
Formatted: English (US)
Formatted: English (US)
Deleted: -
Formatted: English (US)
Deleted: in the framework of
Formatted: English (US)
Deleted: from November to March
Formatted: English (US)
Formatted: English (US)
Formatted: English (US)
Deleted: , more than 20
Formatted: English (US)
Formatted: English (US)
Formatted: English (US)
Formatted: English (US)
Formatted: English (US)
Formatted: English (US)
Deleted: .
Formatted: English (US)
Deleted: →
Formatted: English (US)
Formatted: English (US)
Formatted: English (US)
Formatted: English (US)
Formatted: English (US)
Deleted: For more than a decade, ^{1}H-NMR has been used for the characterization of organic aerosol.
Formatted: English (US)
Deleted: A total of 21 fog and 18 aerosol
Formatted: English (US)

were collected during the winter 2013 campaign using the method described above to identify and quantify major components of WSOC in both fog and aerosol. In the present study, the results of these ^{1}H-NMR analyses were used to characterize and to select the samples for subsequent FT-ICR MS analysis as described in section 3.1.

2.3 HR-ToF-AMS analysis

During the Supersito winter 2013 campaign (4 February 2013 to 15 February 2013) the chemical composition of PM_1 aerosol particles at Bologna was characterized with a 5 minute-time resolution using an HR-ToF-AMS (Aerodyne Research (DeCarlo et al., 2006)). Data was collected in the V-ion mode, at a resolution of 2,200. The influx of aerosol particles was dried below 30% relative humidity with a Nafion drier before analysis. Details on analysis of HR-ToF-AMS data for the Supersito winter 2013 campaign were previously reported (Gilardoni et al., 2016); here we report HR-ToF-AMS characterization averaged over the sampling periods of the selected aerosol samples.

Fog water samples were also analyzed by HR-ToF-AMS after being re-aerosolized (TSI constant output atomizer, Model #3076) in an inert argon gas flow, to characterize dissolved water-soluble organics. To make sure that the re-aerosolized fog water represented the original sample, we verified that the nitrate-to-organic carbon and the sulfate-to-organic carbon ratios from the HR-ToF-AMS analysis were within 20% (measurement uncertainty level) of the ratios measured off-line by ion chromatography and thermo-optical analysis.

2.4 Ultrahigh resolution FT-ICR MS analysis

Four samples were selected for FT-ICR MS analysis based on the characterization by HR-ToF-AMS data and ^{1}H-NMR spectra for the entire Supersito winter 2013 sample set (Section 3.1). High molecular weight WSOC compounds were prepared for FT-ICR MS analysis using a polymeric reversed phase solid phase extraction (SPE) cartridge (Strata-X, Phenomenex) to remove salts and low molecular weight compounds which interfere with electrospray ionization (ESI). The cartridges were loaded with HCl acidified aqueous samples (pH < 2), rinsed with 1 mL of water, and then eluted using 2 mL of ACN:H_2O (90:10 by volume). Fog samples were later re-filtered using a 25 mm quartz filter before SPE. A portion of the aerosol filter samples were extracted with ultrapure water using sonication and the extracts were then filtered using a 25 mm quartz filter to remove insoluble materials; the aerosol extracts were then prepared for FT-ICR MS analysis using SPE as described above. The WSOC described in this paper is operationally defined as the WSOC that is both retained and recovered from the SPE cartridges (SPE-recovered), thus it is not equivalent with the total WSOC. The ACN:H_2O extracts were analyzed at the Woods Hole Oceanographic Institute in Woods Hole, MA, using full-scan ESI ultrahigh-resolution FT-ICR MS (7T LTQ FT-ICR MS, Thermo Scientific) at a resolving power of 400,000 as described in our previous work (Zhao et al., 2013; Dzepina et al., 2015). We used direct infusion analysis to collect mass spectrometry data over the mass range of *m/z* 100-1000 in the negative ionization mode, for approximately 200 scans. Molecular formulas were assigned as previously described in our work (Dzepina et al., 2015; Mazzoleni et al., 2010; Putman et al., 2012; Zhao et al., 2013) using Sierra Analytics Composer software (version 1.0.5) within the limits of $C_{2\text{-}200}H_{4\text{-}1000}O_{1\text{-}20}N_{0\text{-}3}S_{0\text{-}1}$. The formulas were reviewed manually for their credibility; for further details, see the Supplemental Text. Approximately 74% of the measured masses in each of the samples were assigned a molecular formula. Oxygen to carbon (O:C) and hydrogen

Deleted: ;
Deleted: was used
Formatted: English (US)
Formatted: English (US)
Deleted: .
Formatted: English (US)
Deleted: submicron
Formatted: English (US)
Formatted: English (US)
Formatted: English (US)
Formatted: English (US)
Formatted: English (US)
Formatted: English (US)
Deleted: with
Formatted: English (US)
Formatted: English (US)
Formatted: English (US)
Formatted: English (US)
Formatted: English (US)
Deleted: ; Dzepina et al., 2015
Formatted: English (US)

to carbon (H:C) ratios, were calculated from the respective number of C, H or O atoms in the assigned molecular formulas. We calculated Kendrick mass (KM) and Kendrick mass defect (KMD) as described in equations (1) and (2), respectively (Stenson et al., 2003).

$$KM = experimental\ mass * \left(\frac{14.00000}{14.01565}\right) \quad (1)$$

$$KMD = nominal\ mass - KM \quad (2)$$

DBE was calculated by equation (3) for the molecular formula format: $C_cH_hO_oN_nS_s$.

$$DBE = c - \left(\frac{h}{2}\right) + \left(\frac{n}{2}\right) + 1 \quad (3)$$

Note that S and O are divalent in equation (3); additional unsaturated bonds associated with pentavalent nitrogen, and tetravalent or hexavalent sulfur are not included in this DBE calculation. The average oxidation state of carbon (OS_C) in the molecular formulas was estimated using equation (4), based on the approximation described in Kroll et al. (2011); note that the inclusion of nitrogen and sulfur affects the oxidation state of carbon, and equation (4) assumes both are fully oxidized. The modified aromaticity index (AI_{mod}) (Koch and Dittmar, 2006, 2016) was calculated using equations (5-7). Equations (4-7) use the same molecular formula format as DBE in equation (3).

$$OS_C \approx 2\frac{o}{c} - \frac{h}{c} - 5\frac{n}{c} - 6\frac{s}{c} \quad (4)$$

$$DBE_{AI} = 1 + c - \left(\frac{o}{2}\right) - s - \left(\frac{n+h}{2}\right) \quad (5)$$

$$C_{AI} = c - \left(\frac{o}{2}\right) - n - s \quad (6)$$

$$AI_{mod} = \frac{DBE_{AI}}{C_{AI}} \quad (7)$$

In equation (7), the $AI_{mod} = 0$, if $DBE_{AI} \leq 0$ or $C_{AI} \leq 0$, as defined in Koch and Dittmar (2006, 2016).

The resulting data set represents the SPE-recovered higher molecular weight water soluble organic aerosol and is expected to predominantly contain acidic compounds due to the negative ion ESI analytical bias. The observed molecular compositions represent the oxidized fraction of the atmospheric samples thus, useful insights can be made with these limitations in mind. Furthermore, it is important to note that the individual molecular formulas likely represent a mixture of structural isomers co-existing in atmospheric organic matter, as recently observed for deep-sea organic matter (Zark et al., 2017).

3. Results and discussion

3.1 Selection of aerosol and fog water samples

Among the 15 fog and 18 aerosol samples collected during the winter of 2013 at SPC and Bologna, we selected two fog and two aerosol samples for subsequent analysis by FT-ICR MS according to the following rationale. Aerosol samples were selected based on PMF source apportionment of "fresh" and "aged" wood burning emissions using HR-ToF-AMS and ^{1}H-NMR data, as described in Gilardoni et al. (2016). On 13 February 2013, a high concentration of SOA was observed, where the ratio of SOA to POA was ~4, and the aqueous SOA from biomass burning accounted for about 55% of total SOA. Thus, BO0213D was defined as strongly influenced by aged wood burning emissions. During the night of 4 February 2013, the fresh biomass burning concentration was ~6 μg m^{-3},

Formatted ... [44]
Formatted ... [45]
Formatted ... [46]
Formatted ... [47]
Formatted ... [48]
Deleted: formed by
Deleted: and
Formatted ... [50]
Deleted: S
Deleted: the
Deleted: calculations
Formatted ... [49]
Formatted ... [51]
Formatted ... [52]
Formatted ... [53]
Deleted: calculated
Formatted ... [54]
Deleted:) as
Formatted ... [55]
Deleted: the
Formatted ... [56]
Deleted:) with
Formatted ... [57]
Deleted: .
Formatted ... [58]
Formatted ... [59]
Deleted: =
Formatted ... [60]
Deleted: $* (O:C) - (H:C)$
Formatted ... [61]
Formatted ... [62]
Formatted ... [63]
Formatted ... [64]
Formatted ... [65]
Formatted ... [66]
Deleted: . The aerosol
Formatted ... [67]
Deleted: to represent conditions strongly impacted by
Formatted ... [68]
Deleted: based on the evaluation of the PM$_1$ organic aerosol ... [69]
Formatted ... [70]
Deleted: Using PMF source apportionment, we observed the ... [71]
Formatted ... [72]
Deleted: between 11 February 2013 and 20 February 2013. In ... [73]
Formatted ... [74]
Deleted: the
Formatted ... [75]
Deleted: this aerosol sample (
Formatted ... [76]
Deleted:)
Formatted ... [77]

accounting for the 54% of total organic aerosol. Thus, BO0204N was defined as strongly influenced by fresh wood burning emissions. Similarly, HR-ToF-AMS observations were used to select fog samples strongly impacted by "fresh" and "aged" wood burning emissions. Specifically, we used the relative intensity of *m/z* 60 (f_{60}) as a marker of fresh biomass burning influence and *m/z* 44 (f_{44}) as a marker of oxygenated and processed dissolved organic molecules (Aiken et al., 2008; Gilardoni et al., 2016). The f_{44} *vs.* f_{60} space was previously proposed to represent biomass burning *vs.* atmospheric aerosol aging (Cubison et al., 2011) and was extended here to fog samples. This representation is an oversimplification of the complexity of organic molecules in fog water, employed here exclusively to note the major differences in terms of emission sources and atmospheric history. In Fig. 1a, it can be seen that the fog sample SPC0106F had low f_{44} and high f_{60} values, while SPC0201F had high f_{44} and low f_{60} values. Thus, from here on, SPC0106F (fog) and BO0204N (aerosol) will be referred to as the "fresh" biomass burning influenced samples, and SPC0201F (fog) and BO0213D (aerosol) will be referred to as the "aged" biomass burning influenced samples. A summary of the sample collection details and HR-ToF-AMS characterization is given in Table 1.

3.2 ^{1}H-NMR composition

Functional group distributions for the selected PM_1 and fog samples were provided by ^{1}H-NMR analysis. A synthetic representation of the ^{1}H-NMR organic functional groups distribution of all the collected samples is reported in Fig. 1b, following the approach described by Decesari et al. (2007) for source attribution. Briefly, Decesari et al. (2007) presented a survey of ^{1}H-NMR functional group distributions of WSOC samples from diverse environments proposing fingerprints for broad categories of oxygenated organic compounds in aerosol. These categories are: SOA (enriched in acyl groups, H-C-C=O), biomass burning aerosol (enriched in alkoxyls, H-C-O, and aromatics), and marine organic aerosol (enriched in aliphatic groups other than acyls and alkoxyls, mainly amines and sulfoxy groups). In this study, most samples were categorized either as SOA or biomass burning, even if a significant fraction of the aerosol samples exhibited ^{1}H-NMR compositions with a very high alkoxyl contribution, exceeding the boundaries proposed by Decesari et al. (2007). For example, sample BO0204N (representative of fresh biomass burning aerosol) showed by far the largest contribution of alkoxyl groups and the least amount of acyl groups. In contrast, BO0213D (representative of aged aerosols) showed relatively high acyl content and small alkoxyl fractions. Similarly, the two selected fog samples (SPC0106F: fresh, and SPC0201F: aged) were clearly differentiated based on their ^{1}H-NMR functional group distributions (Fig 1b). Therefore, the selected aerosol and fog samples represent extremes in the structural space of this WSOC sample set based on the distribution of ^{1}H-NMR functionalities, and in agreement to the categorization provided by the HR-ToF-AMS measurements.

The differences between the two aerosol samples likely reflect the ambient conditions during sampling: BO0204N was characterized by night-time accumulation of ground-level local emissions from residential heating and an absence of photochemical processes; instead, BO0213D was characterized by daytime photo-chemically processed aerosol and by an enhanced mixing with regional-scale air masses. Similarly, the diversity in the fog samples reflects the collection duration and the associated liquid water content (LWC) of the two considered fog events: SPC0106F was collected over a shorter duration with a lower LWC compared to SPC0201F (Table 1).

Deleted: ; thus, it
Formatted: English (US)
Formatted: English (US)
Formatted: English (US)
Formatted: English (US)
Formatted: English (US)
Formatted: English (US)
Formatted: English (US)
Formatted: English (US)
Formatted: English (US)
Formatted: English (US)
Deleted: , namely
Formatted: English (US)
Deleted: rich of
Formatted: English (US)
Formatted: English (US)
Formatted: English (US)
Deleted: photochemically
Formatted: English (US)

It should be noted that although a pair of fresh and aged samples were selected from each of the sample sets, Fig. 1 shows a clear shift in the average composition between the fog and the aerosol samples, where the fog samples were characterized by a greater amount of acyl groups and a smaller fraction of alkoxyls. So, according to the simple source-attribution scheme based on the major ^{1}H-NMR functionalities presented here, the fog compositions were more oxidized and "SOA-like" than aerosols. As a consequence, the fresh fog composition overlapped with the aged aerosol composition (Fig. 1b). This implies that the fresh fog sample SPC0106F was processed to a similar degree as the most aged aerosol sample BO0213D. This was confirmed by the corresponding HR-ToF-AMS elemental ratios (very similar O:C for SPC0106F and BO0213D, see Table 1) and by the detailed comparison between the ^{1}H-NMR spectra of these two samples (one fog and one aerosol). This difference in the average functional group composition between fog and aerosol samples in the Po Valley can be explained by: (a) the preferential scavenging of more oxidized constituents of organic particles into fog (Gilardoni et al., 2014); (b) the effect of oxidative chemical reactions in fog water leading to the production of carboxylic acids and carbonyls (hence, acyls); and (c) a stronger aging effect from fog processing at the rural site (SPC) with respect to urban areas (Bologna) at the margins of the Po basin.

The ^{1}H-NMR spectra of the selected samples are reported in Fig. 2. The spectra of the aerosol samples (Fig. 2c and 2d) exhibited a clear biomass burning fingerprint, with evident proton resonances from levoglucosan and intense bands from alkoxyl (H-C-O) and aromatic (Ar-H) groups. However, the band of phenols and methoxyphenols, which are primary biomass burning tracers, were clearly found only in the spectrum of BO0204N, representative of fresh primary organic aerosols in our study. Moreover, the fraction of levoglucosan and alkoxyl groups was much greater in BO0204N than in BO0213D. The aged aerosol BO0213D contained higher amounts of two methylamines (mono- and tri-methyl-amines) relative to BO0204N, and especially much larger fractions of methanesulfonate and succinic acid, which are tracers of SOA. The spectral region between the chemical shift of 2.1 and 2.4 ppm showed clear bands representing aliphatic dicarboxylic acids and ketoacids (Suzuki et al., 2001) in the aged aerosol, but were barely visible in the fresh aerosol. The aged aerosol was also characterized by the occurrence of hydroxy-methanesulfonic acid (HMSA), a known tracer of aqueous SOA. Similarly for fog, SPC0106F (Fig. 2A) exhibited a clear biomass burning fingerprint with contributions from levoglucosan, alkoxyl (H-C-O), and aromatic groups (Ar-H), whereas SPC0201F (Fig. 2B) showed tracers of aqueous-phase SOA (HMSA) and high concentrations of acyl groups, (CH-C=O), which demonstrated the effects of the aging process. Additionally, SPC0201F exhibited several low-molecular weight organic acids (phthalic, maleic, succinic, pyruvic and lactic acids) in much greater amounts than SPC0106F, where only traces of phthalic and succinic acids were found. This indicated that the aged fog was enriched in products of the oxidative degradation of particulate and gaseous organic compounds. It should be noted, that the fresh fog (SPC0106F) did not show the prominent band from phenols or methoxyphenols observed in the spectrum of the fresh aerosol (BO0204N). This suggests that the WSOC of the fresh fog had undergone a certain degree of chemical modification respective to primary biomass burning OA.

Formatted: English (US)

Formatted: English (US)

Formatted: English (US)

Formatted: English (US)

Formatted: English (US)

Formatted: English (US)

Formatted: English (US)

Deleted: , even if the secondary products of such transformations were not visible in the ^{1}H-NMR spectrum

Formatted: English (US)

3.3 Ultrahigh resolution FT-ICR MS composition

3.3.1 Overview of the Po Valley ambient fog and aerosol compositions

Approximately 1600-2800 individual monoisotopic molecular formulas were assigned to the ultrahigh resolution mass spectra of the SPE-recovered WSOC from each Po Valley sample. Based on the inclusion of C, H, N, O, and S elements, the molecular formulas were sorted into the following elemental groups: "CHO," "CHNO," "CHOS" and "CHNOS." The percent composition of these elemental groups for each sample is shown in Fig. 3. Most of the molecular formulas were present in the subclasses $O_{4\text{-}10}$, $NO_{3\text{-}13}$, $O_{5\text{-}10}S$ and $NO_{7\text{-}11}S$ (Fig. S1). A summary of the observed numbers of formulas per elemental group, as well as the average O:C, H:C, OS_C and DBE values are provided in Table 2. Although they are not expected to match, the values for the SPE-recovered WSOC do trend with those from the HR-ToF-AMS data shown in Table 1; we note, that not only are the elemental ratios from different fractions of the aerosol, but they are also determined differently.

A great diversity of CHNO, CHOS and CHNOS formulas were observed in the Po Valley samples, likely representing organonitrates, organosulfates, and nitrooxy-organosulfates. These compound classes can be inferred from the analytical bias of the negative mode ESI, as well as the O:N and O:S of the assigned molecular formulas. Nearly all N-containing formulas had O:N > 3, suggesting that a majority of the nitrogen species contained at least one nitro or nitrate group. Multiple nitrogen species, such as those of classes $N_2O_{3\text{-}5}$ and $N_3O_{5\text{-}7}$ have an O:N low enough to indicate amine, imine, or imidazole structures, as these types of products have been reported in cloud water mimic reactions (De Haan et al., 2011), however only a modest number of formulas with multiple nitrogen atoms were observed. All of the S-containing formulas had O:S > 4 ratios, suggesting sulfite, sulfate, and sulfonic acid functionalities. These inferences are consistent with the ionization polarity, where oxidized and acidic components are more efficiently ionized in negative ion ESI. A study by LeClair et al. (2012) who performed FT-ICR MS/MS using negative mode ESI on a variety of CHNO, CHOS, and CHNOS components confirmed that the studied compounds in Fresno fog were indeed multifunctional organonitrates, organosulfates, and nitrooxy-organosulfates. Furthermore, nitrate and sulfate salts are common secondary components present in the Po Valley (Giulianelli et al., 2014) and reactions between these inorganic salts and organics are expected as secondary reactions in the aqueous phase (Noziere et al., 2010; McNeill et al., 2012; Herrmann et al., 2015; McNeill, 2015). Amines have been observed in the Po Valley, emitted by livestock farming and waste treatment activity, and it is possible that some species with amine groups were emitted from smoldering biomass combustion (Andreae and Merlet, 2001; Paglione et al., 2014). However, given the analytical bias for acidic functional groups in the ESI negative ion mode, it is unlikely that reduced nitrogen species were detected. Nitrated phenols are known contributors to light absorbing atmospheric brown carbon and are associated with biomass burning (Desyaterik et al., 2013; Laskin et al., 2015). In this work, a large number of CHNO formulas were observed with low H:C and low O:C, especially in the fresh aerosol and fresh fog samples (Fig. S2); several of the CHNO formulas were also estimated to be aromatic using the AI_{mod} calculation (Fig. 4). Specifically, the molecular formulas for nitrophenol, methyl-nitrophenol, dinitrophenol, nitroguaiacol and nitrosalicylic acid (Kitanovski et al., 2012; Desyaterik et al., 2013) were observed in all four Po Valley samples (Table S1).

Deleted: were observed in the Po Valley samples.
Formatted ... [78]
Formatted ... [79]
Formatted ... [80]
Deleted: nitrooxy (
Formatted ... [81]
Deleted:)
Formatted ... [82]
Deleted: make
Formatted ... [83]
Deleted: and
Formatted ... [84]
Deleted: possible, and
Formatted ... [85]
Deleted: .
Formatted ... [86]
Formatted ... [87]
Deleted: indicating
Formatted ... [88]
Formatted ... [89]
Formatted ... [90]
Formatted ... [91]
Formatted ... [92]
Formatted ... [93]
Formatted ... [94]
Formatted ... [95]
Formatted ... [96]
Formatted ... [97]
Formatted ... [98]
Formatted ... [99]
Deleted: 4-
Formatted ... [100]
Deleted: 2-
Formatted ... [101]
Deleted: 4-
Formatted ... [102]
Deleted: 2,4-
Formatted ... [103]
Deleted: 4-
Formatted ... [104]
Deleted: 3-
Formatted ... [105]
Formatted ... [106]
Formatted ... [107]
Deleted: .
Formatted ... [108]

All of the molecular formulas were plotted in van Krevelen space (H:C *vs*. O:C) partitioned by sample (columns) and elemental group (rows) (Figs. 5, S2). In this space, molecular formulas with O:C ≥ 0.6 and OS_C ≥ 0 are considered to be highly oxidized and formulas with H:C ≥ 1.2 are considered to be highly saturated (Tu et al., 2016). The distribution of the CHO and CHNO formulas is quite similar to WSOC extracted from ambient fog collected in Fresno, CA (Mazzoleni et al., 2010). Additionally, the distribution of CHO formulas from phenolic aqueous SOA reported in Yu et al. (2016) partially covers the same area of the van Krevelen space. The CHOS and CHNOS formulas with high H:C ratios were also distributed similarly to Mazzoleni et al. (2010). The high H:C ratios indicate that a majority of the CHOS and CHNOS formulas represent aliphatic organosulfate compounds, consistent with the aliphatic AI_{mod} values (Fig. 4). In contrast, a majority of the formulas with aromatic AI_{mod} values were in the CHO and CHNO groups, and tended to cluster at low H:C and low O:C in the van Krevelen space, in agreement with previous studies (Mazzoleni et al., 2010; LeClair et al., 2012). Consistent with the ^{1}H-NMR results in Fig. 1B, the van Krevelen diagrams for SPC0106F and BO0213D were similar (see also Fig. S2), barring the additional low H:C CHOS and CHNOS formulas of SPC0106F and the additional CHNO formulas of BO0213D.

Underscoring the influence of biomass burning on these samples, we found several molecular formulas matching previously observed species in biomass burning influenced ambient cloud water from Mt. Tai, China (Desyaterik et al., 2013). There were also several matches with the products of laboratory phenolic aqueous SOA reactions (Yu et al., 2014; Yu et al., 2016) (Table S1). Other notable molecular formulas included those for the compounds: acetosyringone, acetovanillone, azelaic acid, benzoic acid, coumaryc acid, hydroxybenzoicacid, ketolimononaldehyde, nitrocatechol, o-toluic acid, phthalic acid, syringaldehyde, syringic acid, tyrosine, vanillic acid and vanillin (Table S1) (Mazzoleni et al., 2007; Desyaterik et al., 2013; Nguyen et al., 2013; Pietrogrande et al., 2014a; Pietrogrande et al., 2014b; Yu et al., 2014; Dzepina et al., 2015; Pietrogrande et al., 2015; Yu et al., 2016). The molecular formulas for common methoxyphenols (syringol ($C_8H_{10}O_3$), methylsyringol ($C_9H_{12}O_3$), and eugenol ($C_{10}H_{12}O_2$)) were present in all samples except BO0204N; as they are both semi-volatile and water-soluble, they are not expected to be present in aerosol with low liquid water content. Several formulas were also found that could be more oxidized versions of phenolic species produced from biomass burning. These formulas included additional oxygen atoms added to the base formulas for phenol ($C_6H_6O_{3\text{-}5}$), guaiacol ($C_7H_8O_{3\text{-}6}$) and syringol ($C_8H_{10}O_{4\text{-}7}$). Five of these formulas, $C_6H_6O_3$, $C_6H_6O_5$, $C_8H_{10}O_5$, $C_8H_{10}O_6$ and $C_8H_{10}O_7$, were previously observed in biomass burning aerosol (Pietrogrande et al., 2015) and in the products of laboratory phenolic aqueous phase SOA reactions (Yu et al., 2014; Yu et al., 2016).

3.3.2 Molecular trends for ambient fog and aerosol compositions

Molecular formula trends in the form of histograms are a useful way to organize and visualize the thousands of formulas observed here. The trends based on carbon number, oxygen number, and DBE of the assigned molecular formulas are shown in Fig. 6. Although relative abundance does not directly correspond to analyte concentrations, it provides a basis for relative comparisons. For example, the influence of terpene SOA products is indicated from the elevated total relative abundance of molecular formulas near C_{10} (observed in all samples) and an additional increased abundance between $C_{15\text{-}18}$ (observed in most samples). This was especially pronounced in BO0213D (Fig. 6a). These

Deleted: ;
Formatted: English (US)
Formatted: English (US)
Formatted: English (US)
Formatted: English (US)
Formatted: English (US)
Formatted: English (US)
Formatted: English (US)
Formatted: English (US)
Formatted: English (US)
Formatted: English (US)
Formatted: English (US)
Formatted: English (US)
Deleted: 3 and Table
Formatted: English (US)
Formatted: English (US)
Deleted: methyl-nitrophenol,
Formatted: English (US)
Deleted: , nitrophenol
Formatted: English (US)
Deleted: 3
Formatted: English (US)
Formatted: English (US)
Formatted: English (US)
Formatted: English (US)
Formatted: English (US)
Formatted: English (US)
Formatted: English (US)
Deleted: molecular
Formatted: English (US)

formulas are likely derived from monoterpenes (C_{10}) and sesquiterpenes (C_{15}), where terpene emissions have been observed in biomass burning (Andreae and Merlet, 2001). Terpene oxidation products, including organosulfates, were previously observed in biomass burning influenced cloud water (Zhao et al., 2013; Cook et al., 2017) and many of the same molecular formulas were observed in this study (Table S1). Specifically, we observed molecular formulas for pinic acid, ketopinic acid, pinonic acid, hydroxy-dimethylglutaric acid, and methyl-butanetricarboxylic acid (Table S1) (He et al., 2014). Overall, the trends indicate an enhanced abundance of CHO formulas in SPC0201F, CHNO formulas in BO0204N and BO0213D, and CHOS formulas in SPC0106F (Fig 6a). Consistent with the ^{1}H-NMR results in Fig. 1b, there is a strong similarity between samples SPC0106F and BO0213D, especially for the oxygen and DBE trends shown in Figs. 6b and 6c.

Difference mass spectra were constructed from the assigned monoisotopic molecular formulas for the fog and aerosol samples (Fig. S3) and provide a direct comparison of their compositions. Each of the individual relative abundances were normalized by the total abundance of the assigned masses for each sample. In Fig. S3, the individual masses with higher abundances in either the positive or negative direction were substantially greater in the fresh or aged samples, respectively; the masses with similar relative abundances tended to cancel each other. Overall, we observed molecular formulas with higher oxygen content at lower molecular weights in the two aged samples compared to the two fresh samples. To investigate this further, we adapted the approach used for the molecular formula trends described above with the difference relative abundances. The resulting difference trend plots are shown in Fig. 7 for carbon, and Figs. S4 and S5 for oxygen and DBE respectively. In Fig. 7b, it is clear there was an enhanced abundance of CHOS and CHNOS formulas with higher carbon numbers in the fresh fog, while the aged fog showed an enhanced abundance of low carbon number CHO formulas. In Fig. 7a, it is clear that the fresh aerosol had an enhanced abundance of higher carbon number formulas, though unlike the fog samples, they were mainly CHO and CHNO compounds. The aged aerosol had an enhanced abundance of low carbon number formulas from the CHOS and CHNOS groups. In both fog and aerosol, there is an enhanced abundance of higher carbon numbers in the fresh samples relative to the aged samples. Overall, the carbon numbers are shifted to lower values in the fog compared to aerosol (Fig. 7) and the oxygen numbers are shifted to higher values in fog compared to aerosol (Fig. S4).

The subsequent sections discuss the molecular diversity of the different samples, especially considering the sample type, atmospheric processes during sample collection and the unique molecular formulas observed in each sample. The distributions of unique molecular formulas are shown in Fig. 3b and Fig. S1.

3.3.3 Comparison of the fresh and aged biomass burning influenced fog compositions

The molecular formulas of the aged biomass burning influenced fog (SPC0201F) were more oxidized than the fresh biomass burning influenced fog (SPC0106F). This enhancement in oxidation is shown in Fig. S4a, with a greater abundance of higher oxygen number formulas observed in the aged fog. The opposite is true for DBE and carbon numbers, where both trended to higher numbers in the fresh fog compared to the aged fog (See Figs. 7b and S5b). Most of the CHOS and CHNOS formulas in SPC0106F and SPC0201F were classified as aliphatic by AI_{mod} and approximately 30% of these formulas in SPC0106F were classified as olefinic, which was higher than any other sample (Fig. 4). This suggests that the fresh fog molecular formulas represented molecules with large unsaturated

Formatted: English (US)
Formatted: English (US)
Deleted: (Zhao et al., 2013; Cook et al., 2017)
Formatted: English (US)
Deleted: 3-
Formatted: English (US)
Deleted: 4,4-
Formatted: English (US)
Deleted: 3-
Formatted: English (US)
Deleted: 1,2,3-
Formatted: English (US)
Deleted: 3
Formatted: English (US)
Formatted: English (US)
Formatted: English (US)
Deleted: higher numbers of oxygen in the
Formatted: English (US)
Formatted: English (US)
Formatted: English (US)
Deleted: →As expected from the molecular trends, the
Formatted: English (US)
Deleted: The overall average O:C was higher in SPC0201F than in SPC0106F across all groups. Likewise, the average number of oxygen in CHO and CHNO formulas were higher in the aged fog, however the average number of oxygen in CHOS and CHNOS formulas was about the same. Fig. S4a shows this enhancement in oxidation with a greater abundance of higher oxygen number formulas observed in the aged fog. In the van Krevelen space, the molecular formulas in SPC0106F tended to cluster to the left of the O:C = 0.6 line in Fig. 5, but the formulas in SPC0201F tended to cluster on the line and slightly to the right of it, indicating they were significantly more oxygenated. Additionally, there were more molecular formulas in SPC0106F below the H:C = 1.2 line (Fig. 5 and Fig. S2), indicating these formulas were more unsaturated. The average OS_C was higher across all groups in SPC0201F compared to SPC0106F, underscoring the more oxidized nature of the aged fog; this can be seen in Fig. 5 as additional formulas in SPC0201F were shifted towards and below the $OS_C = 0$ diagonal line. The average DBE values for all of the elemental groups were higher in SPC0106F compared to SPC0201F (Table 3); similarly, the average AI_{mod} was higher, indicating there are more aromatic structures in SPC0106F.
Formatted: English (US)
Deleted: . In addition to the higher average DBE and AI_{mod}, the average number of carbon atoms in the SPC0106F molecular formulas was higher as well.
Formatted: English (US)

carbon backbones, which is consistent with pollutants without significant atmospheric aging. In contrast, the molecular formulas that were more oxidized with smaller carbon backbones were more prevalent in the aged fog.

The unique molecular formulas found in the fresh fog (SPC0106F) were mostly of the $O_{5-13}S$ and $NO_{7-12}S$ subclasses. Organosulfates are known products of aqueous secondary processes (Darer et al., 2011; Ervens et al., 2011; McNeill, 2015; Schindelka et al., 2013), and nucleation scavenging from the preceding fog nuclei composition likely plays a significant role as well (Darer et al., 2011; Gilardoni et al., 2014; Herckes et al., 2007; Hu et al., 2011). The aromatic organosulfates and nitooxy-organosulfates observed in fresh biomass burning aerosol (Staudt et al., 2014) were not observed here. In general, organosulfates are the products of aqueous-phase SOA reactions which are expected to be enhanced at acidic pH (Ervens et al., 2011; McNeill et al., 2012; Noziere et al., 2010). Because the pH of SPC0106F was only slightly acidic at 5.81, we propose that the formation of these organosulfates may have been promoted by low LWC, and thus relatively high solute concentrations, during the activation of the fog droplets or possibly in the fully formed fog droplets. Organosulfates may also efficiently nucleate droplets, leading to their eventual presence in the fog samples. A noticeable number of CHOS and CHNOS formulas unique to SPC0106F had higher DBE values than formulas from other samples. There was an overall preference for CHOS and CHNOS formulas with DBE values < 6, except for some of the formulas in SPC0106F which were higher (Fig. 6c). The 10 most abundant unique molecular formulas in the fresh biomass burning influenced fog of SPC0106F were all CHOS and CHNOS formulas: $C_{11}H_{15}NO_8S$, $C_{13}H_{14}O_8S$, $C_{14}H_{16}O_8S$, $C_{15}H_{16}O_9S$, $C_{15}H_{24}O_7S$, $C_{15}H_{24}O_8S$, $C_{16}H_{18}O_9S$, $C_{17}H_{20}O_9S$, $C_{18}H_{30}O_8S$ and $C_{19}H_{24}O_9S$. These formulas may be tracer species for partially fog processed biomass burning emissions.

While all samples contained some unique molecular formulas among the CHO subclasses, a high number of formulas in the O_{9-14} subclasses were unique to the aged fog (SPC0201F). This trend could indicate enhanced oxidation and aging as a result of aqueous phase reactions in fog. The high average O:C ratio (0.577 ± 0.18) and low pH (3.34) of SPC0201F is consistent with the trend observed by Cook et al. (2017) for cloud water, where the average O:C increased with decreasing pH. Overall, we observed a significant number of CHNO, CHOS and CHNOS molecular formulas in SPC0201F, which are expected products of secondary aqueous phase reactions in fog. However, there was a lower percentage of CHNO, CHOS and CHNOS formulas, and an increased percentage of CHO formulas in SPC0201F compared to SPC0106F, suggesting that aqueous SOA products with N or S may have been transformed by acid hydrolysis into more stable CHO species (Darer et al., 2011). This is reasonable given the longer duration of the fog episode as well as the higher LWC of SPC0201F compared to SPC0106F. The increased oxidation is supported by the ^{1}H-NMR analysis, which showed an enrichment of carboxylic acids and other compounds carrying acyl groups. SPC0201F had additional unique formulas which were highly oxygenated in the NO_{13}, $O_{11}S$ and $NO_{13}S$ subclasses, which appeared on the low mass end of the homologous series in the CHOS and CHNOS groups (Fig. S6). The 10 most abundant unique molecular formulas in the aged biomass burning influenced fog (SPC0201F) were CHO, CHOS and CHNOS species with smaller carbon skeletons than the fresh biomass burning influenced fog (SPC0106F), including: $C_4H_9NO_7S$, $C_5H_9NO_7S$, $C_8H_{12}O_7S$, $C_8H_{13}NO_{11}S$, $C_8H_{14}O_7S$, $C_9H_{16}O_8S$, $C_{10}H_{10}O_7$, $C_{10}H_{18}O_5S$, $C_{11}H_8O_7$ and $C_{12}H_{14}O_9$. These formulas may be tracer species for heavily fog processed biomass burning emissions.

Formatted: English (US)
Deleted: that were more oxidized
Formatted: English (US)
Formatted ... [109]
Deleted: Since organosulfates
Formatted: English (US)
Deleted: associated with
Formatted ... [110]
Deleted: ; McNeill, 2015…, the fact that 33% of the formulas in SPC0106F contained sulfur was initially confusing. Likewise, non-aromatic organosulfates and nitooxy-organosulfates would not be expected in fresh biomass burning emissions ... [111]
Formatted: English (US)
Deleted: Staudt…arer et al., 2011; Gilardoni et al., 2014; Herckes et al., 2007; Hu et al., 2011). Furthermore, photolysis reactions were not expected to have influenced the sample composition because it was collected from ~3:10 am to 4:30 am. However, the fog composition is influenced by the preceding fog nuclei composition ... [112]
Formatted: English (US)
Deleted: Herckes et al., 2007; Gilardoni…taudt et al., 2014). ... [113]
Formatted: English (US)
Deleted: Darer…rvens et al., 2011; Hu…cNeill et al., 2011…012; Noziere et al., 2010) indicating that aged aerosol act as fog nuclei. This is further underscored by the similar compositions of the fresh fog and aged aerosol samples. Meanwhile it is well known that organosulfates are products of aqueous-phase SOA reactions, which are enhanced at acidic pH, (Noziere et al., 2010; Ervens et al., 2011; McNeill et al., 2012). Thus, the lower LWC and relatively higher solute concentrations may have promoted CHOS and CHNOS compound formation in the fresh fog. Increasing organosulfate concentrations in aerosol have been shown to be linked to increased aerosol LWC (Huang et al., 2015), although it is unclear if this ... [114]
Formatted: English (US)
Deleted: observed
Formatted: English (US)
Deleted: a significant fraction of
Formatted ... [115]
Deleted: $C_{15}H_{24}O_7S$
Formatted ... [116]
Deleted: $C_{18}H_{30}O_8S$, $C_{15}H_{16}O_9S$,
Formatted ... [117]
Deleted: and $C_{11}H_{15}NO_8S$
Formatted: English (US)
Formatted ... [118]
Deleted: It is possible that an enhanced oxidation from hydrolysis ... [119]
Formatted: English (US)
Deleted: $C_{10}H_{10}O_7$, $C_{11}H_8O_7$, $C_{12}H_{14}O_9$, $C_{10}H_{18}O_5S$, $C_8H_{14}O_7S$ ... [120]
Deleted: and
Formatted: English (US)
Formatted ... [121]

3.3.4 Comparison of the fresh and aged biomass burning influenced aerosol compositions

Similar to the fog samples, the fresh aerosol formulas trended towards higher carbon and DBE numbers relative to the aged aerosol formulas. These carbon number and DBE trends are clearly visible through the difference trends shown in Figs. 7a and S6a, respectively. Both aerosol samples had a high percentage of formulas that contained nitrogen, with a noticeable number of CHNO formulas unique to these samples (Fig. 3b). This larger percentage of CHNO formulas may be attributed enhanced NO_X concentrations associated with urban traffic emissions (Glasius et al., 2006) (Table 1). However, residential wood combustion influenced cloud water collected near Steamboat Springs, CO, was found to be composed of ~52% CHNO molecular formulas (Zhao et al., 2013), and elevated numbers of CHNO formulas were also reported in aerosol with a strong regional biomass burning influence (Schmitt-Kopplin et al., 2010) and wildfire influenced cloud water (Cook et al., 2017).

A majority of the unique formulas in the fresh aerosol (BO0204N) were in the $NO_{6\text{-}12}$ and $N_2O_{7\text{-}11}$ subclasses, which were expected to be products of NO_X reactions and night-time nitrate radical reactions. The formulas of BO0204N were less saturated and less oxygenated, compared to the formulas in the aged aerosol (BO0213D), which would be expected with little to no influence from aqueous phase secondary processes in the dry conditions of BO0204N (Ervens et al., 2011; McNeill, 2015). This could also help to explain the low percentage of CHOS and CHNOS formulas observed in BO0204N. Overall, no unique CHOS formulas were detected in BO0204N and only 1 unique CHNOS formula ($C_8H_{11}NO_8S$) was detected. The small number of observed CHOS and CHNOS formulas in BO0204N may have originated from the increase in LWC (up to ~300 µg m-3) observed in the last 4 hours of sample collection, and thus may have been formed by similar processes as in BO0213D. DBE values in BO0204N trended towards values up to 10, which was much higher than in other samples, where the trend stopped near the DBE of 5 (Fig. 6c). The 10 most abundant unique molecular formulas in the aerosol with a fresh biomass burning influence (BO0204N) were mostly N_1 and N_2 CHNO formulas: $C_8H_4N_2O_6$, $C_{12}H_{10}N_2O_8$, $C_{13}H_{12}N_2O_8$, $C_{15}H_{14}N_2O_{10}$, $C_{16}H_{15}NO_6$, $C_{17}H_{20}O_5$, $C_{20}H_{18}O_8$, $C_{24}H_{21}NO_{10}$, $C_{24}H_{23}NO_{10}$ and $C_{26}H_{23}NO_{10}$. These formulas may be tracer species for biomass burning emissions when night-time gas phase reactions are dominant.

Several unique molecular formulas for the aged aerosol (BO0213D) were found in the $N_2O_{4\text{-}13}$ and $N_3O_{5\text{-}13}$ subclasses, as well as the $O_{4\text{-}7}S$, $NO_{5\text{-}7}S$ and $NO_{10\text{-}12}S$ subclasses. A large fraction of the N_2 formulas, and all of the N_3 formulas were unique to BO0213D. Compared to the other samples, BO0213D was collected during relatively high NO_X conditions, as well as high humidity and aerosol liquid water content compared to the other aerosol sample. The increased frequency of CHOS and CHNOS formulas in BO0213D compared to BO0204N was likely from reactions in the aqueous phase, enhanced by the increased concentration of species in aerosol liquid water (Darer et al., 2011; Hu et al., 2011; McNeill et al., 2012). Accretion reactions such as aldol condensation, acetal, and hemiacetal reactions are also expected to take place at a significant rate in these enhanced concentrations (Herrmann et al., 2015). While there was not a significant trend towards higher masses in BO0213D compared to other samples, the unique molecular formulas of this sample tended to fall on the high mass end of the homologous series, especially for CHNOS formulas (Fig. S6). The 10 most abundant unique molecular formulas for BO0213D were mostly highly oxygenated CHNO formulas: $C_7H_9NO_3$, $C_9H_{15}NO_{10}$, $C_{12}H_{25}NO_8S$, $C_{15}H_{24}O_{12}$, $C_{16}H_{18}N_2O_{11}$, $C_{16}H_{20}N_2O_{11}$, $C_{17}H_{22}N_2O_{11}$, $C_{17}H_{22}N_2O_{13}$,

Deleted: Consistent with the fog samples, the average O:C and H:C values, and average number of oxygen atoms, were higher in the aged aerosol (BO0213D) than in the fresh aerosol (BO0204N). The influence of fresh biomass burning emissions is further supported by the higher average DBE, AI_{mod}, and average number of carbon atoms in BO0204N. These trends were clearly apparent for the CHO and CHNO groups, but less apparent for the CHOS and CHNOS groups. However, a low number of S-containing formulas were observed in BO0204N (~6%), which may have skewed these statistics. CHO and CHNO formulas in BO0204N clustered to the left of the O:C = 0.6 line in Fig. 5, indicating they were not very oxygenated. In contrast, the aged aerosol molecular formulas were distributed on and to the right of the O:C = 0.6 line. Additionally, ... [122]

Formatted: English (US)

Deleted: the

Formatted ... [123]

Deleted: . These unique CHNO

Formatted ... [124]

Deleted:). In BO0204N, these formulas were expected to be ... [125]

Formatted: English (US)

Deleted: low relative humidity and had low aerosol liquid water ... [126]

Formatted: English (US)

Deleted: . The low humidity

Formatted: English (US)

Deleted: explains

Formatted: English (US)

Deleted: non-unique

Formatted: English (US)

Deleted: Less oxygenated species would be expected with little ... [127]

Formatted: English (US)

Deleted: $C_{16}H_{15}NO_6$, $C_{24}H_{23}NO_{10}$, $C_{24}H_{21}NO_{10}$, $C_{26}H_{23}NO_{10}$,

Formatted ... [128]

Deleted: and

Formatted ... [129]

Deleted: in

Formatted ... [130]

Deleted: . Furthermore, this was

Formatted: English (US)

Deleted: only

Formatted: English (US)

Deleted: collected during daylight hours, implying that these N ... [131]

Formatted: English (US)

Deleted: the formation of organosulfates and nitrooxy- ... [132]

Formatted ... [133]

Deleted: $C_{16}H_{18}N_2O_{11}$

Formatted: English (US)

Deleted: $C_{18}H_{24}N_2O_{11}$,

Formatted: English (US)

$C_{18}H_{21}N_3O_{11}$ and $C_{18}H_{24}N_2O_{11}$. These formulas may be tracer species for biomass burning emissions heavily aged by reactions in aerosol liquid water with photolysis.

4. Summary and implications

Hygroscopic species are expected to enhance droplet formation, indicating that organics acting as fog nuclei must be somewhat aged. In fog or wet aerosol, the water-soluble organics are subjected to further transformation in the aqueous phase, as we have observed here. These transformation processes in fog and aerosol water were shown to produce oxygenated and oxidized molecular formulas, as well as N-containing and S-containing formulas with what were likely nitrate and sulfate functional groups. On the basis of the analysis of the selected aerosol and fog samples, representing extreme cases in the HR-ToF-AMS and ^{1}H-NMR projections of the organic aerosol structural space, we can summarize the following observations:

- An overall molecular trend was observed for both fog and aerosol samples, of concurrent shifts from lower H:C and O:C in samples with fresh biomass burning influence, and toward higher H:C and O:C values in samples with aged biomass burning influence. This was consistent with the ^{1}H-NMR functional group distributions, which showed a decrease of aromatic moieties from the fresh to the aged aerosol, largely due to the disappearance of phenolic structures. The lower number of carbon atoms observed in aged samples suggests that the secondary formation of oligomers was somewhat counterbalanced by fragmentation reactions and/or by the uptake of low-molecular weight compounds from the gas-phase.
- Overall, the fog composition was generally more oxidized and "SOA-like" than the aerosol, where the fresh fog composition was similar to the aged aerosol composition in both the ^{1}H-NMR analysis and the molecular formula trends.
- CHOS and CHNOS formulas were detected with high frequencies in samples with high water content during collection (all samples except BO0204N). This supports an enhanced production of S-containing SOA species via reactions in the aqueous phase.
- When comparing the unique formulas of the two aged samples (SPC0201F and BO0213D), aging reactions in aerosol liquid water appeared to produce less highly oxygenated CHO formulas than in fog and a greater number of formulas in the CHNO, CHOS and CHNOS groups. This difference could be explained by the increased chance of reactions with inorganic nitrate and sulfate ions in the relatively higher solute concentrations of aerosol liquid water compared to the increased likelihood of hydration reactions in fog (Darer et al., 2011; Hu et al., 2011). This conclusion agrees with the quantitative analysis of functional group composition of aqueous SOA isolated by PMF analysis reported previously (Gilardoni et al., 2016).
- The variability of ^{1}H-NMR fingerprints between samples reflects the change in oxidation state of the CHO family detected by FT-ICR MS (reaching a maximum for SPC0201F), but seems rather insensitive to the changes in content of heteroatom-containing groups (CHNO, CHOS, CHNOS). In fact, the formation of CHOS compounds detected in the FT-ICR MS analysis in deliquesced aerosols (BO0213D) or in low-LWC fog water (SPC0106F) could not be traced to parallel changes in ^{1}H-NMR spectral characteristics. It is possible, however,

Deleted: , $C_9H_{15}NO_{10}$, $C_{12}H_{25}NO_8S$
Deleted: $C_{15}H_{24}O_{12}$
Formatted: English (US)
Formatted: English (US)
Deleted: Hydrophilic
Formatted: English (US)
Deleted: Aged sample molecular formulas contained on average a higher number of oxygen atoms, while fresh sample molecular formulas contained on average a higher number of carbon atoms.
Formatted: English (US)
Deleted: However, some evidence of dimerization of C_{10} compounds was found in all samples, especially for C_8-C_9 CHNO compounds in the aged aerosol.
Formatted: English (US)
Formatted: English (US)
Deleted: that were collected as activated fog (both samples) or had a substantial aerosol liquid
Formatted: English (US)
Deleted: as in the case of BO0213D).
Deleted: provided strong evidence that the
Formatted: English (US)
Formatted: English (US)
Deleted: is dominated by
Formatted: English (US)
Deleted: The occurrence of S-containing SOA in the fog can be explained by formation in incipient droplets (at very low LWC), through radical reactions mediated by the sulfate radical (Noziere et al., 2010; McNeill et al., 2012; Schindelka et al., 2013), or possibly acid catalyzed substitution reactions with the sulfate ion (Darer et al., 2011; Hu et al., 2011; McNeill, 2015).
Formatted: English (US)
Formatted: English (US)
Formatted: English (US)
Formatted: English (US)
Deleted: positive matrix factorization analysis of HR-ToF-AMS mass spectra and ^{1}H-NMR spectra
Formatted: English (US)
Formatted: English (US)
Formatted: English (US)

that a fraction of the ^{1}H-NMR–detected alkoxyl groups (H-C-O) were bound to sulfate esters and misclassified as alcohols.

- Compared to fresh fog (SPC0106F), the aged fog (SPC0201F) had an enhancement in the highly oxidized CHO formulas and an overall lower percentage of CHNO and CHOS formulas. This is likely due to hydrolysis reactions in the low pH environment (Darer et al., 2011; Hu et al., 2011). The ^{1}H-NMR analysis also highlighted that SPC0201F included highly oxidized low-molecular weight organic acids (phthalic, maleic, succinic, pyruvic acids) which originated from the degradation of particulate WSOC, the oxidation of condensable water-soluble volatile organic compounds, and the uptake of condensable products of gas-phase oxidative reactions.

In this work, we used the detailed molecular composition to describe the differences in aging and aqueous phase processes for a select set of samples from the Supersito 2013 winter campaign. A majority of the molecular formulas observed in this study have not been previously reported, but correlate with anticipated molecular trends. This emphasizes the importance of detailed molecular analysis of atmospheric samples for the study of biomass burning emissions processed in the aqueous phase of aerosol and fog, as well as the potential of aqueous phase processing to act as a source of SOA in the atmosphere.

Data availability

An abbreviated list of the complete FT-ICR MS dataset is provided and is available on Digital Commons: http://digitalcommons.mtu.edu/chemistry-fp/98/

Acknowledgments

This research was supported with a NASA Earth and Space Science Fellowship for Matthew Brege. The Italian CNR contribution was supported by the BACCHUS project, European Commission FP7-603445. The authors thank Drs. Melissa Soule and Elizabeth Kujawinski of the Woods Hole Oceanographic Institution (WHOI) Mass Spectrometry Facility for instrument time and assistance with data FT-ICR MS acquisition (NSF OCE-0619608 and Gordon and Betty Moore Foundation).

Formatted: English (US)

Formatted: English (US)

Formatted: English (US)

Deleted: several

Formatted: English (US)

Deleted: The resulting ^{1}H-NMR spectral fingerprint of the aged fog (SPC0201F) is clearly distinct from those of the fresh fog and the two aerosol samples, which are instead dominated by spectral features of primary biomass burning components. Overall, the variability of ^{1}H-NMR fingerprints between samples reflects the change in oxidation state of the CHO family detected by FT-ICR MS (reaching a maximum for SPC0201F), but seems rather insensitive to the changes in content of heteroatom-containing groups (CHNO, CHOS, CHNOS). In fact, the formation of CHOS compounds detected by ultrahigh resolution FT-ICR MS analysis in deliquesced aerosols or in low-LWC fog water (e.g., BO0213D and SPC0106F) could not be traced to parallel changes in ^{1}H-NMR spectral characteristics. It is possible, however, that a fraction of the ^{1}H-NMR–detected alkoxyl groups (H-C-O) were in fact bound to sulfate esters and misclassified as alcohols.

Formatted: English (US)

Formatted: English (US)

Formatted: English (US)

Formatted: English (US)

Figures

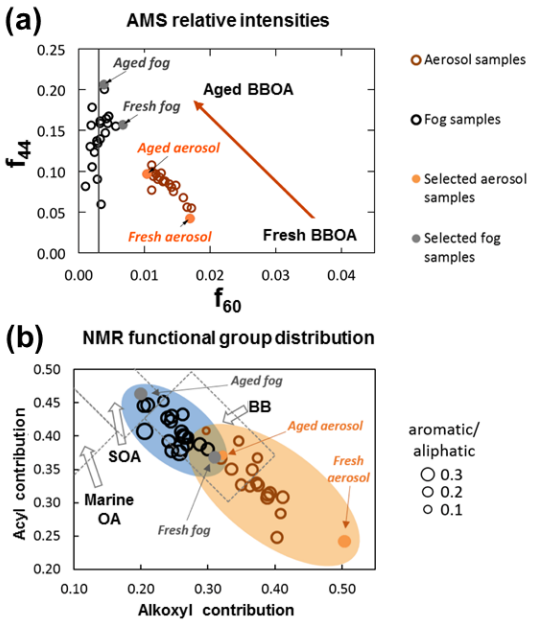

Figure 1: Preliminary characterization of fog and PM_1 aerosol samples collected in SPC and Bologna, respectively, during the 2013 Supersito field campaign. Characterization was performed via HR-ToF-AMS analysis as described by Cubison et al. (2011), utilizing the relative intensity of peak *m/z* 60 (f_{60}) and peak *m/z* 44 (f_{44}) as markers of fresh biomass burning influence and oxygenated and processed dissolved organic molecules respectively (a). Further characterization was performed via ^{1}H-NMR analysis, as described by Decesari et al. (2007), where samples were mapped by ^{1}H-NMR functional group fractions (b). In (b), dashed lines indicate the boundaries of the source fingerprints according to Decesari et al. (2007), ("BB": biomass burning aerosol) and the x and y axes report the contributions of alkoxyl (H-C-O) and acyl (H-C-C=O) groups to the total aliphatic fraction of WSOC respectively. The sample names Fresh Fog, Aged Fog, Fresh Aerosol, and Aged Aerosol correspond to SPC0106F, SPC0201F, BO0204N, and BO0213D, respectively.

Formatted: English (US)

Formatted: English (US)

Formatted: English (US)

Formatted: English (US)

Formatted: English (US)

Formatted: English (US)

Formatted: English (US)

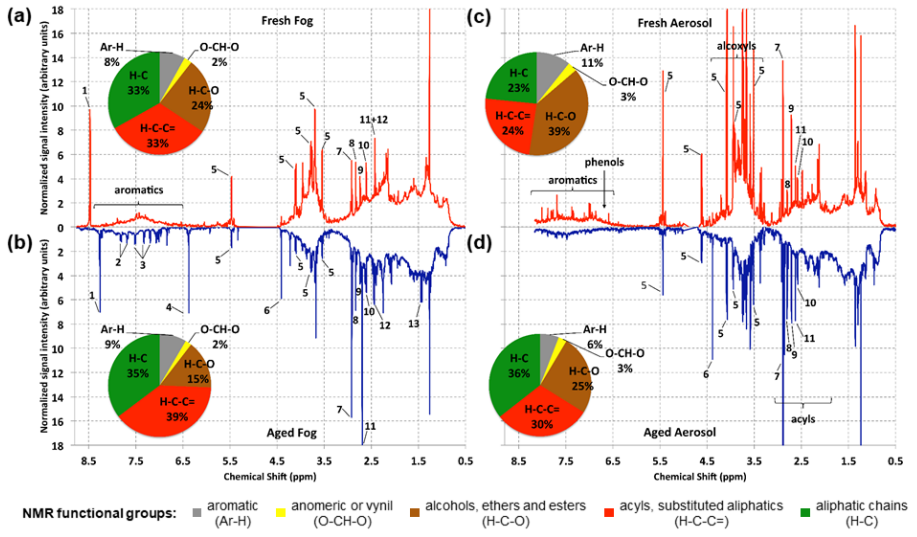

Figure 2: The ^{1}H-NMR spectra of selected fog water (a and b) and aerosol (c and d) samples, and their corresponding functional groups distribution. A set of specific resonances was attributed to individual compounds: 1) formate, 2) phthalic acid, 3) ammonium, 4) maleic acid, 5) levoglucosan, 6) hydroxy-methanesulfonic acid, 7) trimethylamine, 8) methanesulfonic acid, 9) dimethylamine, 10) monomethylamine, 11) succinic acid, 12) pyruvic acid, 13) lactic acid. The sample names Fresh Fog, Aged Fog, Fresh Aerosol, and Aged Aerosol correspond to SPC0106F, SPC0201F, BO0204N, and BO0213D, respectively.

Formatted: English (US)

Deleted:

Formatted: English (US)

Deleted:

Formatted: English (US)

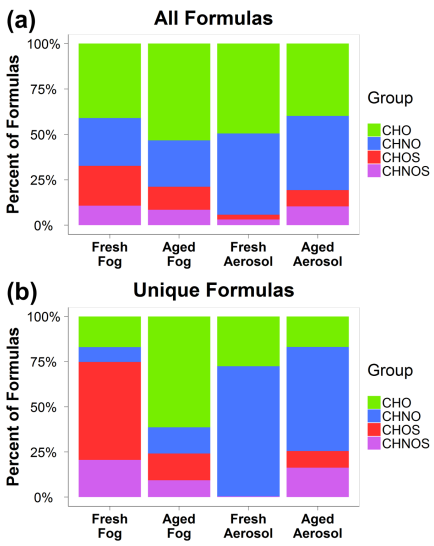

Formatted: English (US)

Figure 3: Percentage of assigned molecular formulas to each of the elemental groups in the Po Valley samples, where (a) includes all identified molecular formulas and (b) includes only the unique molecular formulas. The sample names Fresh Fog, Aged Fog, Fresh Aerosol, and Aged Aerosol correspond to SPC0106F, SPC0201F, BO0204N, and BO0213D, respectively.

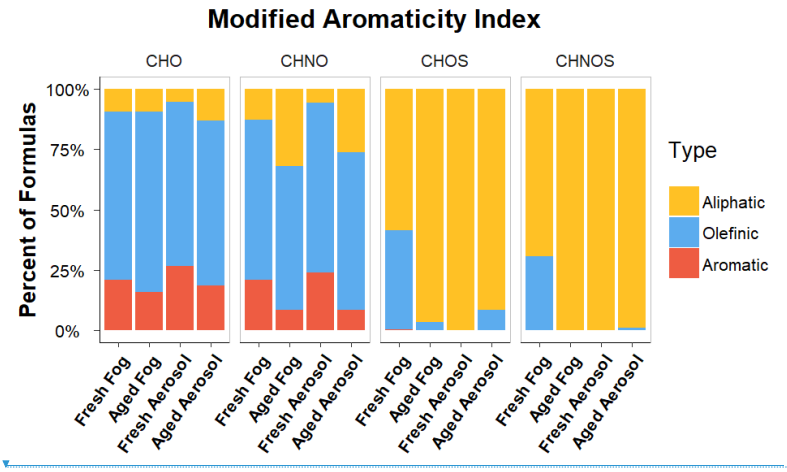

Figure 4: The modified aromaticity index (AI_{mod}) for the assigned molecular formulas (Equations 5-7) and the percentage of each AI_{mod} type, as defined by Koch and Dittmar (2016): aliphatic ($AI_{mod} = 0$), olefinic ($0 < AI_{mod} \leq 0.5$), aromatic ($AI_{mod} > 0.5$), and condensed aromatic ($AI_{mod} \geq 0.67$). Here aromatic and condensed aromatic formulas were combined, because a small fraction of condensed aromatics was observed. The results are partitioned by elemental group, where it can be seen that the majority of olefinic and aromatic compounds belong to the CHO and CHNO groups. The sample names Fresh Fog, Aged Fog, Fresh Aerosol, and Aged Aerosol correspond to SPC0106F, SPC0201F, BO0204N, and BO0213D, respectively.

Deleted:

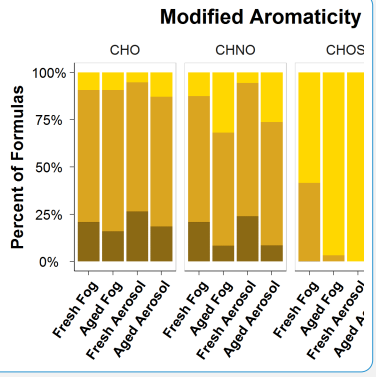

Formatted: English (US)

Formatted: English (US)

Formatted: English (US)

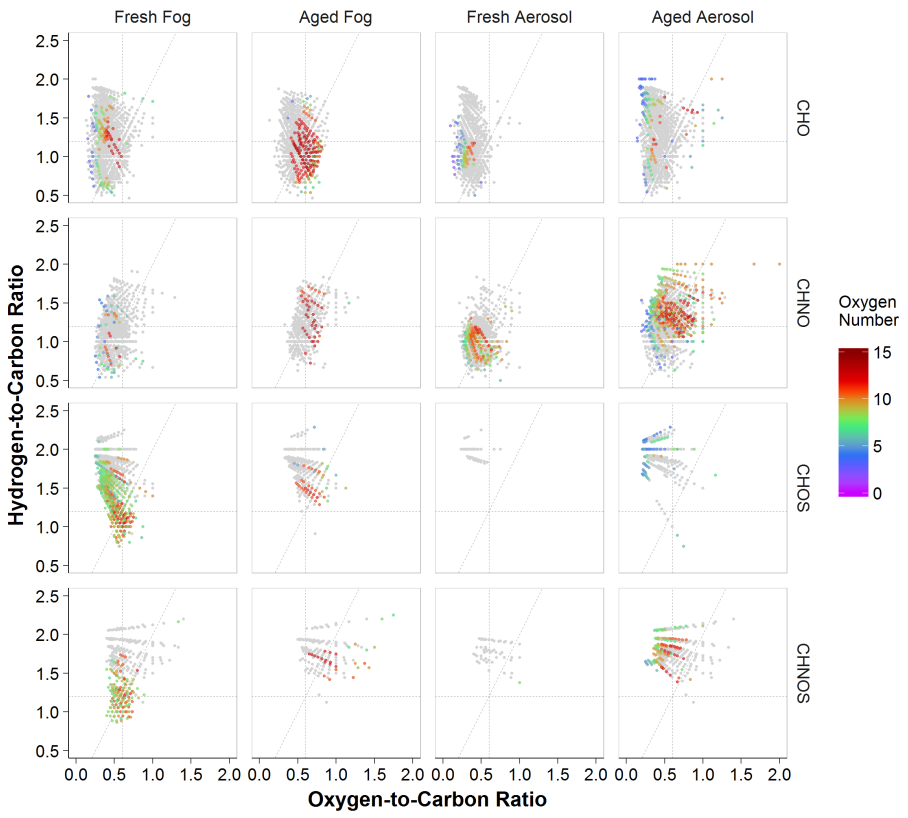

Figure 5: van Krevelen diagrams for the SPE-recovered WSOC by elemental group (rows) and sample (columns) as indicated in the Figure. Dashed lines represent H:C = 1.2 (horizontal), O:C = 0.6 (vertical) and OS_C = 0 (diagonal) as described in Tu et al. (2016). Formulas unique to each sample are color scaled to the number of oxygen atoms in the assigned formula; grey points represent common molecular formula assignments. The sample names Fresh Fog, Aged Fog, Fresh Aerosol, and Aged Aerosol correspond to SPC0106F, SPC0201F, BO0204N, and BO0213D, respectively. A similar plot with all of the molecular formulas scaled to indicate the number of oxygen atoms is provided as Fig. S2.

Formatted: English (US)

Formatted: English (US)

Formatted: English (US)

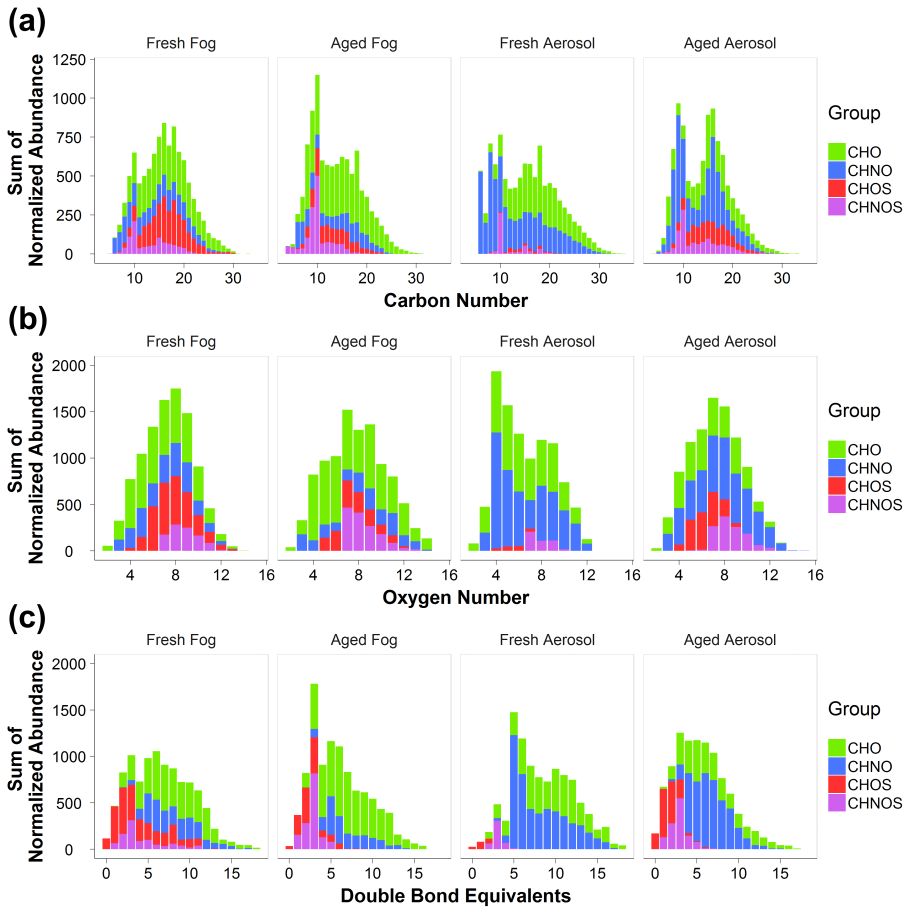

Figure 6: Molecular formula trends for carbon (a), oxygen (b) and the number of double bond equivalents (c). All detected molecular formula abundances were normalized to the total assigned ion abundance for each sample and then summed across the integer values for carbon number, oxygen number, or double bond equivalent values. The sample names Fresh Fog, Aged Fog, Fresh Aerosol, and Aged Aerosol correspond to SPC0106F, SPC0201F, BO0204N, and BO0213D, respectively.

Formatted: English (US)

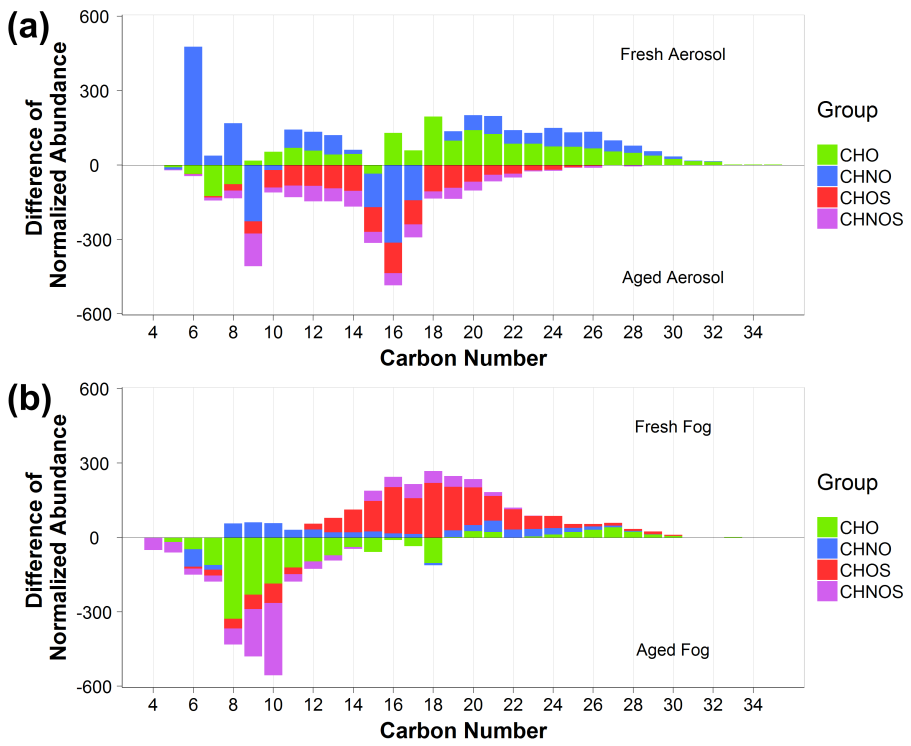

Figure 7: Carbon difference trend plots for aerosol (a) and fog (b) sample types. Difference trends were calculated as in Figure 6 and then the respective aged sample was subtracted from the fresh sample for each integer carbon number value. Positive values indicate an enhanced relative abundance of the formulas in the fresh sample compared to the aged sample. Similarly, negative values indicate an enhanced abundance of formulas in the aged sample compared to the fresh sample. The sample names Fresh Fog, Aged Fog, Fresh Aerosol, and Aged Aerosol correspond to SPC0106F, SPC0201F, BO0204N, and BO0213D, respectively.

Formatted: English (US)

Tables

Table 1: Sample collection, identification and HR-ToF-AMS data. Relative humidity (RH), liquid water content (LWC), and aerosol liquid water content (ALWC) are averaged over the sample collection time. Fog samples were collected at Capofiume (SPC). Fog water samples were re-aerosolized for HR-ToF-AMS data analysis, while aerosol sample data is from on-line measurements. For aerosol samples, the standard deviation of on-line measurements corresponding to the sample collection period are shown.

Sample name	SPC01016F	SPC0201F	BO0204N	BO0213D
Collection site	SPC	SPC	Bologna	Bologna
Sample type	Fog water	Fog water	PM_1 aerosol	PM_1 aerosol
Fresh *vs.* Aged influence	Fresh	Aged	Fresh	Aged
Start collection date and time[a]	6 January 2013, 3:10	1 February 2013, 19:40	4 February 2013, 18:18	13 February 2013, 9:24
Collection time (h)	1.33	15.37	14.62	8.60
Temperature (°C)[b]	1.0	3.0	5.9	3.0
pH	5.81	3.34	NA	NA
[NO_X] (ppb)[b]	73	15	146	101
RH (%)[b, c]	100	100	58	80
LWC (mL m^{-3})[b]	0.190	0.258	NA	NA
ALWC (µg m^{-3})[b, d]	NA	NA	69	515
f_{44}[e]	0.16	0.21	0.042 ± 0.006	0.097 ± 0.004
f_{60}[e]	0.007	0.004	0.016 ± 0.003	0.010 ± 0.001
OM:OC[b, f]	1.9	2.2	1.5 ± 0.1	1.9 ± 0.1
O:C[b, f]	0.58	0.8	0.24 ± 0.04	0.56 ± 0.03
H:C[b, f]	1.37	1.29	1.65 ± 0.03	1.60 ± 0.01
OSc[b, f]	-0.21	0.32	-1.17 ± 0.08	-0.48 ± 0.06

[a]Start collection times given in local time; [b]Average values corresponding to the collection times of individual samples; [c]Average RH was assumed to be 100% for fog samples, as super-saturation levels could not be measured; [d]ALWC is an average of E-AIM and ISORROPIA modeled data for the sampling period; [e]Fractional abundance of a mass fragment (f_X) was calculated as the ratio between that fragment signal and the total organic concentration; [f]Elemental ratios were calculated according to Aiken et al. (2008).

Formatted Table
Formatted: English (US)
Formatted: English (US)
Formatted: English (US)
Formatted: English (US)
Formatted: English (US)
Formatted: English (US)
Formatted: English (US)
Formatted: English (US)
Formatted: English (US)
Formatted: English (US)
Formatted: English (US)
Formatted: English (US)
Formatted: English (US)
Formatted: English (US)
Formatted: English (US)
Formatted: English (US)
Formatted: English (US)
Formatted: English (US)
Formatted: English (US)

Table 2: Summary of FT-ICR MS formula assignment data. Mass, O:C, H:C, OS_C, DBE, AI, C_n, and O_n values represent mathematical averages based on formula assignment, with standard deviation provided. These values were obtained using equations 1-7.

		All	CHO	CHNO	CHOS	CHNOS
SPC0106F	Number	2824	1158 (41%)	744 (26%)	619 (22%)	303 (11%)
	Molecular weight (Da)	368.44 ± 94.21	359.05 ± 101.35	342.88 ± 90.69	404.68 ± 83.64	393.12 ± 61.72
	O:C	0.479 ± 0.16	0.415 ± 0.13	0.503 ± 0.14	0.488 ± 0.14	0.642 ± 0.18
	H:C	1.30 ± 0.36	1.21 ± 0.32	1.14 ± 0.27	1.56 ± 0.34	1.53 ± 0.34
	OS_C	-0.623 ± 0.48	-0.379 ± 0.42	-0.563 ± 0.33	-0.950 ± 0.49	-1.039 ± 0.37
	DBE	7.24 ± 3.65	8.29 ± 3.67	8.35 ± 3.01	4.93 ± 3.08	5.20 ± 2.93
	AI_{mod}	0.24 ± 0.22	0.31 ± 0.20	0.32 ± 0.21	0.08 ± 0.12	0.06 ± 0.11
	C_N	17.2 ± 5.2	18.3 ± 5.5	15.7 ± 4.9	17.8 ± 4.8	15 ± 3.7
	O_N	7.8 ± 2.3	7.4 ± 2.5	7.6 ± 2.2	8.3 ± 2.0	9.1 ± 1.3
SPC0201F	Number	1671	890 (53%)	427 (26%)	212 (13%)	142 (8%)
	Molecular weight (Da)	360.12 ± 97.52	358.18 ± 108.61	364.33 ± 90.94	360.12 ± 78.27	359.66 ± 63.56
	O:C	0.577 ± 0.18	0.509 ± 0.13	0.617 ± 0.14	0.592 ± 0.15	0.858 ± 0.24
	H:C	1.31 ± 0.35	1.18 ± 0.29	1.23 ± 0.26	1.74 ± 0.23	1.77 ± 0.20
	OS_C	-0.399 ± 0.51	-0.161 ± 0.41	-0.369 ± 0.28	-1.006 ± 0.42	-1.075 ± 0.35
	DBE	6.83 ± 3.53	8.05 ± 3.38	7.49 ± 2.69	3.01 ± 1.81	2.93 ± 1.13
	AI_{mod}	0.22 ± 0.21	0.30 ± 0.19	0.22 ± 0.20	0.00 ± 0.03	0.00 ± 0.00
	C_N	15.8 ± 5.0	16.9 ± 5.2	15.4 ± 4.4	14.4 ± 4.0	11.8 ± 3.4
	O_N	8.7 ± 2.7	8.5 ± 3.0	9.2 ± 2.4	8.2 ± 2.0	9.5 ± 1.6
BO0204N	Number	1634	808 (49%)	732 (45%)	42 (3%)	52 (3%)
	Molecular weight (Da)	364.99 ± 100.13	358.24 ± 105.13	373.63 ± 98.27	332.45 ± 54.27	374.39 ± 50.93
	O:C	0.433 ± 0.14	0.377 ± 0.11	0.480 ± 0.14	0.405 ± 0.11	0.652 ± 0.17
	H:C	1.13 ± 0.32	1.12 ± 0.30	1.04 ± 0.22	1.96 ± 0.10	1.77 ± 0.14
	OS_C	-0.471 ± 0.41	-0.368 ± 0.38	-0.461 ± 0.28	-1.578 ± 0.22	-1.303 ± 0.21
	DBE	9.26 ± 3.94	9.42 ± 4.03	9.99 ± 3.11	1.31 ± 0.64	3.08 ± 0.9
	AI_{mod}	0.36 ± 0.20	0.38 ± 0.19	0.39 ± 0.18	0.00 ± 0.00	0.00 ± 0.00
	C_N	18.0 ± 5.6	18.9 ± 5.7	17.6 ± 5.5	15.0 ± 3.5	13.9 ± 3.4
	O_N	7.5 ± 2.4	7.0 ± 2.5	8.1 ± 2.3	5.8 ± 0.9	8.6 ± 0.7
BO0213D	Number	2753	1097 (40%)	1123 (41%)	249 (9%)	284 (10%)
	Molecular weight (Da)	361.82 ± 96.19	351.26 ± 102.62	360.99 ± 94.43	354.82 ± 75.64	412.02 ± 76.3

Formatted Table ... [134]
Formatted ... [135]
Deleted: Mass
Formatted ... [136]
Formatted ... [138]
Formatted ... [137]
Formatted ... [139]
Formatted ... [140]
Deleted: 583
Deleted: 247 ± 0.43
Formatted ... [141]
Deleted: 345
Formatted ... [142]
Deleted: 45
Formatted ... [143]
Deleted: 133
Formatted ... [144]
Formatted ... [145]
Formatted ... [147]
Deleted: 51
Formatted ... [146]
Formatted ... [148]
Formatted ... [149]
Formatted ... [150]
Formatted ... [151]
Formatted ... [152]
Formatted ... [153]
Formatted ... [154]
Deleted: Mass
Formatted ... [156]
Formatted ... [155]
Formatted ... [157]
Formatted ... [158]
Formatted ... [159]
Deleted: 158
Formatted ... [160]
Deleted: 43
Formatted ... [161]
Formatted ... [162]
Deleted: 007
Formatted ... [163]
Deleted: 30
Formatted ... [164]
Formatted ... [165]
Deleted: 551 ± 0.45
Formatted ... [166]
Formatted ... [167]
Deleted: 050 ± 0.50
Formatted ... [168]
Formatted ... [169]
Formatted ... [170]
Formatted ... [171]
Formatted ... [172]
Formatted ... [173]
Formatted ... [174]
Deleted: Mass
Formatted ... [176]
Formatted ... [175]
Formatted ... [177]
Formatted ... [178]
Formatted ... [179]
Deleted: 262

O:C	0.498 ± 0.19	0.424 ± 0.15	0.555 ± 0.18	0.435 ± 0.16	0.617 ± 0.21
H:C	1.37 ± 0.37	1.25 ± 0.34	1.26 ± 0.27	1.9 ± 0.22	1.8 ± 0.18
OS_C	-0.683 ± 0.53	-0.399 ± 0.46	-0.631 ± 0.34	-1.445 ± 0.37	-1.322 ± 0.30
DBE	6.64 ± 3.65	7.81 ± 3.88	7.44 ± 2.6	1.8 ± 1.43	3.19 ± 1.47
AI_{mod}	0.21 ± 0.21	0.29 ± 0.21	0.22 ± 0.20	0.01 ± 0.06	0.00 ± 0.00
C_N	16.7 ± 5.3	17.9 ± 5.7	15.8 ± 4.9	16 ± 4.9	16 ± 4.7
O_N	7.8 ± 2.5	7.2 ± 2.4	8.3 ± 2.5	6.3 ± 1.4	9.1 ± 1.6

Formatted: English (US)
Formatted: English (US)
Formatted: English (US)
Deleted: 372
Deleted: 5
Deleted: 152
Deleted: 39
Deleted: 562 ± 0.45
Formatted: English (US)
Deleted: 027
Deleted: 44
Formatted: English (US)
Formatted: English (US)
Formatted: English (US)
Formatted: English (US)
Formatted: English (US)
Formatted: English (US)
Formatted: English (US)
Formatted: English (US)
Formatted: English (US)
Formatted: English (US)
Formatted: English (US)
Deleted: ¶
Page Break
¶
Table 3: Summary of the possible identified molecular formulas from the present study. Identical formulas from the literature are provided with their references. Additional possible identified molecular formulas are listed in Table S1.¶
Formula ... [195]
Formatted: Font: Bold, English (US)

References

Aiken, A. C., Decarlo, P. F., Kroll, J. H., Worsnop, D. R., Huffman, J. A., Docherty, K. S., Ulbrich, I. M., Mohr, C., Kimmel, J. R., Sueper, D., Sun, Y., Zhang, Q., Trimborn, A., Northway, M., Ziemann, P. J., Canagaratna, M. R., Onasch, T. B., Alfarra, M. R., Prevot, A. S. H., Dommen, J., Duplissy, J., Metzger, A., Baltensperger, U., and Jimenez, J. L.: O/C and OM/OC ratios of primary, secondary, and ambient organic aerosols with high-resolution time-of-flight aerosol mass spectrometry, Environ Sci Technol, 42, 4478-4485, 2008.

Andreae, M. O., and Merlet, P.: Emission of trace gases and aerosols from biomass burning, Global Biogeochem Cy, 15, 955-966, 2001.

Bond, T. C., Streets, D. G., Yarber, K. F., Nelson, S. M., Woo, J. H., and Klimont, Z.: A technology-based global inventory of black and organic carbon emissions from combustion, J Geophys Res-Atmos, 109, 2004.

Boone, E. J., Laskin, A., Laskin, J., Wirth, C., Shepson, P. B., Stirm, B. H., and Pratt, K. A.: Aqueous Processing of Atmospheric Organic Particles in Cloud Water Collected via Aircraft Sampling, Environ Sci Technol, 49, 8523-8530, 2015.

Chang, J. L., and Thompson, J. E.: Characterization of colored products formed during irradiation of aqueous solutions containing H2O2 and phenolic compounds, Atmos Environ, 44, 541-551, 2010.

Cook, R. D., Lin, Y. H., Peng, Z. Y., Boone, E., Chu, R. K., Dukett, J. E., Gunsch, M. J., Zhang, W. L., Tolic, N., Laskin, A., and Pratt, K. A.: Biogenic, urban, and wildfire influences on the molecular composition of dissolved organic compounds in cloud water, Atmos Chem Phys, 17, 15167-15180, 10.5194/acp-17-15167-2017, 2017.

Cubison, M. J., Ortega, A. M., Hayes, P. L., Farmer, D. K., Day, D., Lechner, M. J., Brune, W. H., Apel, E., Diskin, G. S., Fisher, J. A., Fuelberg, H. E., Hecobian, A., Knapp, D. J., Mikoviny, T., Riemer, D., Sachse, G. W., Sessions, W., Weber, R. J., Weinheimer, A. J., Wisthaler, A., and Jimenez, J. L.: Effects of aging on organic aerosol from open biomass burning smoke in aircraft and laboratory studies, Atmos Chem Phys, 11, 12049-12064, 2011.

Dall'Osto, M., Paglione, M., Decesari, S., Facchini, M. C., O'Dowd, C., Plass-Duellmer, C., and Harrison, R. M.: On the Origin of AMS "Cooking Organic Aerosol" at a Rural Site, Environ Sci Technol, 49, 13964-13972, 2015.

Darer, A. I., Cole-Filipiak, N. C., O'Connor, A. E., and Elrod, M. J.: Formation and Stability of Atmospherically Relevant Isoprene-Derived Organosulfates and Organonitrates, Environ Sci Technol, 45, 1895-1902, 2011.

De Haan, D. O., Hawkins, L. N., Kononenko, J. A., Turley, J. J., Corrigan, A. L., Tolbert, M. A., and Jimenez, J. L.: Formation of Nitrogen-Containing Oligomers by Methylglyoxal and Amines in Simulated Evaporating Cloud Droplets, Environ Sci Technol, 45, 984-991, 10.1021/es102933x, 2011.

DeCarlo, P. F., Kimmel, J. R., Trimborn, A., Northway, M. J., Jayne, J. T., Aiken, A. C., Gonin, M., Fuhrer, K., Horvath, T., Docherty, K. S., Worsnop, D. R., and Jimenez, J. L.: Field-deployable, high-resolution, time-of-flight aerosol mass spectrometer, Anal Chem, 78, 8281-8289, 2006.

Decesari, S., Facchini, M. C., Fuzzi, S., and Tagliavini, E.: Characterization of water-soluble organic compounds in atmospheric aerosol: A new approach, J Geophys Res-Atmos, 105, 1481-1489, 2000.

Formatted: English (US)

Formatted: English (US)

Formatted: Indent: Left: 0"

Decesari, S., Mircea, M., Cavalli, F., Fuzzi, S., Moretti, F., Tagliavini, E., and Facchini, M. C.: Source attribution of water-soluble organic aerosol by nuclear magnetic resonance spectroscopy, Environ Sci Technol, 41, 2479-2484, 2007.

Desyaterik, Y., Sun, Y., Shen, X. H., Lee, T. Y., Wang, X. F., Wang, T., and Collett, J. L.: Speciation of "brown" carbon in cloud water impacted by agricultural biomass burning in eastern China, J Geophys Res-Atmos, 118, 7389-7399, 2013.

Dzepina, K., Mazzoleni, C., Fialho, P., China, S., Zhang, B., Owen, R. C., Helmig, D., Hueber, J., Kumar, S., Perlinger, J. A., Kramer, L. J., Dziobak, M. P., Ampadu, M. T., Olsen, S., Wuebbles, D. J., and Mazzoleni, L. R.: Molecular characterization of free tropospheric aerosol collected at the Pico Mountain Observatory: a case study with a long-range transported biomass burning plume, Atmos Chem Phys, 15, 5047-5068, 2015.

Ervens, B., Turpin, B. J., and Weber, R. J.: Secondary organic aerosol formation in cloud droplets and aqueous particles (aqSOA): a review of laboratory, field and model studies, Atmos Chem Phys, 11, 11069-11102, 2011.

Fuzzi, S., Orsi, G., Bonforte, G., Zardini, B., and Franchini, P. L.: An automated fog water collector suitable for deposition networks: Design, operation and field tests, Water Air Soil Poll, 93, 383-394, 1997.

Gilardoni, S., Massoli, P., Giulianelli, L., Rinaldi, M., Paglione, M., Pollini, F., Lanconelli, C., Poluzzi, V., Carbone, S., Hillamo, R., Russell, L. M., Facchini, M. C., and Fuzzi, S.: Fog scavenging of organic and inorganic aerosol in the Po Valley, Atmos Chem Phys, 14, 6967-6981, 2014.

Gilardoni, S., Massoli, P., Paglione, M., Giulianelli, L., Carbone, C., Rinaldi, M., Decesari, S., Sandrini, S., Costabile, F., Gobbi, G. P., Pietrogrande, M. C., Visentin, M., Scotto, F., Fuzzi, S., and Facchini, M. C.: Direct observation of aqueous secondary organic aerosol from biomass-burning emissions, P Natl Acad Sci USA, 113, 10013-10018, 2016.

Giulianelli, L., Gilardoni, S., Tarozzi, L., Rinaldi, M., Decesari, S., Carbone, C., Facchini, M. C., and Fuzzi, S.: Fog occurrence and chemical composition in the Po valley over the last twenty years, Atmos Environ, 98, 394-401, 2014.

Glasius, M., Ketzel, M., Wahlin, P., Jensen, B., Monster, J., Berkowicz, R., and Palmgren, F.: Impact of wood combustion on particle levels in a residential area in Denmark, Atmos Environ, 40, 7115-7124, 10.1016/j.atmosenv.2006.06.047, 2006.

Hand, J. L., Malm, W. C., Laskin, A., Day, D., Lee, T., Wang, C., Carrico, C., Carrillo, J., Cowin, J. P., Collett, J., and Iedema, M. J.: Optical, physical, and chemical properties of tar balls observed during the Yosemite Aerosol Characterization Study, J Geophys Res-Atmos, 110, 2005.

Hawkins, L. N., Lemire, A. N., Galloway, M. M., Corrigan, A. L., Turley, J. J., Espelien, B. M., and De Haan, D. O.: Maillard Chemistry in Clouds and Aqueous Aerosol As a Source of Atmospheric Humic-Like Substances, Environ Sci Technol, 50, 7443-7452, 10.1021/acs.est.6b00909, 2016.

He, Q. F., Ding, X., Wang, X. M., Yu, J. Z., Fu, X. X., Liu, T. Y., Zhang, Z., Xue, J., Chen, D. H., Zhong, L. J., and Donahue, N. M.: Organosulfates from Pinene and Isoprene over the Pearl River Delta, South China: Seasonal Variation and Implication in Formation Mechanisms, Environ Sci Technol, 48, 9236-9245, 2014.

Herckes, P., Chang, H., Lee, T., and Collett, J. L.: Air pollution processing by radiation fogs, Water Air Soil Poll, 181, 65-75, 10.1007/s11270-006-9276-x, 2007.

Herckes, P., Valsaraj, K. T., and Collett, J. L.: A review of observations of organic matter in fogs and clouds: Origin, processing and fate, Atmos Res, 132, 434-449, 10.1016/j.atmosres.2013.06.005, 2013.

Herrmann, H., Schaefer, T., Tilgner, A., Styler, S. A., Weller, C., Teich, M., and Otto, T.: Tropospheric Aqueous-Phase Chemistry: Kinetics, Mechanisms, and Its Coupling to a Changing Gas Phase, Chem Rev, 115, 4259-4334, 2015.

Hertkorn, N., Ruecker, C., Meringer, M., Gugisch, R., Frommberger, M., Perdue, E. M., Witt, M., and Schmitt-Kopplin, P.: High-precision frequency measurements: indispensable tools at the core of the molecular-level analysis of complex systems, Anal Bioanal Chem, 389, 1311-1327, 2007.

Hu, K. S., Darer, A. I., and Elrod, M. J.: Thermodynamics and kinetics of the hydrolysis of atmospherically relevant organonitrates and organosulfates, Atmos Chem Phys, 11, 8307-8320, 2011.

Kitanovski, Z., Grgic, I., Vermeylen, R., Claeys, M., and Maenhaut, W.: Liquid chromatography tandem mass spectrometry method for characterization of monoaromatic nitro-compounds in atmospheric particulate matter, J Chromatogr A, 1268, 35-43, 10.1016/j.chroma.2012.10.021, 2012.

Koch, B. P., and Dittmar, T.: From mass to structure: an aromaticity index for high-resolution mass data of natural organic matter, Rapid Commun Mass Sp, 20, 926-932, 2006.

Koch, B. P., and Dittmar, T.: From mass to structure: an aromaticity index for high-resolution mass data of natural organic matter (vol 20, pg 926, 2006), Rapid Commun Mass Sp, 30, 250-250, 2016.

Kroll, J. H., Donahue, N. M., Jimenez, J. L., Kessler, S. H., Canagaratna, M. R., Wilson, K. R., Altieri, K. E., Mazzoleni, L. R., Wozniak, A. S., Bluhm, H., Mysak, E. R., Smith, J. D., Kolb, C. E., and Worsnop, D. R.: Carbon oxidation state as a metric for describing the chemistry of atmospheric organic aerosol, Nat Chem, 3, 133-139, 2011.

Larsen, B. R., Gilardoni, S., Stenstrom, K., Niedzialek, J., Jimenez, J., and Belis, C. A.: Sources for PM air pollution in the Po Plain, Italy: II. Probabilistic uncertainty characterization and sensitivity analysis of secondary and primary sources, Atmos Environ, 50, 203-213, 2012.

Laskin, A., Laskin, J., and Nizkorodov, S. A.: Chemistry of Atmospheric Brown Carbon, Chem Rev, 115, 4335-4382, 2015.

Laskin, A., Gilles, M. K., Knopf, D. A., Wang, B. B., and China, S.: Progress in the Analysis of Complex Atmospheric Particles, Annu Rev Anal Chem, 9, 117-143, 10.1146/annurev-anchem-071015-041521, 2016.

LeClair, J. P., Collett, J. L., and Mazzoleni, L. R.: Fragmentation Analysis of Water-Soluble Atmospheric Organic Matter Using Ultrahigh-Resolution FT-ICR Mass Spectrometry, Environ Sci Technol, 46, 4312-4322, 2012.

Lee, A. K. Y., Hayden, K. L., Herckes, P., Leaitch, W. R., Liggio, J., Macdonald, A. M., and Abbatt, J. P. D.: Characterization of aerosol and cloud water at a mountain site during WACS 2010: secondary organic aerosol formation through oxidative cloud processing, Atmos Chem Phys, 12, 7103-7116, 10.5194/acp-12-7103-2012, 2012.

Deleted: Huang, D. D., Li, Y. J., Lee, B. P., and Chan, C. K.: Analysis of Organic Sulfur Compounds in Atmospheric Aerosols at the HKUST Supersite in Hong Kong Using HR-ToF-AMS, Environ Sci Technol, 49, 3672-3679, 2015.¶

Lee, A. K. Y., Zhao, R., Li, R., Liggio, J., Li, S. M., and Abbatt, J. P. D.: Formation of Light Absorbing Organo-Nitrogen Species from Evaporation of Droplets Containing Glyoxal and Ammonium Sulfate, Environ Sci Technol, 47, 12819-12826, 2013.

Mazzoleni, L. R., Zielinska, B., and Moosmuller, H.: Emissions of levoglucosan, methoxy phenols, and organic acids from prescribed burns, laboratory combustion of wildland fuels, and residential wood combustion, Environ Sci Technol, 41, 2115-2122, 2007.

Mazzoleni, L. R., Ehrmann, B. M., Shen, X. H., Marshall, A. G., and Collett, J. L.: Water-Soluble Atmospheric Organic Matter in Fog: Exact Masses and Chemical Formula Identification by Ultrahigh-Resolution Fourier Transform Ion Cyclotron Resonance Mass Spectrometry, Environ Sci Technol, 44, 3690-3697, 2010.

McNeill, V. F., Woo, J. L., Kim, D. D., Schwier, A. N., Wannell, N. J., Sumner, A. J., and Barakat, J. M.: Aqueous-Phase Secondary Organic Aerosol and Organosulfate Formation in Atmospheric Aerosols: A Modeling Study, Environ Sci Technol, 46, 8075-8081, 2012.

McNeill, V. F.: Aqueous Organic Chemistry in the Atmosphere: Sources and Chemical Processing of Organic Aerosols, Environ Sci Technol, 49, 1237-1244, 10.1021/es5043707, 2015.

Nguyen, T. B., Laskin, A., Laskin, J., and Nizkorodov, S. A.: Brown carbon formation from ketoaldehydes of biogenic monoterpenes, Faraday Discuss, 165, 473-494, 2013.

Nizkorodov, S. A., Laskin, J., and Laskin, A.: Molecular chemistry of organic aerosols through the application of high resolution mass spectrometry, Phys Chem Chem Phys, 13, 3612-3629, 2011.

Noziere, B., Ekstrom, S., Alsberg, T., and Holmstrom, S.: Radical-initiated formation of organosulfates and surfactants in atmospheric aerosols, Geophys Res Lett, 37, 2010.

Noziere, B., Kaberer, M., Claeys, M., Allan, J., D'Anna, B., Decesari, S., Finessi, E., Glasius, M., Grgic, I., Hamilton, J. F., Hoffmann, T., Iinuma, Y., Jaoui, M., Kahno, A., Kampf, C. J., Kourtchev, I., Maenhaut, W., Marsden, N., Saarikoski, S., Schnelle-Kreis, J., Surratt, J. D., Szidat, S., Szmigielski, R., and Wisthaler, A.: The Molecular Identification of Organic Compounds in the Atmosphere: State of the Art and Challenges, Chem Rev, 115, 3919-3983, 10.1021/cr5003485, 2015.

Paglione, M., Saarikoski, S., Carbone, S., Hillamo, R., Facchini, M. C., Finessi, E., Giulianelli, L., Carbone, C., Fuzzi, S., Moretti, F., Tagliavini, E., Swietlicki, E., Stenstrom, K. E., Prevot, A. S. H., Massoli, P., Canaragatna, M., Worsnop, D., and Decesari, S.: Primary and secondary biomass burning aerosols determined by proton nuclear magnetic resonance (H-1-NMR) spectroscopy during the 2008 EUCAARI campaign in the Po Valley (Italy), Atmos Chem Phys, 14, 5089-5110, 2014.

Pietrogrande, M. C., Bacco, D., Visentin, M., Ferrari, S., and Casali, P.: Polar organic marker compounds in atmospheric aerosol in the Po Valley during the Supersito campaigns - Part 2: Seasonal variations of sugars, Atmos Environ, 97, 215-225, 2014a.

Pietrogrande, M. C., Bacco, D., Visentin, M., Ferrari, S., and Poluzzi, V.: Polar organic marker compounds in atmospheric aerosol in the Po Valley during the Supersito campaigns - Part 1: Low molecular weight carboxylic acids in cold seasons, Atmos Environ, 86, 164-175, 2014b.

Deleted: Lin, P., Laskin, J., Nizkorodov, S. A., and Laskin, A.: Revealing Brown Carbon Chromophores Produced in Reactions of Methylglyoxal with Ammonium Sulfate, Environ Sci Technol, 49, 14257-14266, 10.1021/acs.est.5b03608, 2015.¶

Pietrogrande, M. C., Sacco, D., Ferrari, S., Kaipainen, J., Ricciardelli, I., Riekkola, M. L., Trentini, A., and Visentin, M.: Characterization of atmospheric aerosols in the Po valley during the supersito campaigns - Part 3: Contribution of wood combustion to wintertime atmospheric aerosols in Emilia Romagna region (Northern Italy), Atmos Environ, 122, 291-305, 2015.

Poluzzi, V., Trentini, A., Scotto, F., Ricciardelli, I., Ferrari, S., Maccone, C., Bacco, D., Zigola, C., Bonafè, G., and Ugolini, P.: Preliminary results of the project "Supersito" concerning the atmospheric aerosol composition in Emilia-Romagna region, Italy: PM source apportionment and aerosol size distribution, WIT Transactions on The Built Environment, 168, 689-698, 2015.

Pratt, K. A., Fiddler, M. N., Shepson, P. B., Carlton, A. G., and Surratt, J. D.: Organosulfates in cloud water above the Ozarks' isoprene source region, Atmos Environ, 77, 231-238, 10.1016/j.atmosenv.2013.05.011, 2013.

Putman, A. L., Offenberg, J. H., Fisseha, R., Kundu, S., Rahn, T. A., and Mazzoleni, L. R.: Ultrahigh-resolution FT-ICR mass spectrometry characterization of alpha-pinene ozonolysis SOA, Atmos Environ, 46, 164-172, 2012.

Rinaldi, M., Emblico, L., Decesari, S., Fuzzi, S., Facchini, M. C., and Librando, V.: Chemical characterization and source apportionment of size-segregated aerosol collected at an urban site in sicily, Water Air Soil Poll, 185, 311-321, 2007.

Saarikoski, S., Carbone, S., Decesari, S., Giulianelli, L., Angelini, F., Canagaratna, M., Ng, N. L., Trimborn, A., Facchini, M. C., Fuzzi, S., Hillamo, R., and Worsnop, D.: Chemical characterization of springtime submicrometer aerosol in Po Valley, Italy, Atmos Chem Phys, 12, 8401-8421, 2012.

Schindelka, J., Iinuma, Y., Hoffmann, D., and Herrmann, H.: Sulfate radical-initiated formation of isoprene-derived organosulfates in atmospheric aerosols, Faraday Discuss, 165, 237-259, 2013.

Schmitt-Kopplin, P., Gelencser, A., Dabek-Zlotorzynska, E., Kiss, G., Hertkorn, N., Harir, M., Hong, Y., and Gebefugi, I.: Analysis of the Unresolved Organic Fraction in Atmospheric Aerosols with Ultrahigh-Resolution Mass Spectrometry and Nuclear Magnetic Resonance Spectroscopy: Organosulfates As Photochemical Smog Constituents, Anal Chem, 82, 8017-8026, 2010.

Staudt, S., Kundu, S., Lehmler, H. J., He, X. R., Cui, T. Q., Lin, Y. H., Kristensen, K., Glasius, M., Zhang, X. L., Weber, R. J., Surratt, J. D., and Stone, E. A.: Aromatic organosulfates in atmospheric aerosols: Synthesis, characterization, and abundance, Atmos Environ, 94, 366-373, 2014.

Stenson, A. C., Marshall, A. G., and Cooper, W. T.: Exact masses and chemical formulas of individual Suwannee River fulvic acids from ultrahigh resolution electrospray ionization Fourier transform ion cyclotron resonance mass spectra, Anal Chem, 75, 1275-1284, 2003.

Surratt, J. D., Gomez-Gonzalez, Y., Chan, A. W. H., Vermeylen, R., Shahgholi, M., Kleindienst, T. E., Edney, E. O., Offenberg, J. H., Lewandowski, M., Jaoui, M., Maenhaut, W., Claeys, M., Flagan, R. C., and Seinfeld, J. H.: Organosulfate formation in biogenic secondary organic aerosol, J Phys Chem A, 112, 8345-8378, 2008.

Suzuki, Y., Kawakami, M., and Akasaka, K.: H-1 NMR application for characterizing water-soluble organic compounds in urban atmospheric particles, Environ Sci Technol, 35, 2656-2664, 2001.

Tu, P. J., Hall, W. A., and Johnston, M. V.: Characterization of Highly Oxidized Molecules in Fresh and Aged Biogenic Secondary Organic Aerosol, Anal Chem, 88, 4495-4501, 2016.

Willoughby, A. S., Wozniak, A. S., and Hatcher, P. G.: Detailed Source-Specific Molecular Composition of Ambient Aerosol Organic Matter Using Ultrahigh Resolution Mass Spectrometry and H-1 NMR, Atmosphere-Basel, 7, 2016.

Xu, X., Chen, J., Zhu, C., Li, J., Sui, X., Liu, L., and Sun, J.: Fog composition along the Yangtze River basin: Detecting emission sources of pollutants in fog water, J Environ Sci-China, 11, 2017.

Yu, L., Smith, J., Laskin, A., Anastasio, C., Laskin, J., and Zhang, Q.: Chemical characterization of SOA formed from aqueous-phase reactions of phenols with the triplet excited state of carbonyl and hydroxyl radical, Atmos Chem Phys, 14, 13801-13816, 2014.

Yu, L., Smith, J., Laskin, A., George, K. M., Anastasio, C., Laskin, J., Dillner, A. M., and Zhang, Q.: Molecular transformations of phenolic SOA during photochemical aging in the aqueous phase: competition among oligomerization, functionalization, and fragmentation, Atmos Chem Phys, 16, 4511-4527, 2016.

Zark, M., Christoffers, J., and Dittmar, T.: Molecular properties of deep-sea dissolved organic matter are predictable by the central limit theorem: Evidence from tandem FT-ICR-MS, Mar Chem, 191, 9-15, 10.1016/j.marchem.2017.02.005, 2017.

Zhang, Q., Jimenez, J. L., Canagaratna, M. R., Allan, J. D., Coe, H., Ulbrich, I., Alfarra, M. R., Takami, A., Middlebrook, A. M., Sun, Y. L., Dzepina, K., Dunlea, E., Docherty, K., DeCarlo, P. F., Salcedo, D., Onasch, T., Jayne, J. T., Miyoshi, T., Shimono, A., Hatakeyama, S., Takegawa, N., Kondo, Y., Schneider, J., Drewnick, F., Borrmann, S., Weimer, S., Demerjian, K., Williams, P., Bower, K., Bahreini, R., Cottrell, L., Griffin, R. J., Rautiainen, J., Sun, J. Y., Zhang, Y. M., and Worsnop, D. R.: Ubiquity and dominance of oxygenated species in organic aerosols in anthropogenically-influenced Northern Hemisphere midlatitudes, Geophys Res Lett, 34, 2007.

Zhang, Q., Jimenez, J. L., Canagaratna, M. R., Ulbrich, I. M., Ng, N. L., Worsnop, D. R., and Sun, Y. L.: Understanding atmospheric organic aerosols via factor analysis of aerosol mass spectrometry: a review, Anal Bioanal Chem, 401, 3045-3067, 2011.

Zhao, Y., Hallar, A. G., and Mazzoleni, L. R.: Atmospheric organic matter in clouds: exact masses and molecular formula identification using ultrahigh-resolution FT-ICR mass spectrometry, Atmos Chem Phys, 13, 12343-12362, 2013.

Formatted: Indent: Left: 0"

Formatted: English (US)

Page 2: [1] Formatted	mabrege	8/20/18 3:30:00 PM

English (US)

Page 2: [1] Formatted	mabrege	8/20/18 3:30:00 PM

English (US)

Page 2: [1] Formatted	mabrege	8/20/18 3:30:00 PM

English (US)

Page 2: [1] Formatted	mabrege	8/20/18 3:30:00 PM

English (US)

Page 2: [1] Formatted	mabrege	8/20/18 3:30:00 PM

English (US)

Page 2: [2] Formatted	mabrege	8/20/18 3:30:00 PM

English (US)

Page 2: [2] Formatted	mabrege	8/20/18 3:30:00 PM

English (US)

Page 2: [2] Formatted	mabrege	8/20/18 3:30:00 PM

English (US)

Page 2: [3] Formatted	mabrege	8/20/18 3:30:00 PM

English (US)

Page 2: [3] Formatted	mabrege	8/20/18 3:30:00 PM

English (US)

Page 2: [3] Formatted	mabrege	8/20/18 3:30:00 PM

English (US)

Page 2: [3] Formatted	mabrege	8/20/18 3:30:00 PM

English (US)

Page 2: [3] Formatted	mabrege	8/20/18 3:30:00 PM

English (US)

Page 2: [3] Formatted	mabrege	8/20/18 3:30:00 PM

English (US)

Page 2: [3] Formatted	mabrege	8/20/18 3:30:00 PM

English (US)

Page 2: [4] Formatted	mabrege	8/20/18 3:30:00 PM

English (US)

Page 2: [4] Formatted	mabrege	8/20/18 3:30:00 PM

English (US)

Page 2: [4] Formatted	mabrege	8/20/18 3:30:00 PM

English (US)

Page 2: [5] Formatted	mabrege	8/20/18 3:30:00 PM

English (US)

Page 2: [5] Formatted	mabrege	8/20/18 3:30:00 PM

English (US)

Page 2: [5] Formatted	mabrege	8/20/18 3:30:00 PM

English (US)

Page 2: [5] Formatted	mabrege	8/20/18 3:30:00 PM

English (US)

Page 2: [6] Formatted	mabrege	8/20/18 3:30:00 PM

English (US)

Page 2: [6] Formatted	mabrege	8/20/18 3:30:00 PM

English (US)

Page 2: [7] Formatted	mabrege	8/20/18 3:30:00 PM

English (US)

Page 2: [7] Formatted	mabrege	8/20/18 3:30:00 PM

English (US)

Page 2: [7] Formatted	mabrege	8/20/18 3:30:00 PM

English (US)

Page 2: [7] Formatted	mabrege	8/20/18 3:30:00 PM

English (US)

Page 2: [7] Formatted	mabrege	8/20/18 3:30:00 PM

English (US)

Page 2: [7] Formatted	mabrege	8/20/18 3:30:00 PM

English (US)

Page 2: [7] Formatted	mabrege	8/20/18 3:30:00 PM

English (US)

Page 2: [7] Formatted	mabrege	8/20/18 3:30:00 PM

English (US)

Page 2: [7] Formatted	mabrege	8/20/18 3:30:00 PM

English (US)

Page 2: [7] Formatted	mabrege	8/20/18 3:30:00 PM

English (US)

Page 2: [7] Formatted	mabrege	8/20/18 3:30:00 PM

English (US)

Page 2: [7] Formatted	mabrege	8/20/18 3:30:00 PM

English (US)

Page 2: [7] Formatted	mabrege	8/20/18 3:30:00 PM

English (US)

Page 2: [7] Formatted	mabrege	8/20/18 3:30:00 PM

English (US)

Page 2: [7] Formatted	mabrege	8/20/18 3:30:00 PM

English (US)

Page 3: [8] Formatted	mabrege	8/20/18 3:30:00 PM

English (US)

Page 3: [9] Formatted	mabrege	8/20/18 3:30:00 PM

English (US)

Page 3: [10] Formatted	mabrege	8/20/18 3:30:00 PM

English (US)

Page 3: [11] Formatted	mabrege	8/20/18 3:30:00 PM

English (US)

Page 3: [12] Formatted	mabrege	8/20/18 3:30:00 PM

English (US)

Page 3: [13] Formatted	mabrege	8/20/18 3:30:00 PM

English (US)

Page 3: [14] Deleted	mabrege	8/20/18 3:30:00 PM

The valley contains a mixture of dense population areas and intensively cultivated agricultural regions.

Page 3: [15] Formatted	mabrege	8/20/18 3:30:00 PM

English (US)

Page 3: [16] Formatted	mabrege	8/20/18 3:30:00 PM

English (US)

Page 3: [17] Formatted	mabrege	8/20/18 3:30:00 PM

English (US)

Page 3: [18] Formatted	mabrege	8/20/18 3:30:00 PM

English (US)

Page 3: [19] Formatted	mabrege	8/20/18 3:30:00 PM

English (US)

Page 3: [20] Formatted	mabrege	8/20/18 3:30:00 PM

English (US)

Page 3: [21] Formatted	mabrege	8/20/18 3:30:00 PM

English (US)

Page 3: [22] Formatted	mabrege	8/20/18 3:30:00 PM

English (US)

Page 3: [23] Formatted	mabrege	8/20/18 3:30:00 PM

English (US)

Page 3: [24] Formatted	mabrege	8/20/18 3:30:00 PM

English (US)

Page 3: [25] Formatted	mabrege	8/20/18 3:30:00 PM

English (US)

Page 3: [26] Formatted	mabrege	8/20/18 3:30:00 PM

English (US)

Page 3: [27] Formatted	mabrege	8/20/18 3:30:00 PM

English (US)

Page 3: [28] Formatted	mabrege	8/20/18 3:30:00 PM

English (US)

Page 3: [29] Formatted	mabrege	8/20/18 3:30:00 PM

English (US)

Page 3: [30] Formatted	mabrege	8/20/18 3:30:00 PM

English (US)

Page 3: [31] Formatted	mabrege	8/20/18 3:30:00 PM

English (US)

Page 3: [32] Formatted	mabrege	8/20/18 3:30:00 PM

English (US)

Page 3: [33] Formatted	mabrege	8/20/18 3:30:00 PM

English (US)

Page 3: [34] Formatted	mabrege	8/20/18 3:30:00 PM

English (US)

Page 3: [35] Formatted	**mabrege**	**8/20/18 3:30:00 PM**

English (US)

Page 3: [36] Formatted	**mabrege**	**8/20/18 3:30:00 PM**

English (US)

Page 3: [37] Formatted	**mabrege**	**8/20/18 3:30:00 PM**

English (US)

Page 3: [38] Formatted	**mabrege**	**8/20/18 3:30:00 PM**

English (US)

Page 3: [39] Formatted	**mabrege**	**8/20/18 3:30:00 PM**

English (US)

Page 3: [40] Formatted	**mabrege**	**8/20/18 3:30:00 PM**

English (US)

Page 3: [41] Formatted	**mabrege**	**8/20/18 3:30:00 PM**

English (US)

Page 3: [42] Formatted	**mabrege**	**8/20/18 3:30:00 PM**

English (US)

Page 3: [43] Formatted	**mabrege**	**8/20/18 3:30:00 PM**

English (US)

Page 6: [44] Formatted	**mabrege**	**8/20/18 3:30:00 PM**

English (US)

Page 6: [44] Formatted	**mabrege**	**8/20/18 3:30:00 PM**

English (US)

Page 6: [45] Formatted	**mabrege**	**8/20/18 3:30:00 PM**

English (US)

Page 6: [45] Formatted	**mabrege**	**8/20/18 3:30:00 PM**

English (US)

Page 6: [45] Formatted	**mabrege**	**8/20/18 3:30:00 PM**

English (US)

Page 6: [46] Formatted	**mabrege**	**8/20/18 3:30:00 PM**

English (US)

Page 6: [46] Formatted	**mabrege**	**8/20/18 3:30:00 PM**

English (US)

Page 6: [46] Formatted	mabrege	8/20/18 3:30:00 PM

English (US)

Page 6: [46] Formatted	mabrege	8/20/18 3:30:00 PM

English (US)

Page 6: [46] Formatted	mabrege	8/20/18 3:30:00 PM

English (US)

Page 6: [46] Formatted	mabrege	8/20/18 3:30:00 PM

English (US)

Page 6: [47] Formatted	mabrege	8/20/18 3:30:00 PM

Indent: First line: 0.5"

Page 6: [48] Formatted	mabrege	8/20/18 3:30:00 PM

English (US)

Page 6: [49] Formatted	mabrege	8/20/18 3:30:00 PM

English (US)

Page 6: [50] Formatted	mabrege	8/20/18 3:30:00 PM

English (US)

Page 6: [51] Formatted	mabrege	8/20/18 3:30:00 PM

English (US)

Page 6: [52] Formatted	mabrege	8/20/18 3:30:00 PM

English (US)

Page 6: [53] Formatted	mabrege	8/20/18 3:30:00 PM

English (US)

Page 6: [54] Formatted	mabrege	8/20/18 3:30:00 PM

English (US)

Page 6: [55] Formatted	mabrege	8/20/18 3:30:00 PM

English (US)

Page 6: [55] Formatted	mabrege	8/20/18 3:30:00 PM

English (US)

Page 6: [55] Formatted	mabrege	8/20/18 3:30:00 PM

English (US)

Page 6: [56] Formatted	mabrege	8/20/18 3:30:00 PM

English (US)

Page 6: [56] Formatted	mabrege	8/20/18 3:30:00 PM

English (US)

Page 6: [56] Formatted	mabrege	8/20/18 3:30:00 PM

English (US)

Page 6: [57] Formatted	mabrege	8/20/18 3:30:00 PM

English (US)

Page 6: [58] Formatted	mabrege	8/20/18 3:30:00 PM

English (US)

Page 6: [59] Formatted	mabrege	8/20/18 3:30:00 PM

English (US)

Page 6: [59] Formatted	mabrege	8/20/18 3:30:00 PM

English (US)

Page 6: [60] Formatted	mabrege	8/20/18 3:30:00 PM

English (US)

Page 6: [61] Formatted	mabrege	8/20/18 3:30:00 PM

English (US)

Page 6: [62] Formatted	mabrege	8/20/18 3:30:00 PM

English (US)

Page 6: [62] Formatted	mabrege	8/20/18 3:30:00 PM

English (US)

Page 6: [62] Formatted	mabrege	8/20/18 3:30:00 PM

English (US)

Page 6: [62] Formatted	mabrege	8/20/18 3:30:00 PM

English (US)

Page 6: [62] Formatted	mabrege	8/20/18 3:30:00 PM

English (US)

Page 6: [62] Formatted	mabrege	8/20/18 3:30:00 PM

English (US)

Page 6: [62] Formatted	mabrege	8/20/18 3:30:00 PM

English (US)

Page 6: [62] Formatted	mabrege	8/20/18 3:30:00 PM

English (US)

Page 6: [62] Formatted	mabrege	8/20/18 3:30:00 PM

English (US)

Page 6: [63] Formatted	mabrege	8/20/18 3:30:00 PM

English (US)

Page 6: [63] Formatted	mabrege	8/20/18 3:30:00 PM

English (US)

Page 6: [63] Formatted	mabrege	8/20/18 3:30:00 PM

English (US)

Page 6: [63] Formatted	mabrege	8/20/18 3:30:00 PM

English (US)

Page 6: [63] Formatted	mabrege	8/20/18 3:30:00 PM

English (US)

Page 6: [63] Formatted	mabrege	8/20/18 3:30:00 PM

English (US)

Page 6: [64] Formatted	mabrege	8/20/18 3:30:00 PM

English (US)

Page 6: [64] Formatted	mabrege	8/20/18 3:30:00 PM

English (US)

Page 6: [64] Formatted	mabrege	8/20/18 3:30:00 PM

English (US)

Page 6: [64] Formatted	mabrege	8/20/18 3:30:00 PM

English (US)

Page 6: [64] Formatted	mabrege	8/20/18 3:30:00 PM

English (US)

Page 6: [64] Formatted	mabrege	8/20/18 3:30:00 PM

English (US)

Page 6: [64] Formatted	mabrege	8/20/18 3:30:00 PM

English (US)

Page 6: [64] Formatted	mabrege	8/20/18 3:30:00 PM

English (US)

Page 6: [65] Formatted	mabrege	8/20/18 3:30:00 PM

English (US)

Page 6: [65] Formatted	mabrege	8/20/18 3:30:00 PM

English (US)

Page 6: [66] Formatted **mabrege** **8/20/18 3:30:00 PM**

English (US)

Page 6: [67] Formatted **mabrege** **8/20/18 3:30:00 PM**

English (US)

Page 6: [68] Formatted **mabrege** **8/20/18 3:30:00 PM**

English (US)

Page 6: [69] Deleted **mabrege** **8/20/18 3:30:00 PM**

based on the evaluation of the PM_1 organic aerosol composition in the winter

Page 6: [70] Formatted **mabrege** **8/20/18 3:30:00 PM**

English (US)

Page 6: [70] Formatted **mabrege** **8/20/18 3:30:00 PM**

English (US)

Page 6: [70] Formatted **mabrege** **8/20/18 3:30:00 PM**

English (US)

Page 6: [70] Formatted **mabrege** **8/20/18 3:30:00 PM**

English (US)

Page 6: [71] Deleted **mabrege** **8/20/18 3:30:00 PM**

Using PMF source apportionment, we observed the highest

Page 6: [72] Formatted **mabrege** **8/20/18 3:30:00 PM**

English (US)

Page 6: [73] Deleted **mabrege** **8/20/18 3:30:00 PM**

between 11 February 2013 and 20 February 2013. In particular, on 13 February 2013,

Page 6: [74] Formatted **mabrege** **8/20/18 3:30:00 PM**

English (US)

Page 6: [74] Formatted **mabrege** **8/20/18 3:30:00 PM**

English (US)

Page 6: [75] Formatted **mabrege** **8/20/18 3:30:00 PM**

English (US)

Page 6: [76] Formatted **mabrege** **8/20/18 3:30:00 PM**

English (US)

Page 6: [77] Formatted **mabrege** **8/20/18 3:30:00 PM**

English (US)

Page 6: [77] Formatted	mabrege	8/20/18 3:30:00 PM

English (US)

Page 9: [78] Formatted	mabrege	8/20/18 3:30:00 PM

English (US)

Page 9: [79] Formatted	mabrege	8/20/18 3:30:00 PM

English (US)

Page 9: [80] Formatted	mabrege	8/20/18 3:30:00 PM

English (US)

Page 9: [81] Formatted	mabrege	8/20/18 3:30:00 PM

English (US)

Page 9: [82] Formatted	mabrege	8/20/18 3:30:00 PM

English (US)

Page 9: [83] Formatted	mabrege	8/20/18 3:30:00 PM

English (US)

Page 9: [84] Formatted	mabrege	8/20/18 3:30:00 PM

English (US)

Page 9: [85] Formatted	mabrege	8/20/18 3:30:00 PM

English (US)

Page 9: [86] Formatted	mabrege	8/20/18 3:30:00 PM

English (US)

Page 9: [87] Formatted	mabrege	8/20/18 3:30:00 PM

English (US)

Page 9: [88] Formatted	mabrege	8/20/18 3:30:00 PM

English (US)

Page 9: [89] Formatted	mabrege	8/20/18 3:30:00 PM

English (US)

Page 9: [90] Formatted	mabrege	8/20/18 3:30:00 PM

English (US)

Page 9: [91] Formatted	mabrege	8/20/18 3:30:00 PM

English (US)

Page 9: [92] Formatted	mabrege	8/20/18 3:30:00 PM

English (US)

Page 9: [93] Formatted	mabrege	8/20/18 3:30:00 PM

English (US)

Page 9: [94] Formatted	**mabrege**	**8/20/18 3:30:00 PM**

English (US)

Page 9: [95] Formatted	**mabrege**	**8/20/18 3:30:00 PM**

English (US)

Page 9: [96] Formatted	**mabrege**	**8/20/18 3:30:00 PM**

English (US)

Page 9: [97] Formatted	**mabrege**	**8/20/18 3:30:00 PM**

English (US)

Page 9: [98] Formatted	**mabrege**	**8/20/18 3:30:00 PM**

English (US)

Page 9: [99] Formatted	**mabrege**	**8/20/18 3:30:00 PM**

English (US)

Page 9: [100] Formatted	**mabrege**	**8/20/18 3:30:00 PM**

English (US)

Page 9: [101] Formatted	**mabrege**	**8/20/18 3:30:00 PM**

English (US)

Page 9: [102] Formatted	**mabrege**	**8/20/18 3:30:00 PM**

English (US)

Page 9: [103] Formatted	**mabrege**	**8/20/18 3:30:00 PM**

English (US)

Page 9: [104] Formatted	**mabrege**	**8/20/18 3:30:00 PM**

English (US)

Page 9: [105] Formatted	**mabrege**	**8/20/18 3:30:00 PM**

English (US)

Page 9: [106] Formatted	**mabrege**	**8/20/18 3:30:00 PM**

English (US)

Page 9: [107] Formatted	**mabrege**	**8/20/18 3:30:00 PM**

English (US)

Page 9: [108] Formatted	**mabrege**	**8/20/18 3:30:00 PM**

English (US)

Page 12: [109] Formatted	**mabrege**	**8/20/18 3:30:00 PM**

English (US)

Page 12: [109] Formatted	mabrege	8/20/18 3:30:00 PM

English (US)

Page 12: [109] Formatted	mabrege	8/20/18 3:30:00 PM

English (US)

Page 12: [109] Formatted	mabrege	8/20/18 3:30:00 PM

English (US)

Page 12: [109] Formatted	mabrege	8/20/18 3:30:00 PM

English (US)

Page 12: [109] Formatted	mabrege	8/20/18 3:30:00 PM

English (US)

Page 12: [110] Formatted	mabrege	8/20/18 3:30:00 PM

English (US)

Page 12: [110] Formatted	mabrege	8/20/18 3:30:00 PM

English (US)

Page 12: [110] Formatted	mabrege	8/20/18 3:30:00 PM

English (US)

Page 12: [111] Deleted	mabrege	8/20/18 3:30:00 PM

; McNeill, 2015

Page 12: [111] Deleted	mabrege	8/20/18 3:30:00 PM

; McNeill, 2015

Page 12: [112] Deleted	mabrege	8/20/18 3:30:00 PM

Staudt

Page 12: [112] Deleted	mabrege	8/20/18 3:30:00 PM

Staudt

Page 12: [113] Deleted	mabrege	8/20/18 3:30:00 PM

Herckes et al., 2007; Gilardoni

Page 12: [113] Deleted	mabrege	8/20/18 3:30:00 PM

Herckes et al., 2007; Gilardoni

Page 12: [114] Deleted	mabrege	8/20/18 3:30:00 PM

Darer

Page 12: [114] Deleted	mabrege	8/20/18 3:30:00 PM

Darer

Page 12: [114] Deleted **mabrege** **8/20/18 3:30:00 PM**

Darer

Page 12: [114] Deleted **mabrege** **8/20/18 3:30:00 PM**

Darer

Page 12: [115] Formatted **mabrege** **8/20/18 3:30:00 PM**

English (US)

Page 12: [115] Formatted **mabrege** **8/20/18 3:30:00 PM**

English (US)

Page 12: [116] Formatted **mabrege** **8/20/18 3:30:00 PM**

English (US)

Page 12: [116] Formatted **mabrege** **8/20/18 3:30:00 PM**

English (US)

Page 12: [117] Formatted **mabrege** **8/20/18 3:30:00 PM**

English (US)

Page 12: [117] Formatted **mabrege** **8/20/18 3:30:00 PM**

English (US)

Page 12: [118] Formatted **mabrege** **8/20/18 3:30:00 PM**

English (US)

Page 12: [118] Formatted **mabrege** **8/20/18 3:30:00 PM**

English (US)

Page 12: [118] Formatted **mabrege** **8/20/18 3:30:00 PM**

English (US)

Page 12: [118] Formatted **mabrege** **8/20/18 3:30:00 PM**

English (US)

Page 12: [118] Formatted **mabrege** **8/20/18 3:30:00 PM**

English (US)

Page 12: [119] Deleted **mabrege** **8/20/18 3:30:00 PM**

It is possible that an enhanced oxidation from hydroxyl radicals and photolysis reactions played a role in the composition of this sample, as sunrise was ~3.5 hours before the sample collection ended.

Page 12: [120] Deleted **mabrege** **8/20/18 3:30:00 PM**

$C_{10}H_{10}O_7$, $C_{11}H_8O_7$, $C_{12}H_{14}O_9$, $C_{10}H_{18}O_5S$, $C_8H_{14}O_7S$, $C_8H_{12}O_7S$, $C_9H_{16}O_8S$,

Page 12: [121] Formatted **mabrege** **8/20/18 3:30:00 PM**

English (US)

Consistent with the fog samples, the average O:C and H:C values, and average number of oxygen atoms, were higher in the aged aerosol (BO0213D) than in the fresh aerosol (BO0204N). The influence of fresh biomass burning emissions is further supported by the higher average DBE, AI_{mod}, and average number of carbon atoms in BO0204N. These trends were clearly apparent for the CHO and CHNO groups, but less apparent for the CHOS and CHNOS groups. However, a low number of S-containing formulas were observed in BO0204N (~6%), which may have skewed these statistics. CHO and CHNO formulas in BO0204N clustered to the left of the O:C = 0.6 line in Fig. 5, indicating they were not very oxygenated. In contrast, the aged aerosol molecular formulas were distributed on and to the right of the O:C = 0.6 line. Additionally, there were more formulas above the H:C = 1.2 line in BO0213D compared to BO0204N. The distribution of CHOS and CHNOS formulas in the van Krevelen space was similar for BO0204N and BO0213D, however there was a greater number of formulas in the aged aerosol BO0213D.

Like the fog samples, more formulas that represent molecules with larger carbon backbones and higher DBE were found in the fresh aerosol sample compared to the aged aerosol sample, and molecular formulas that represent molecules with smaller carbon backbones that were more oxidized and oxygenated were comparatively more prevalent in the aged aerosol sample.

Page 13: [124] Formatted **mabrege** **8/20/18 3:30:00 PM**

English (US)

Page 13: [124] Formatted **mabrege** **8/20/18 3:30:00 PM**

English (US)

Page 13: [125] Deleted **mabrege** **8/20/18 3:30:00 PM**

). In BO0204N, these formulas were expected to be products of NO_X reactions and night-time nitrate radical reactions. Since BO0204N was collected during a period

Page 13: [126] Deleted **mabrege** **8/20/18 3:30:00 PM**

low relative humidity and had low aerosol liquid water, it seems unlikely that these products were formed by

Page 13: [127] Deleted **mabrege** **8/20/18 3:30:00 PM**

Less oxygenated species would be expected with little to no influence from aqueous phase secondary processes (Ervens et al., 2011; McNeill, 2015), such as observed in the low humidity and low aerosol liquid water conditions of the fresh aerosol in BO0204N. We also observed an overall decrease in the relative abundances of molecular formulas with DBE $\geq$ 5 in all samples except for BO0204N, where there was a secondary spike near DBE 10 (Fig.

Page 13: [128] Formatted **mabrege** **8/20/18 3:30:00 PM**

English (US)

Page 13: [128] Formatted **mabrege** **8/20/18 3:30:00 PM**

English (US)

Page 13: [129] Formatted **mabrege** **8/20/18 3:30:00 PM**

English (US)

Page 13: [129] Formatted **mabrege** **8/20/18 3:30:00 PM**

English (US)

Page 13: [130] Formatted **mabrege** **8/20/18 3:30:00 PM**

English (US)

Page 13: [130] Formatted **mabrege** **8/20/18 3:30:00 PM**

English (US)

Page 13: [131] Deleted **mabrege** **8/20/18 3:30:00 PM**

collected during daylight hours, implying that these N_2 and N_3 formulas are related to photochemical reactions.

Page 13: [132] Deleted **mabrege** **8/20/18 3:30:00 PM**

the formation of organosulfates and nitrooxy-organosulfates

Page 13: [133] Formatted **mabrege** **8/20/18 3:30:00 PM**

English (US)

Page 13: [133] Formatted **mabrege** **8/20/18 3:30:00 PM**

English (US)

Page 13: [133] Formatted	mabrege	8/20/18 3:30:00 PM

English (US)

Page 13: [133] Formatted	mabrege	8/20/18 3:30:00 PM

English (US)

Page 13: [133] Formatted	mabrege	8/20/18 3:30:00 PM

English (US)

Page 13: [133] Formatted	mabrege	8/20/18 3:30:00 PM

English (US)

Page 24: [134] Formatted Table	mabrege	8/20/18 3:30:00 PM

Formatted Table

Page 24: [135] Formatted	mabrege	8/20/18 3:30:00 PM

English (US)

Page 24: [136] Formatted	mabrege	8/20/18 3:30:00 PM

English (US)

Page 24: [137] Formatted	mabrege	8/20/18 3:30:00 PM

English (US)

Page 24: [138] Formatted	mabrege	8/20/18 3:30:00 PM

Left

Page 24: [139] Formatted	mabrege	8/20/18 3:30:00 PM

English (US)

Page 24: [140] Formatted	mabrege	8/20/18 3:30:00 PM

English (US)

Page 24: [141] Formatted	mabrege	8/20/18 3:30:00 PM

English (US)

Page 24: [142] Formatted	mabrege	8/20/18 3:30:00 PM

English (US)

Page 24: [143] Formatted	mabrege	8/20/18 3:30:00 PM

English (US)

Page 24: [144] Formatted	mabrege	8/20/18 3:30:00 PM

English (US)

Page 24: [145] Formatted	mabrege	8/20/18 3:30:00 PM

English (US)

Page 24: [146] Formatted	mabrege	8/20/18 3:30:00 PM

English (US)

Page 24: [147] Formatted	mabrege	8/20/18 3:30:00 PM

English (US)

Page 24: [148] Formatted	mabrege	8/20/18 3:30:00 PM

English (US)

Page 24: [149] Formatted	mabrege	8/20/18 3:30:00 PM

English (US)

Page 24: [150] Formatted	mabrege	8/20/18 3:30:00 PM

English (US)

Page 24: [151] Formatted	mabrege	8/20/18 3:30:00 PM

English (US)

Page 24: [152] Formatted	mabrege	8/20/18 3:30:00 PM

English (US)

Page 24: [153] Formatted	mabrege	8/20/18 3:30:00 PM

English (US)

Page 24: [154] Formatted	mabrege	8/20/18 3:30:00 PM

English (US)

Page 24: [155] Formatted	mabrege	8/20/18 3:30:00 PM

English (US)

Page 24: [156] Formatted	mabrege	8/20/18 3:30:00 PM

Left

Page 24: [157] Formatted	mabrege	8/20/18 3:30:00 PM

English (US)

Page 24: [158] Formatted	mabrege	8/20/18 3:30:00 PM

English (US)

Page 24: [159] Formatted	mabrege	8/20/18 3:30:00 PM

English (US)

Page 24: [160] Formatted	mabrege	8/20/18 3:30:00 PM

English (US)

Page 24: [161] Formatted	mabrege	8/20/18 3:30:00 PM

English (US)

Page 24: [162] Formatted	mabrege	8/20/18 3:30:00 PM

English (US)

Page 24: [163] Formatted	mabrege	8/20/18 3:30:00 PM

English (US)

Page 24: [164] Formatted	mabrege	8/20/18 3:30:00 PM

English (US)

Page 24: [165] Formatted	mabrege	8/20/18 3:30:00 PM

English (US)

Page 24: [166] Formatted	mabrege	8/20/18 3:30:00 PM

English (US)

Page 24: [167] Formatted	mabrege	8/20/18 3:30:00 PM

English (US)

Page 24: [168] Formatted	mabrege	8/20/18 3:30:00 PM

English (US)

Page 24: [169] Formatted	mabrege	8/20/18 3:30:00 PM

English (US)

Page 24: [170] Formatted	mabrege	8/20/18 3:30:00 PM

English (US)

Page 24: [171] Formatted	mabrege	8/20/18 3:30:00 PM

English (US)

Page 24: [172] Formatted	mabrege	8/20/18 3:30:00 PM

English (US)

Page 24: [173] Formatted	mabrege	8/20/18 3:30:00 PM

English (US)

Page 24: [174] Formatted	mabrege	8/20/18 3:30:00 PM

English (US)

Page 24: [175] Formatted	mabrege	8/20/18 3:30:00 PM

English (US)

Page 24: [176] Formatted	mabrege	8/20/18 3:30:00 PM

Left

Page 24: [177] Formatted	mabrege	8/20/18 3:30:00 PM

English (US)

Page 24: [178] Formatted	mabrege	8/20/18 3:30:00 PM

English (US)

Page 24: [179] Formatted	mabrege	8/20/18 3:30:00 PM

English (US)

Page 24: [180] Formatted	mabrege	8/20/18 3:30:00 PM

English (US)

Page 24: [181] Formatted	mabrege	8/20/18 3:30:00 PM

English (US)

Page 24: [182] Formatted	mabrege	8/20/18 3:30:00 PM

English (US)

Page 24: [183] Formatted	mabrege	8/20/18 3:30:00 PM

English (US)

Page 24: [184] Formatted	mabrege	8/20/18 3:30:00 PM

English (US)

Page 24: [185] Formatted	mabrege	8/20/18 3:30:00 PM

English (US)

Page 24: [186] Formatted	mabrege	8/20/18 3:30:00 PM

English (US)

Page 24: [187] Formatted	mabrege	8/20/18 3:30:00 PM

English (US)

Page 24: [188] Formatted	mabrege	8/20/18 3:30:00 PM

English (US)

Page 24: [189] Formatted	mabrege	8/20/18 3:30:00 PM

English (US)

Page 24: [190] Formatted	mabrege	8/20/18 3:30:00 PM

English (US)

Page 24: [191] Formatted	mabrege	8/20/18 3:30:00 PM

English (US)

Page 24: [192] Formatted	mabrege	8/20/18 3:30:00 PM

English (US)

Page 24: [193] Formatted	mabrege	8/20/18 3:30:00 PM

English (US)

Page 24: [194] Formatted	mabrege	8/20/18 3:30:00 PM

Left

Page 25: [195] Deleted	mabrege	8/20/18 3:30:00 PM

Table 3: Summary of the possible identified molecular formulas from the present study. Identical formulas from the literature are provided with their references. Additional possible identified molecular formulas are listed in Table S1.

Formula	SPC0106F	SPC0201F	BO0204N	BO0213D	Possible Identity	Reference
$C_6H_4N_2O_5$	X	X	X	X	2,4-dinitrophenol	a
$C_6H_5NO_3$	X	X	X	X	4-nitrophenol	a, b
$C_6H_5NO_4$	X	X	X	X	4-nitrocatechol	b
$C_6H_6O_3$				X	phenol SOA (pyrogallol)	c-e
$C_6H_6O_4$		X		X	phenol SOA	
$C_6H_6O_5$				X	phenol SOA	f
$C_6H_{10}O_5$		X		X	levoglucosan	b-e, g, h
$C_7H_5NO_5$	X	X	X	X	3-nitrosalicylic acid	a
$C_7H_6O_2$	X	X		X	benzoic acid	b, h
$C_7H_6O_3$	X	X	X	X	4-hydroxybenzoic acid	c-f
$C_7H_7NO_3$	X	X	X	X	2-methyl-4-nitrophenol	a, b
$C_7H_7NO_4$	X	X	X	X	4-nitroguaiacol	a
$C_7H_8O_3$	X	X		X	guaiacol SOA	
$C_7H_8O_4$	X	X	X	X	guaiacol SOA	
$C_7H_8O_5$	X	X	X	X	guaiacol SOA	
$C_7H_8O_6$	X	X		X	guaiacol SOA	
$C_7H_{12}O_5$		X	X	X	3-hydroxy-4,4-dimethylglutaric acid	i
$C_8H_6O_4$	X	X	X	X	phthalic acid	b-e, h
$C_8H_8O_2$	X	X	X	X	o-toluic acid	b, h
$C_8H_8O_3$	X	X	X	X	vanillin	b-e
$C_8H_8O_4$	X	X	X	X	vanillic acid	c-e, g, h
$C_8H_{10}O_3$	X	X		X	syringol	f-h, j
$C_8H_{10}O_4$	X	X		X	syringol SOA	
$C_8H_{10}O_5$	X	X	X	X	syringol aqSOA	j
$C_8H_{10}O_6$	X	X	X	X	syringol aqSOA	f
$C_8H_{10}O_7$		X		X	syringol aqSOA	f
$C_8H_{12}O_6$	X	X	X	X	3-methyl-1,2,3-butanetricarboxylic acid	i
$C_9H_8O_3$	X	X	X	X	coumaryc acid	b-e
$C_9H_{10}O_3$	X	X	X	X	acetovanillone	c-e, f, j, k
$C_9H_{10}O_4$	X	X	X	X	syringaldehyde	c-e, g, h, j
$C_9H_{10}O_5$	X	X	X	X	syringic acid	c-e, g, h
$C_9H_{11}NO_3$	X	X	X	X	tyrosine	
$C_9H_{12}O_3$	X	X		X	4-methylsyringol	h

$C_9H_{14}O_3$	X	X		X	ketolimononaldehyde	l
$C_9H_{14}O_4$	X	X		X	pinic acid	i
$C_9H_{16}O_4$	X	X	X	X	azelaic acid	c-e, h
$C_{10}H_{12}O_2$	X	X		X	eugenol	h
$C_{10}H_{12}O_4$	X	X	X	X	acetosyringone	c-e
$C_{10}H_{14}O_3$	X	X		X	ketopinic acid	i
$C_{10}H_{16}O_3$	X	X		X	pinonic acid	c-e, i

*References are (a) Kitanovski et al. (2012); (b) Desyaterik et al. (2013); (c) Pietrogrande et al. (2014a); (d) Pietrogrande et al. (2014b); (e) Pietrogrande et al. (2015); (f) Yu et al. (2016); (g) Dzepina et al. (2015); (h) Mazzoleni et al. (2007); (i) He et al. (2014); (j) Yu et al. (2014); (k) Lin et al. (2015); and (l) Nguyen et al. (2013).

Style Definition: EndNote Bibliography Title: Font: 11 pt
Style Definition: EndNote Bibliography: Font: 11 pt
Formatted: Different first page header
Formatted: Suppress line numbers

Supplemental Information

Molecular insights on aging and aqueous phase processing from ambient biomass burning emissions-influenced Po Valley fog and aerosol

Matthew Brege[1], Marco Paglione[2], Stefania Gilardoni[2], Stefano Decesari[2], Maria Cristina Facchini[2], and Lynn R. Mazzoleni[1,3]

[1]Department of Chemistry, Michigan Technological University, Houghton, MI, USA.
[2]Institute of Atmospheric Sciences and Climate, Italian National Research Council, Bologna, Italy.
[3]Atmospheric Sciences Program, Michigan Technological University, Houghton, MI, USA.

Correspondence to: Lynn R. Mazzoleni (lrmazzol@mtu.edu)

Table of Contents

1. FT-ICR MS data processing and molecular formula assignment review

The individual transient scans of FT-ICR MS data for each sample were reviewed manually and the unacceptable scans with an abrupt change in the total ion current were removed; the remaining transient scans were co-added together to create the working file for each sample (this helped to increase signal to noise and enhance sensitivity). Molecular formula assignments were made as previously described (Mazzoleni et al., 2010; Putman et al., 2012; Zhao et al., 2013; Dzepina et al., 2015) using Sierra Analytics Composer software (version 1.0.5) within the limits of: $C_{2\text{-}200}H_{4\text{-}1000}O_{1\text{-}20}N_{0\text{-}3}S_{0\text{-}1}$. Masses were calculated from measured *m/z* values, assuming an ion charge of -1 from the electrospray. The calculator uses a CH_2 Kendrick mass defect (KMD) analysis to sort homologous ion series and extend the molecular formula assignments to higher masses (Hughey et al., 2001; Kujawinski and Behn, 2006). A de novo cut-off at *m/z* 500 was applied, indicating that no new formula assignments would occur above *m/z* 500, unless the formula was part of an existing CH_2 homologous series that began at a point lower than *m/z* 500. This is necessary because the number of possible molecular formulas increases at higher values. The minimum relative abundance required for molecular formula assignment was > 10 times the estimated signal-to-noise ratio, determined for each sample between *m/z* 900–1000. Only integer values up to 40 were allowed for the double bond equivalents (DBE). The data set was manually reviewed to remove: formulas with an absolute error > 3 ppm, elemental ratios that were not chemically sensible (such as O:C > 3 or H:C < 0.3), and formulas which violated the rule of 13 or violated the nitrogen rule. The rule of 13 checks for a reasonable number of heteroatoms in a formula. A base formula (C_nH_{n+r}) can be generated for any measured mass by solving: $\frac{M}{13} = n + \frac{r}{13}$ (Pavia, 2009). Then, the maximum number of "large atoms" (C, O, N, S) in a formula is defined as the mass divided by 13, because substituting for a heteroatom (O, N or S) involves a substitution for at least one carbon. This maximum number is then compared to the actual number of "large atoms" in a formula, and those formulas exceeding the maximum number are rejected. The nitrogen rule removes formulas with odd masses that do not contain an odd number of nitrogen atoms, and even masses that do not contain an even number (or no) nitrogen atoms; this is due to the odd numbered valence of nitrogen (Pavia, 2009). Molecular formulas that contained ^{13}C or ^{34}S were also removed from the data set. Homologous series with large gaps in the DBE trend were removed, as well as homologous series with a length of one. The assigned formulas were also analyzed with consideration to the DBE and oxygen number trends, (Herzsprung et al., 2014) where unreliable formula assignments were also removed.

2. Ultrahigh resolution FT-ICR MS results

The total ion abundance of the identified monoisotopic molecular formulas reported for each sample was determined by their summation. Then, these values were used to normalize the individual ion abundances within each sample using a ratio of the individual ion intensity to this total ion abundance. Then, the values were rescaled using a normalization constant (10,000). This normalization procedure was done to remove analytical biases introduced by trace contaminants with high electrospray efficiency.

Reconstructed difference mass spectra of the assigned molecular formulas for both fog and aerosol samples are shown in Fig. S3. These difference mass spectra permit a direct comparison of the samples using normalized

Deleted: and the

Deleted: →

Formatted: Indent: First line: 0.5"

relative abundances. The individual relative abundances were normalized by the total abundance of the assigned molecular formulas identified in each of the samples. In Fig. S3, the individual masses with higher abundances in either the positive or negative direction were substantially greater in one of the two samples, whereas the masses of similar abundance tended to cancel each other. To enhance the interpretation of the compositional differences, the individual masses were color-coded to represent the number of oxygen atoms in the assigned formula. Overall, we observed higher numbers of oxygen in the masses of the two samples with aged biomass burning emissions influence compared to the two samples with fresh biomass burning emissions influence. The molecular formulas assigned to the fresh samples had approximately 0-5 oxygen atoms over the mass range of 50-250 Da, 5-10 oxygen atoms over 250-550 Da, and a few molecular formulas were assigned with 10-15 oxygen atoms over 500-600 Da. In contrast, the aged samples had a large number of molecular formulas with 10-15 oxygen atoms in the range of 400-550 Da. This clearly shows a greater amount of oxidation in the aged influenced samples compared to the fresh influenced samples.

KMD diagrams can be used as useful tools to visualize the relationships between the many molecular formulas of complex mixtures such as atmospheric samples. We used Kendrick mass defect to sort the molecular formulas into CH_2 homologous series of identical heteroatom content and DBE, where the formulas in the same series differ only by a number of CH_2 units (Stenson et al., 2003). It should be noted that the presence of multiple formulas in the same homologous series does not necessarily imply a related chemical structure. The homologous series are visible as horizontal rows of formulas in Figs. S6 and S7. There were multiple homologous series per subclass, where the base formula for each series differ in DBE and increase in KMD to form an ensemble of "steps" within each subclass. In our samples individual CHO and CHNO subclasses had approximately 5-16 different homologous series, while CHOS and CHNOS subclasses had approximately 3-10 different homologous series. The number of homologous series in a subclass increased with oxygen number, and peaked near the median oxygen number, then decreased again towards the maximum number of oxygen; this led to fewer molecular formulas in subclasses with higher and lower oxygen numbers, and more formulas in subclasses near the median oxygen number. The subclasses with the highest numbers of molecular formulas per elemental group were: O_7, NO_8, O_7S and NO_9S. It was atypical for the unique formulas of a sample to be completely unrelated to other formulas across the data set; often the unique formulas were extensions of homologous series that appeared across samples.

Deleted: (Stenson et al., 2003)

3. FT-ICR MS data set

An abbreviated list of the complete FT-ICR MS dataset is provided and is available on Digital Commons: http://digitalcommons.mtu.edu/chemistry-fp/98/

4. Supplemental Figures and tables

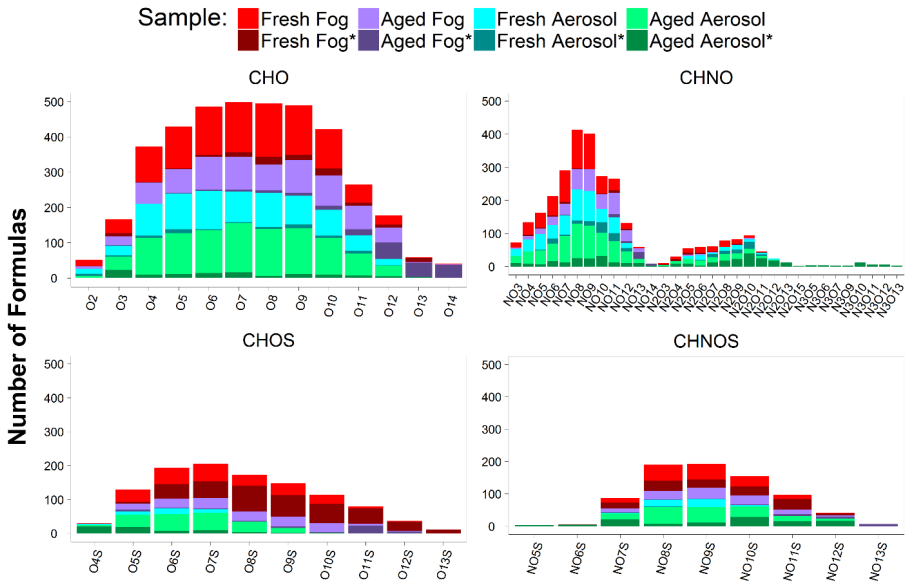

Figure S1: Distributions of the molecular formulas within all 64 elemental group subclasses for CHO, CHNO, CHOS and CHNOS groups as indicated in the Figure. The total number of molecular formulas for each SPE-recovered WSOC sample were split into two groups of unique and non-unique formulas; the darker shade represents formulas unique to a sample, (denoted in the Figure legend with an asterisk after the sample name, e.g. "Fresh Fog*") while the lighter shade represents common formulas. The sample names Fresh Fog, Aged Fog, Fresh Aerosol, and Aged Aerosol correspond to SPC0106F, SPC0201F, BO0204N, and BO0213D, respectively.

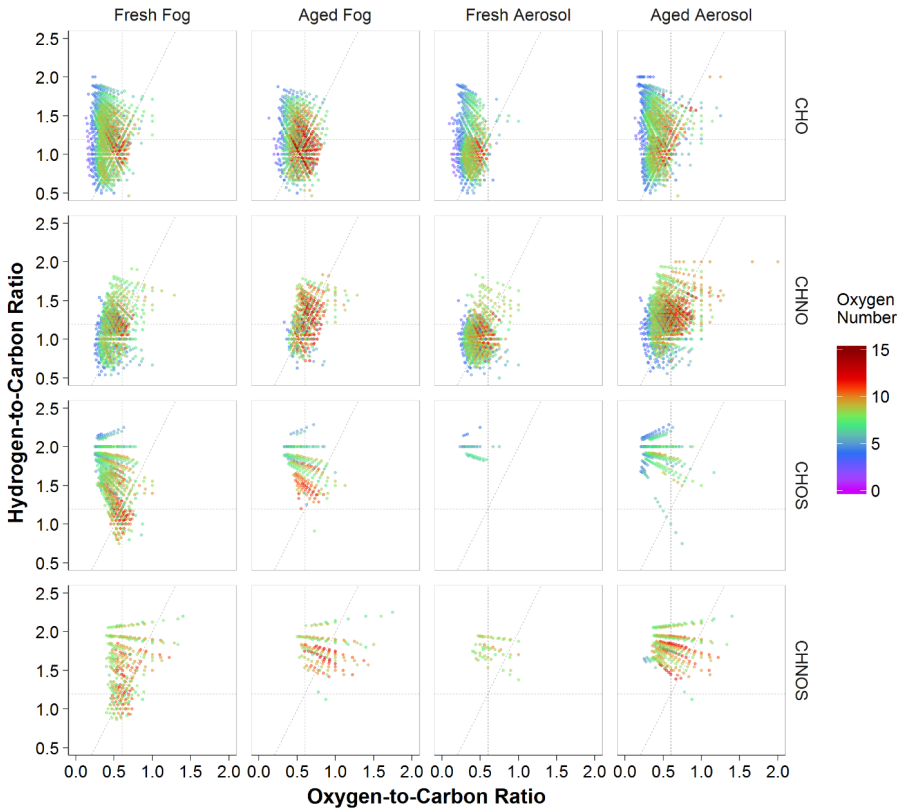

Figure S2: van Krevelen diagrams for the SPE-recovered WSOC by elemental group (rows) and sample (columns) as indicated in the Figure. Dashed lines represent H:C = 1.2 (horizontal), O:C = 0.6 (vertical) and OS_C = 0 (diagonal) as described in Tu et al. (2016). Formulas are color scaled to the number of oxygen atoms in the assigned formula. The sample names Fresh Fog, Aged Fog, Fresh Aerosol, and Aged Aerosol correspond to SPC0106F, SPC0201F, BO0204N, and BO0213D, respectively.

Deleted: Tu et al. (2016)

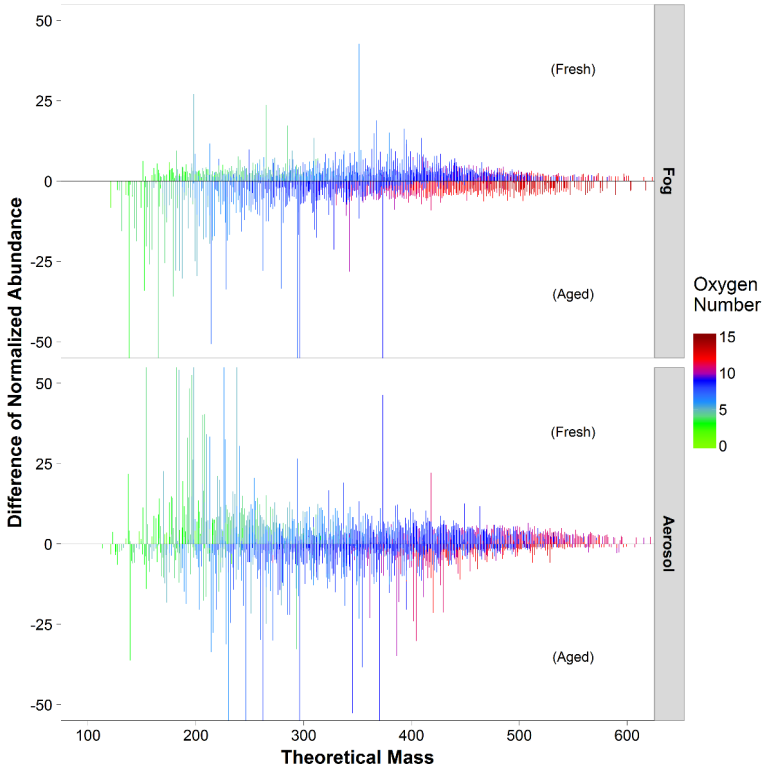

Figure S3: Reconstructed difference mass spectra for theoretical masses of assigned molecular formulas in the Po Valley samples with normalized relative abundance. Fresh influenced samples (SPC0106F and BO0204N) are plotted with positive abundance and aged influenced samples (SPC0201F and BO0213D) are plotted with negative abundance. Molecular compositions in both samples with the same mass and similar normalized relative abundance are reduced toward zero. The peaks in the mass spectra are color scaled to the number of oxygen atoms in the assigned molecular formula, where it can be observed that the aged samples shift towards species with higher oxygen numbers at lower masses, compared to the fresh samples. The sample names Fresh Fog, Aged Fog, Fresh Aerosol, and Aged Aerosol correspond to SPC0106F, SPC0201F, BO0204N, and BO0213D, respectively.

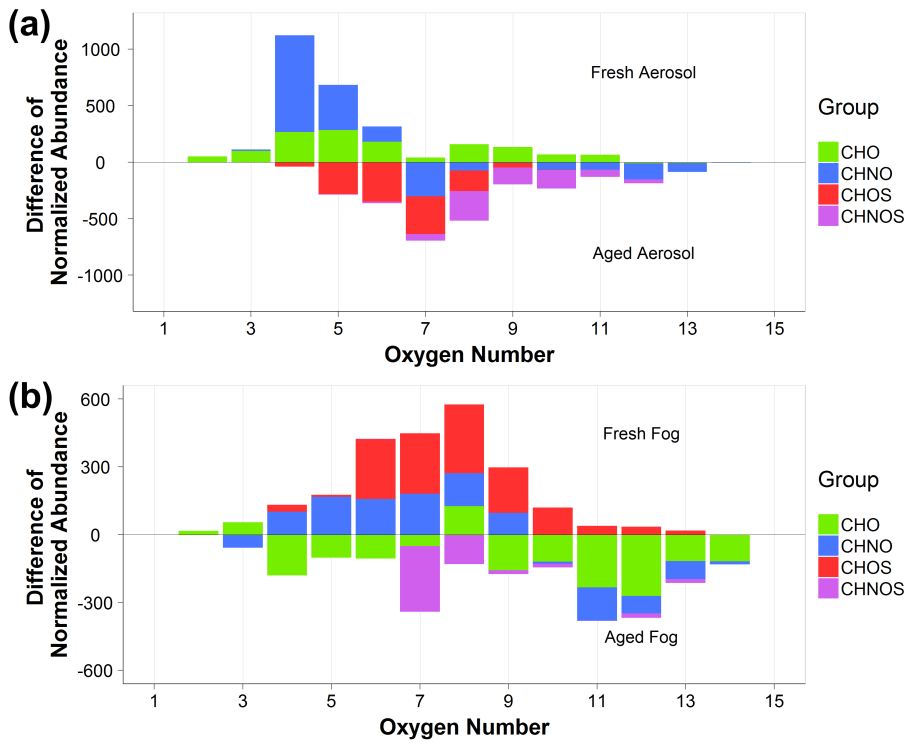

Figure S4: Oxygen difference trends for aerosol (a) and fog (b) samples. Abundance trends were calculated as in Figure 6 of the main text, and then the respective aged sample normalized abundance was subtracted from the fresh sample normalized abundance for each oxygen number value. A positive difference of abundance indicates an enhanced abundance of formulas in the fresh sample compared to the aged sample. Similarly, a negative difference of abundance indicates an enhanced abundance of formulas in the aged sample compared to the fresh sample. The sample names Fresh Fog, Aged Fog, Fresh Aerosol, and Aged Aerosol correspond to SPC0106F, SPC0201F, BO0204N, and BO0213D, respectively.

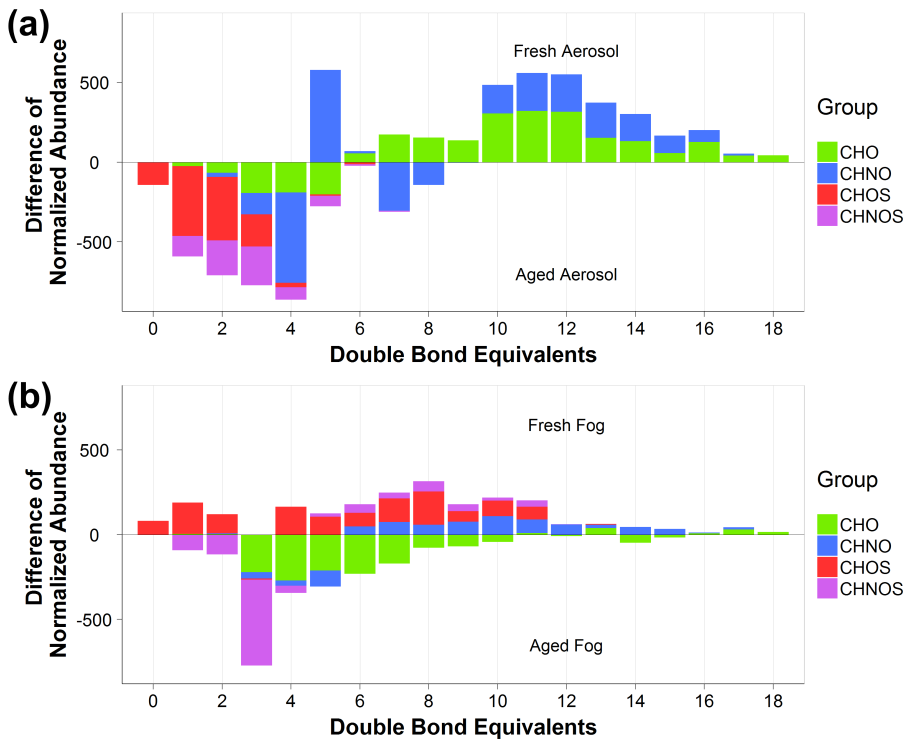

Figure S5: Double bond equivalent difference trends for aerosol (a) and fog (b) samples. Abundance trends were calculated as in Figure 6 of the main text, and then the respective aged sample normalized abundance was subtracted from the fresh sample normalized abundance for each integer double bond equivalent value. A positive difference of abundance indicates an enhanced abundance of formulas in the fresh sample compared to the aged sample. Similarly, a negative difference of abundance indicates an enhanced abundance of formulas in the aged sample compared to the fresh sample. The sample names Fresh Fog, Aged Fog, Fresh Aerosol, and Aged Aerosol correspond to SPC0106F, SPC0201F, BO0204N, and BO0213D, respectively.

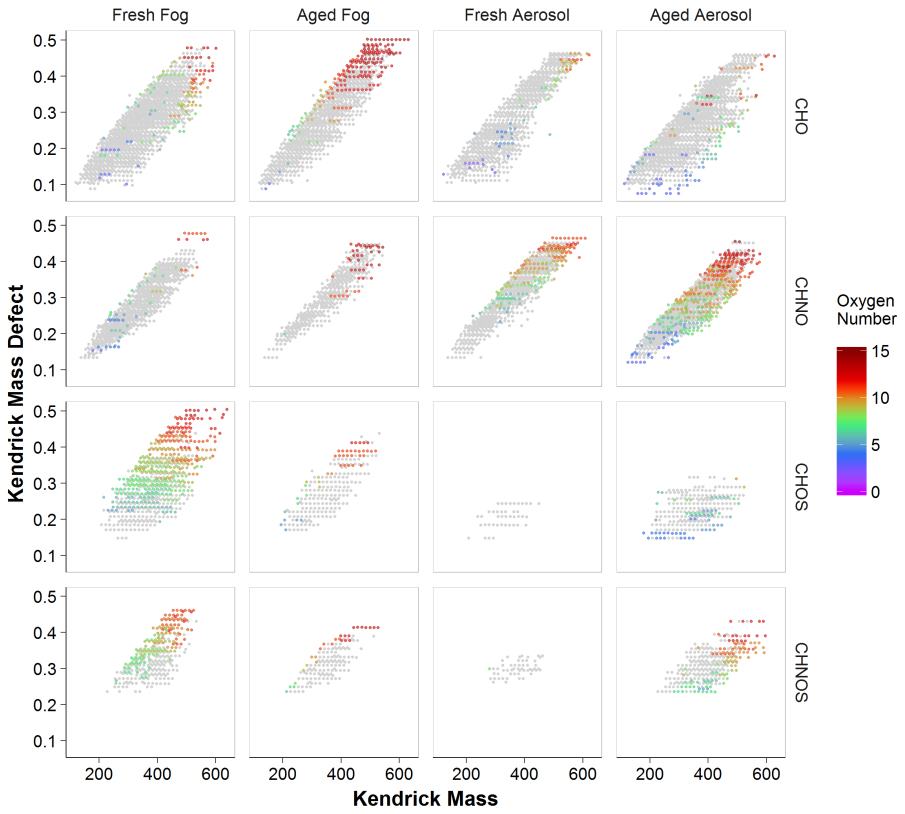

Figure S6: Kendrick mass defect diagrams for each of the Po Valley samples, partitioned by elemental group (rows) and sample (columns) as indicated in the Figure. The molecular formulas unique to each sample are color scaled to the number of oxygen atoms in the assigned formula; grey points represent formulas which are common. Homologous series of molecular formulas are visible as horizontal rows of points, where formulas which are unique to a sample may make up all or only part of an individual homologous series. The sample names Fresh Fog, Aged Fog, Fresh Aerosol, and Aged Aerosol correspond to SPC0106F, SPC0201F, BO0204N, and BO0213D, respectively.

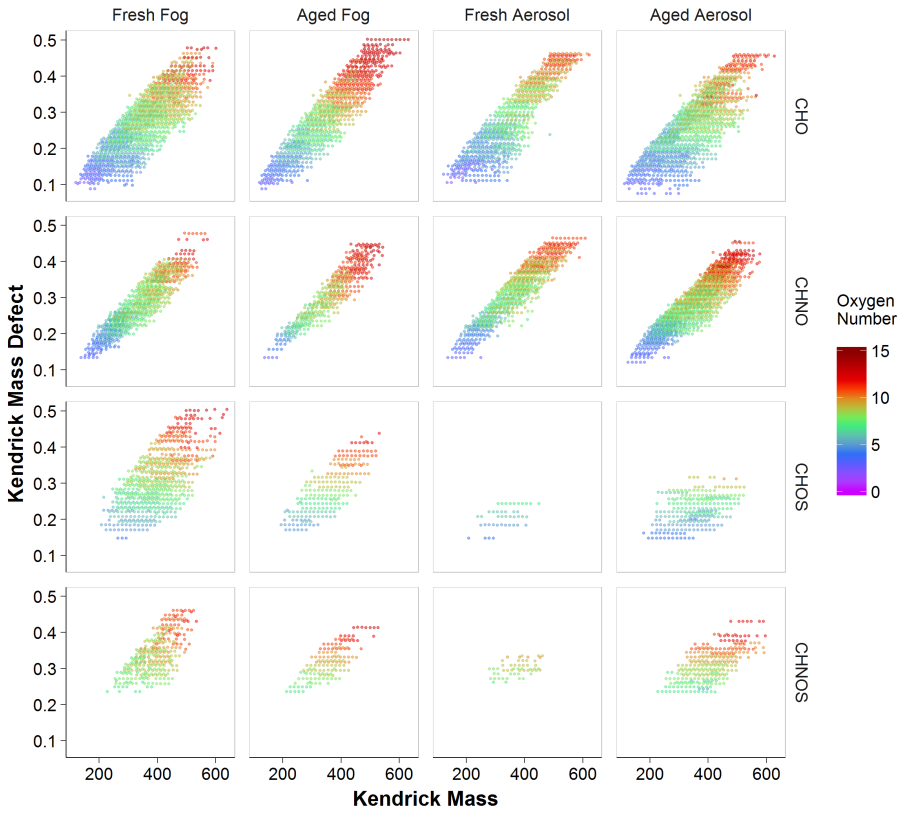

Figure S7: Kendrick mass defect diagrams for each of the Po Valley samples, partitioned by elemental group (rows) and sample (columns) as indicated in the Figure. Molecular formulas are color scaled to the number of oxygen atoms in the assigned formula. The sample names Fresh Fog, Aged Fog, Fresh Aerosol, and Aged Aerosol correspond to SPC0106F, SPC0201F, BO0204N, and BO0213D, respectively.

Table S1: Summary of the literature structural insights associated with the identified molecular formulas observed in this study. Because the identified molecular formulas may represent a variety of structural isomers, we note that matched molecular formulas do not necessarily correspond to the same molecular structure or atmospheric origin. The normalized abundances are indicated for each sample, where "ND" (not detected), "Low" (≤ 3%), "Med", (> 3% and ≤ 15%), "High" (> 15% and ≤ 50%) and "Very High" (> 50%). Molecular formulas from the literature are provided with their references.

Formula	SPC0106F	SPC0201F	BO0204N	BO0213D	Possible Identity	Reference*
$C_4H_6O_5$	ND	ND	ND	Low	syringol aqSOA	A
$C_5H_6O_3$	ND	ND	ND	Low	ambient cloud water	B
$C_5H_6O_4$	ND	Low	ND	Low	syringol aqSOA	A, B
$C_5H_6O_5$	ND	ND	ND	Low	syringol aqSOA (ketoglutaric acid)	A, C-E
$C_5H_8O_4$	ND	Med	ND	Low	ambient cloud water (methylsuccinic acid and glutatric acid)	B-F
$C_5H_8O_5$	ND	ND	ND	Low	ambient cloud water (hydroxyglutaric acid)	B, G
$C_6H_4N_2O_5$	High	Med	Low	Low	dinitrophenol	H
$C_6H_5NO_3$	High	High	Med	Med	nitrophenol	B, H
$C_6H_5NO_4$	High	High	Very High	Med	nitrocatechol	B, H
$C_6H_5NO_5$	ND	ND	Med	Low	ambient cloud water	B
$C_6H_6O_3$	ND	ND	ND	Low	pyrogallol	C-E
$C_6H_6O_4$	ND	Low	ND	Med	phenol SOA	
$C_6H_6O_5$	ND	ND	ND	Low	syringol aqSOA	A
$C_6H_8O_4$	Low	Med	ND	Med	ambient cloud water	B
$C_6H_8O_6$	ND	ND	ND	Low	syringol aqSOA	A
$C_6H_{10}O_3$	ND	Low	ND	Low	ambient cloud water	B
$C_6H_{10}O_4$	ND	Med	ND	Low	ambient cloud water (methylglutaric acid and adipic acid)	B-F
$C_6H_{10}O_5$	ND	Low	ND	Low	levoglucosan	B-F, I
$C_6H_{10}O_6$	ND	ND	ND	Low	dimethyltartaric acid	J
$C_7H_5NO_5$	High	Med	Med	Med	nitrosalicylic acid	H
$C_7H_6O_2$	Med	Med	ND	Low	ambient cloud water (benzoic acid)	B, F
$C_7H_6O_3$	Med	Med	Med	Med	phenol aqSOA (dihydroxybenzaldehyde and hydroxybenzoic acid)	A, C-E
$C_7H_6O_4$	Med	Low	Low	Med	phenol aqSOA	A

Deleted: possible
Deleted: from the present
Deleted: Identical
Formatted: Font: Not Bold

Formula	SPC0106F	SPC0201F	BO0204N	BO0213D	Possible Identity	Reference*
$C_7H_6O_5$	ND	Low	ND	Low	syringol aqSOA	K
$C_7H_6N_2O_5$	Med	Med	Med	Low	ambient cloud water	B, L
$C_7H_6N_2O_6$	Med	ND	Med	Low	ambient cloud water	B, L
$C_7H_7NO_3$	High	High	Med	High	methyl-nitrophenol	B, H
$C_7H_7NO_4$	High	Med	Med	Med	ambient cloud water (nitroguaiacol and methyl-nitrocatechol)	B,H
$C_7H_7NO_5$	Med	Low	Med	Med	ambient cloud water	B
$C_7H_8O_3$	Med	Low	ND	High	guaiacol SOA	
$C_7H_8O_4$	Med	Med	Low	Low	guaiacol SOA	
$C_7H_8O_5$	Low	Med	Low	Med	guaiacol SOA	
$C_7H_8O_6$	Low	Low	ND	Med	guaiacol SOA	
$C_7H_{10}O_4$	Low	Med	Low	Med	ambient cloud water	L
$C_7H_{10}O_6$	Low	Low	Low	Med	guaiacol aqSOA	A
$C_7H_{12}O_4$	ND	Med	ND	Low	ambient cloud water (pimelic acid)	C-E, L
$C_7H_{12}O_5$	ND	Low	Low	Med	biogenic SOA (hydroxy-dimethylglutaric acid)	G
$C_7H_{12}O_6S$	ND	Low	ND	Low	ambient cloud water	L
$C_7H_{12}O_7$	Low	ND	ND	ND	syringol aqSOA	A
$C_7H_{14}O_5S$	Low	Med	ND	Low	dodecane aqSOA	L
$C_7H_{14}O_6S$	ND	Low	ND	Low	ambient cloud water	L
$C_8H_5NO_4$	Med	Low	Med	Low	ambient cloud water	B
$C_8H_6O_3$	Med	Med	Low	Low	ambient cloud water and guaiacol aqSOA	A, B
$C_8H_6O_4$	Med	Very High	Low	Low	ambient cloud water (phthalic acid)	B-F
$C_8H_6O_5$	Med	Med	ND	Low	phenol aqSOA	A
$C_8H_7NO_3$	Med	ND	Med	High	ambient cloud water	B
$C_8H_7NO_4$	Med	Med	Med	High	ambient cloud water	B
$C_8H_7NO_5$	High	Med	Med	High	ambient cloud water	B
$C_8H_8O_2$	Med	Med	Low	Low	ambient cloud water (o-toluic acid)	B, F
$C_8H_8O_3$	High	Med	Med	Low	ambient cloud water (vanillin)	B-E

Formula	SPC0106F	SPC0201F	BO0204N	BO0213D	Possible Identity	Reference*
$C_8H_8O_4$	Med	Med	Low	Low	vanillic acid	C-F, I
$C_8H_9NO_3$	Med	Med	Med	Low	ambient cloud water	B
$C_8H_9NO_4$	High	Med	Very High	High	ambient cloud water	B
$C_8H_9NO_5$	High	Med	High	High	ambient cloud water	B
$C_8H_{10}O_3$	Med	Low	ND	Low	syringol	A,F, I, K
$C_8H_{10}O_4$	Low	Med	ND	Low	syringol SOA	
$C_8H_{10}O_5$	Med	Med	Low	Med	syringol aqSOA	K-L
$C_8H_{10}O_6$	Low	Med	Low	Med	syringol aqSOA	A
$C_8H_{10}O_7$	ND	Low	ND	Low	syringol aqSOA	A
$C_8H_{12}O_6$	Med	Med	Low	Med	biogenic SOA (methyl-butanetricarboxylic acid)	G
$C_8H_{12}O_7S$	ND	Low	ND	ND	ambient cloud water	L
$C_8H_{12}O_8S$	Med	Low	ND	Low	ambient cloud water	L
$C_8H_{14}O_6S$	Low	Med	ND	Low	ambient cloud water	L
$C_8H_{14}O_7$	Med	ND	ND	ND	methylglyceric acid dimer	J
$C_8H_{14}O_7S$	ND	Low	ND	ND	ambient cloud water	L
$C_8H_{16}O_6S$	Med	Med	Low	Med	ambient cloud water	M
$C_9H_7NO_4$	Med	Low	Med	Low	ambient cloud water	B
$C_9H_8O_2$	Med	Low	Low	ND	ambient cloud water	B
$C_9H_8O_3$	Med	Med	Med	Med	ambient cloud water (coumaryc acid)	B-E
$C_9H_8N_2O_6$	Low	ND	Low	Med	ambient cloud water	L
$C_9H_9NO_3$	Med	ND	Low	Med	ambient cloud water	B
$C_9H_9NO_3$	Med	ND	Low	Med	laboratory brown carbon aqSOA	N
$C_9H_9NO_4$	Med	Low	Med	Med	ambient cloud water	B
$C_9H_{10}O_3$	Med	Low	Low	Low	laboratory brown carbon aqSOA (acetovanillone and dimethoxybenzaldehyde)	A, C-F, K, O
$C_9H_{10}O_4$	Med	Med	Low	Low	syringol aqSOA (syringaldehyde)	C-F, I, K
$C_9H_{10}O_5$	Med	Med	Low	Low	syringic acid	C-F, I
$C_9H_{11}NO_3$	Med	Low	Low	Med	tyrosine	

Formula	SPC0106F	SPC0201F	BO0204N	BO0213D	Possible Identity	Reference*
$C_9H_{11}NO_4$	Med	Low	Med	Med	ambient cloud water	B
$C_9H_{12}O_3$	Low	Low	ND	Low	methylsyringol	F
$C_9H_{12}O_5$	Med	Med	Low	Low	ambient cloud water	L
$C_9H_{12}O_7S$	Low	ND	ND	ND	ambient cloud water	L
$C_9H_{12}N_2O_3$	ND	ND	ND	Low	laboratory brown carbon aqSOA	O
$C_9H_{12}N_2O_3$	ND	ND	ND	Low	laboratory brown carbon aqSOA	N
$C_9H_{13}NO_5$	Low	ND	ND	Med	laboratory brown carbon aqSOA	N
$C_9H_{14}O_3$	Low	Low	ND	Low	ketolimononaldehyde	P
$C_9H_{14}O_4$	Med	Med	ND	Low	biogenic SOA (pinic acid)	G
$C_9H_{14}O_6S$	Med	ND	ND	ND	ambient cloud water	L
$C_9H_{14}O_7S$	Low	Med	ND	Low	ambient cloud water	L
$C_9H_{14}O_8S$	Med	Med	ND	Low	ambient cloud water	L
$C_9H_{14}O_9S$	Low	Low	ND	ND	ambient cloud water	L
$C_9H_{15}NO_8S$	Very High	Very High	Low	Very High	ambient cloud water	L
$C_9H_{16}O_4$	High	Med	Low	Low	azelaic acid	C-F
$C_9H_{16}O_6S$	Med	Med	ND	Med	ambient cloud water	L
$C_9H_{16}O_7S$	Low	Med	ND	Low	ambient cloud water	L
$C_9H_{16}O_8S$	ND	Low	ND	ND	ambient cloud water	L
$C_9H_{18}O_6S$	Med	Med	Low	Med	ambient cloud water, marine SOA	I, M
$C_9H_{18}O_8S$	ND	ND	ND	Low	ambient cloud water	M
$C_{10}H_8O_3$	Med	Low	Med	Low	syringol aqSOA	A
$C_{10}H_{10}O_4$	High	Med	Med	ND	ferrulic acid	C-E
$C_{10}H_{12}O_2$	Low	Low	ND	Low	eugenol	F
$C_{10}H_{12}O_4$	Med	Low	Low	Low	acetosyringone	C-E
$C_{10}H_{14}O_3$	Low	Low	ND	Low	ketopinic acid	G
$C_{10}H_{14}O_5$	Med	Med	Low	Low	ambient cloud water	L
$C_{10}H_{14}O_6$	Med	Med	ND	Low	ambient cloud water	L
$C_{10}H_{14}O_7S$	Med	ND	ND	ND	ambient cloud water	L
$C_{10}H_{14}O_8S$	Low	Low	ND	ND	ambient cloud water	L
$C_{10}H_{16}O_3$	Low	Low	ND	Low	pinonic acid	C-E, G

Formula	SPC0106F	SPC0201F	BO0204N	BO0213D	Possible Identity	Reference*
$C_{10}H_{16}O_6S$	Med	ND	ND	ND	ambient cloud water	L
$C_{10}H_{16}O_7S$	Med	High	ND	Low	ambient cloud water	L
$C_{10}H_{16}O_8S$	ND	Med	ND	Low	ambient cloud water	L
$C_{10}H_{16}O_9S$	Low	Low	ND	ND	ambient cloud water	L
$C_{10}H_{17}NO_7S$	Very High	Very High	High	Very High	ambient cloud water	L
$C_{10}H_{17}NO_{10}S$	Med	Med	Low	Med	ambient cloud water	L
$C_{10}H_{18}O_5S$	ND	Med	ND	ND	ambient cloud water	L
$C_{10}H_{18}O_7S$	Med	Med	ND	Low	ambient cloud water	L
$C_{10}H_{18}O_8S$	Low	Med	ND	ND	ambient cloud water	L
$C_{10}H_{19}NO_9S$	High	Med	Low	Med	ambient cloud water	M
$C_{10}H_{20}O_5S$	Med	Med	Low	High	ambient cloud water	M
$C_{10}H_{20}O_6S$	Med	Med	ND	Med	marine SOA	I
$C_{10}H_{20}O_7S$	Low	Low	ND	Low	ambient cloud water	L
$C_{11}H_{10}O_8$	ND	Low	ND	ND	phenol aqSOA	A
$C_{11}H_{21}NO_9S$	Med	Med	Low	Med	ambient cloud water	M
$C_{11}H_{22}O_5S$	Med	Med	Low	High	ambient cloud water	M
$C_{11}H_{22}O_6S$	Med	Med	ND	Med	marine SOA	I
$C_{12}H_{10}O_2$	Low	ND	Low	ND	phenol aqSOA	A, K
$C_{12}H_{10}O_3$	Low	ND	Low	Low	phenol aqSOA	A
$C_{12}H_{10}O_4$	ND	ND	Low	Low	phenol aqSOA	A
$C_{12}H_{10}O_7$	Med	Med	Low	Low	syringol aqSOA	K
$C_{12}H_{10}N_2O_8$	ND	ND	Low	ND	ambient cloud water	B
$C_{12}H_{11}NO_4$	Med	ND	Low	Low	laboratory brown carbon aqSOA	N
$C_{12}H_{12}O_6$	Med	Med	Low	Low	syringol aqSOA	K, L
$C_{12}H_{12}O_7$	Med	Med	Low	Low	syringol aqSOA	A, K, L
$C_{12}H_{14}O_4$	Med	Low	Low	Med	syringol aqSOA	A
$C_{12}H_{14}N_2O_4$	ND	ND	ND	Low	laboratory brown carbon aqSOA	O
$C_{12}H_{14}N_2O_4$	ND	ND	ND	Low	laboratory brown carbon aqSOA	N
$C_{12}H_{16}N_2O_5$	ND	ND	ND	Low	laboratory brown carbon aqSOA	O
$C_{12}H_{17}NO_7$	Low	Low	Low	Low	laboratory brown carbon aqSOA	N

Formula	SPC0106F	SPC0201F	BO0204N	BO0213D	Possible Identity	Reference*
$C_{12}H_{20}O_7S$	Med	Med	ND	Med	ambient cloud water	L
$C_{12}H_{22}O_7S$	Med	Med	Low	Med	ambient cloud water	M
$C_{12}H_{23}NO_9S$	Med	Med	Low	Med	ambient cloud water	M
$C_{12}H_{24}O_5S$	Med	Low	Low	High	ambient cloud water	M
$C_{12}H_{24}O_6S$	Med	Med	ND	Med	marine SOA	I
$C_{12}H_{26}O_4S$	High	ND	Med	Low	ambient cloud water	M
$C_{13}H_{10}O_3$	ND	ND	ND	Low	guaiacol aqSOA	A
$C_{13}H_{10}O_4$	Med	Low	Low	ND	guaiacol aqSOA	A
$C_{13}H_{10}O_5$	Med	ND	Low	Low	guaiacol aqSOA	A
$C_{13}H_{12}O_4$	ND	ND	Low	Low	guaiacol aqSOA	A
$C_{13}H_{12}O_6$	Med	Med	Low	Low	guaiacol aqSOA	A, L
$C_{13}H_{14}O_5$	Med	Med	Med	Med	syringol aqSOA	A
$C_{13}H_{14}O_7$	Med	Med	Low	Low	syringol aqSOA	A
$C_{13}H_{16}O_8$	Med	ND	Low	ND	syringol aqSOA	A
$C_{13}H_{24}O_7S$	Med	Med	Low	Med	ambient cloud water	M
$C_{13}H_{26}O_6S$	Med	Low	Low	Med	ambient cloud water, marine SOA	I, M
$C_{14}H_{10}O_5$	Med	Low	Low	Low	phenol aqSOA	A
$C_{14}H_{12}O_6$	Med	Low	Low	Low	guaiacol aqSOA	A, L
$C_{14}H_{12}O_7$	Med	Med	ND	Low	syringol aqSOA	A
$C_{14}H_{14}O_4$	ND	ND	Med	Low	guaiacol aqSOA	A, I, K
$C_{14}H_{14}O_5$	Med	Low	Low	Med	guaiacol aqSOA	A, K, L
$C_{14}H_{14}O_6$	Med	Med	Low	Med	syringol aqSOA and guaiacol aqSOA	A, K
$C_{14}H_{14}O_8$	Med	Med	ND	Low	Syringol aqSOA	A
$C_{14}H_{16}O_8$	Med	Med	Low	Low	syringol aqSOA	A
$C_{14}H_{16}O_9$	Med	Low	ND	Low	syringol aqSOA	A
$C_{14}H_{16}O_{10}$	Low	Low	ND	Low	syringol aqSOA	A
$C_{14}H_{20}O_9$	Low	Low	ND	Med	ambient cloud water	L
$C_{14}H_{24}O_8$	ND	Low	ND	ND	ambient cloud water	L
$C_{14}H_{27}NO_9S$	Med	Low	Low	Med	ambient cloud water	M
$C_{14}H_{28}O_5S$	Med	Low	Low	Med	ambient cloud water	M
$C_{14}H_{28}O_6S$	Med	Low	Low	Med	ambient cloud water	M
$C_{14}H_{30}O_4S$	Med	ND	Low	Med	ambient cloud water	M
$C_{15}H_{14}O_6$	Med	Low	Low	Low	syringol aqSOA	K, L
$C_{15}H_{14}O_8$	Med	Med	Low	Low	syringol aqSOA	K

Formula	SPC0106F	SPC0201F	BO0204N	BO0213D	Possible Identity	Reference*
$C_{15}H_{16}O_6$	Med	Med	Low	Low	syringol aqSOA	A, K, L
$C_{15}H_{16}O_8$	Med	Med	ND	Low	syringol aqSOA	A
$C_{15}H_{16}O_9$	Med	Med	ND	Low	syringol aqSOA	A, K, L
$C_{15}H_{18}O_7$	Med	Med	Low	Low	syringol aqSOA	A, K, L
$C_{15}H_{18}O_9$	Med	Med	Low	Low	syringol aqSOA	A
$C_{15}H_{18}O_{10}$	Low	Low	ND	Low	syringol aqSOA	A
$C_{15}H_{24}O_9$	Low	Low	ND	Low	ambient cloud water	L
$C_{15}H_{29}NO_9S$	Med	Low	Low	Med	ambient cloud water	M
$C_{15}H_{30}O_6S$	Med	Low	Low	Med	ambient cloud water	M
$C_{16}H_{18}O_6$	Med	Low	Low	ND	syringol aqSOA	A, I, K, L
$C_{16}H_{18}O_7$	Med	Med	Low	Low	syringol aqSOA	A
$C_{16}H_{18}O_9$	Med	Med	ND	Low	syringol aqSOA	K
$C_{16}H_{24}O_{11}S$	ND	Low	ND	ND	ambient cloud water	L
$C_{16}H_{31}NO_9S$	Med	Low	Low	Med	ambient cloud water	M
$C_{17}H_{33}NO_9S$	Med	Low	Low	Med	ambient cloud water	M
$C_{18}H_{12}O_5$	Low	ND	ND	Low	phenol aqSOA	A
$C_{18}H_{14}O_4$	Low	ND	Low	Low	phenol aqSOA	A
$C_{18}H_{26}O_{12}S$	ND	Low	ND	ND	ambient cloud water	L
$C_{18}H_{28}O_{11}S$	Low	Low	ND	ND	ambient cloud water	L
$C_{18}H_{38}O_6S$	Low	ND	ND	Low	ambient cloud water	M
$C_{19}H_{30}O_{12}S$	Low	ND	ND	ND	ambient cloud water	L
$C_{20}H_{14}O_6$	Low	ND	Low	ND	phenol aqSOA	A
$C_{20}H_{16}O_7$	Med	ND	Low	Low	guaiacol aqSOA	A
$C_{20}H_{18}O_6$	Med	ND	Low	Low	guaiacol aqSOA	A
$C_{20}H_{26}O_3$	Low	ND	Low	ND	oxodehydroabietic acid	F
$C_{20}H_{28}O_2$	ND	ND	Low	ND	dehydroabietic acid	F
$C_{21}H_{18}O_8$	Med	Low	Low	Low	guaiacol aqSOA	A
$C_{21}H_{20}O_6$	Low	ND	Low	Low	guaiacol aqSOA	A, K
$C_{21}H_{20}O_8$	Med	ND	Low	ND	guaiacol aqSOA	A
$C_{28}H_{26}O_8$	ND	ND	Low	Low	guaiacol aqSOA	A

*References: (A) Yu et al. (2016); (B) Desyaterik et al. (2013); (C) Pietrogrande et al. (2014a); (D) Pietrogrande et al. (2014b); (E) Pietrogrande et al. (2015); (F) Mazzoleni et al. (2007); (G) He et al. (2014); (H) Kitanovski et al. (2012); (I) Dzepina et al. (2015); (J) Herrmann et al. (2015); (K) Yu et al. (2014); (L) Cook et al. (2017); (M) Zhao et al. (2013); (N) Hawkins et al. (2018); (O) Lin et al. (2015) and (P) Nguyen et al. (2013).

Deleted: a
Field Code Changed
Deleted: b
Field Code Changed
Deleted: ; (c) Pietrogrande et al. (2014a); (d)
Field Code Changed
Deleted: (e
Field Code Changed
Deleted: ; (f) Mazzoleni et al. (2007); (g)
Field Code Changed
Deleted: ; (h) Herrmann et al. (2015); (i)
Deleted: Cook
Deleted: 2017
Deleted: ; (j) Yu et al. (2014); and (k) Dzepina et al. (2015).¶

References

Cook, R. D., Lin, Y. H., Peng, Z. Y., Boone, E., Chu, R. K., Dukett, J. E., Gunsch, M. J., Zhang, W. L., Tolic, N., Laskin, A., and Pratt, K. A.: Biogenic, urban, and wildfire influences on the molecular composition of dissolved organic compounds in cloud water, Atmos Chem Phys, 17, 15167-15180, 10.5194/acp-17-15167-2017, 2017.

Desyaterik, Y., Sun, Y., Shen, X. H., Lee, T. Y., Wang, X. F., Wang, T., and Collett, J. L.: Speciation of "brown" carbon in cloud water impacted by agricultural biomass burning in eastern China, J Geophys Res-Atmos, 118, 7389-7399, 2013.

Dzepina, K., Mazzoleni, C., Fialho, P., China, S., Zhang, B., Owen, R. C., Helmig, D., Hueber, J., Kumar, S., Perlinger, J. A., Kramer, L. J., Dziobak, M. P., Ampadu, M. T., Olsen, S., Wuebbles, D. J., and Mazzoleni, L. R.: Molecular characterization of free tropospheric aerosol collected at the Pico Mountain Observatory: a case study with a long-range transported biomass burning plume, Atmos Chem Phys, 15, 5047-5068, 2015.

Hawkins, L., Welsh, H., and Alexander, M.: Evidence for pyrazine-based chromophores in cloudwater mimics containing methylglyoxal and ammonium sulfate, Atmos. Chem. Phys. Discuss., 29, https://doi.org/10.5194/acp-2018-63, 2018.

He, Q. F., Ding, X., Wang, X. M., Yu, J. Z., Fu, X. X., Liu, T. Y., Zhang, Z., Xue, J., Chen, D. H., Zhong, L. J., and Donahue, N. M.: Organosulfates from Pinene and Isoprene over the Pearl River Delta, South China: Seasonal Variation and Implication in Formation Mechanisms, Environ Sci Technol, 48, 9236-9245, 2014.

Herrmann, H., Schaefer, T., Tilgner, A., Styler, S. A., Weller, C., Teich, M., and Otto, T.: Tropospheric Aqueous-Phase Chemistry: Kinetics, Mechanisms, and Its Coupling to a Changing Gas Phase, Chem Rev, 115, 4259-4334, 2015.

Herzsprung, P., Hertkorn, N., von Tumpling, W., Harir, M., Friese, K., and Schmitt-Kopplin, P.: Understanding molecular formula assignment of Fourier transform ion cyclotron resonance mass spectrometry data of natural organic matter from a chemical point of view, Anal Bioanal Chem, 406, 7977-7987, 2014.

Hughey, C. A., Hendrickson, C. L., Rodgers, R. P., Marshall, A. G., and Qian, K. N.: Kendrick mass defect spectrum: A compact visual analysis for ultrahigh-resolution broadband mass spectra, Anal Chem, 73, 4676-4681, 2001.

Kitanovski, Z., Grgic, I., Vermeylen, R., Claeys, M., and Maenhaut, W.: Liquid chromatography tandem mass spectrometry method for characterization of monoaromatic nitro-compounds in atmospheric particulate matter, J Chromatogr A, 1268, 35-43, 10.1016/j.chroma.2012.10.021, 2012.

Kujawinski, E. B., and Behn, M. D.: Automated analysis of electrospray ionization Fourier transform ion cyclotron resonance mass spectra of natural organic matter, Anal Chem, 78, 4363-4373, 2006.

Lin, P., Laskin, J., Nizkorodov, S. A., and Laskin, A.: Revealing Brown Carbon Chromophores Produced in Reactions of Methylglyoxal with Ammonium Sulfate, Environ Sci Technol, 49, 14257-14266, 10.1021/acs.est.5b03608, 2015.

Mazzoleni, L. R., Zielinska, B., and Moosmuller, H.: Emissions of levoglucosan, methoxy phenols, and organic acids from prescribed burns, laboratory combustion of wildland fuels, and residential wood combustion, Environ Sci Technol, 41, 2115-2122, 2007.

Formatted: Indent: Left: 0.1", Hanging: 0.25"

Mazzoleni, L. R., Ehrmann, B. M., Shen, X. H., Marshall, A. G., and Collett, J. L.: Water-Soluble Atmospheric Organic Matter in Fog: Exact Masses and Chemical Formula Identification by Ultrahigh-Resolution Fourier Transform Ion Cyclotron Resonance Mass Spectrometry, Environ Sci Technol, 44, 3690-3697, 2010.

Nguyen, T. B., Laskin, A., Laskin, J., and Nizkorodov, S. A.: Brown carbon formation from ketoaldehydes of biogenic monoterpenes, Faraday Discuss, 165, 473-494, 2013.

Pavia, D., Lampman, G., Kriz, G., Vyvyan, J.: Introduction to Spectroscopy, 4th ed., Brooks/Cole, Cengage Learning, 656 pp., 2009.

Pietrogrande, M. C., Bacco, D., Visentin, M., Ferrari, S., and Casali, P.: Polar organic marker compounds in atmospheric aerosol in the Po Valley during the Supersito campaigns - Part 2: Seasonal variations of sugars, Atmos Environ, 97, 215-225, 2014a.

Pietrogrande, M. C., Bacco, D., Visentin, M., Ferrari, S., and Poluzzi, V.: Polar organic marker compounds in atmospheric aerosol in the Po Valley during the Supersito campaigns - Part 1: Low molecular weight carboxylic acids in cold seasons, Atmos Environ, 86, 164-175, 2014b.

Pietrogrande, M. C., Sacco, D., Ferrari, S., Kaipainen, J., Ricciardelli, I., Riekkola, M. L., Trentini, A., and Visentin, M.: Characterization of atmospheric aerosols in the Po valley during the supersito campaigns - Part 3: Contribution of wood combustion to wintertime atmospheric aerosols in Emilia Romagna region (Northern Italy), Atmos Environ, 122, 291-305, 2015.

Putman, A. L., Offenberg, J. H., Fisseha, R., Kundu, S., Rahn, T. A., and Mazzoleni, L. R.: Ultrahigh-resolution FT-ICR mass spectrometry characterization of alpha-pinene ozonolysis SOA, Atmos Environ, 46, 164-172, 2012.

Stenson, A. C., Marshall, A. G., and Cooper, W. T.: Exact masses and chemical formulas of individual Suwannee River fulvic acids from ultrahigh resolution electrospray ionization Fourier transform ion cyclotron resonance mass spectra, Anal Chem, 75, 1275-1284, 2003.

Tu, P. J., Hall, W. A., and Johnston, M. V.: Characterization of Highly Oxidized Molecules in Fresh and Aged Biogenic Secondary Organic Aerosol, Anal Chem, 88, 4495-4501, 2016.

Yu, L., Smith, J., Laskin, A., Anastasio, C., Laskin, J., and Zhang, Q.: Chemical characterization of SOA formed from aqueous-phase reactions of phenols with the triplet excited state of carbonyl and hydroxyl radical, Atmos Chem Phys, 14, 13801-13816, 2014.

Yu, L., Smith, J., Laskin, A., George, K. M., Anastasio, C., Laskin, J., Dillner, A. M., and Zhang, Q.: Molecular transformations of phenolic SOA during photochemical aging in the aqueous phase: competition among oligomerization, functionalization, and fragmentation, Atmos Chem Phys, 16, 4511-4527, 2016.

Zhao, Y., Hallar, A. G., and Mazzoleni, L. R.: Atmospheric organic matter in clouds: exact masses and molecular formula identification using ultrahigh-resolution FT-ICR mass spectrometry, Atmos Chem Phys, 13, 12343-12362, 2013.

Formatted: Indent: Left: 0.1", Hanging: 0.25"